K. TAKEDA

Ph.D.

1981

UNSW

Form 2
RETENTION

THE UNIVERSITY OF NEW SOUTH WALES

DECLARATION RELATING TO DISPOSITION OF THESIS

This is to certify that I Kenneth Takeda being a candidate for the degree of Ph.D. am fully aware of the policy of the University relating to the retention and use of higher degree theses, namely that the University retains the copies of any thesis submitted for examination, "and is free to allow the thesis to be consulted or borrowed. Subject to the provisions of the Copyright Act (1968) the University may issue the thesis in whole or in part, in photostat or microfilm or other copying medium."

In the light of these provisions I declare that I wish to retain my full privileges of copyright in my thesis and request that neither the whole nor any portion of the thesis may be published by the University Librarian nor may he authorise the publication of the whole or any part of the thesis, and I further declare that this preservation of my copyright privileges in the thesis shall lapse from the 1st day of January 1984 unless it shall previously have been extended or revoked in writing over my hand.

I also authorize the publication by University Microfilms of a 600 word abstract in Dissertation Abstracts International (D.A.I.).

Signature.....

Witness.....

Date 3 D. 1981

ION PERMEATION THROUGH END-PLATE CHANNELS

by

KENNETH TAKEDA

A thesis submitted for the degree of

DOCTOR OF PHILOSOPHY

in the Faculty of Medicine, University of New South Wales

1981

ABSTRACT

The nature of ion permeation through acetylcholine-activated ionic channels at the motor end-plate of the toad, *Bufo marinus*, was investigated. Spontaneous end-plate currents were recorded from sartorius muscle fibres using a focal, extracellular technique or under voltage clamp. Iontophoretic application of acetylcholine resulted in fluctuations of end-plate current in voltage-clamped, glycerol-treated fibres. Analysis of this 'noise', together with measurements of spontaneous currents allowed the properties of individual end-plate channels to be characterized.

When sodium ions were replaced with ammonium ions in the bathing solution,both the average channel lifetime and single channel conductance were increased. These changes were mirrored by the slower decay and increased peak amplitude of miniature end-plate currents. The results were consistent with an end-plate channel model containing high field strength, neutral sites and also suggested a role for intra-channel hydrogen bonding during ion permeation through end-plate channels.

In isosmotic solutions containing 20 mM calcium or magnesium, miniature end-plate currents had time constants of decay about 30% slower than normal. In isotonic calcium solutions (sodium-free), greater increases in channel lifetime were seen and single channel conductance was significantly decreased. Low concentrations (0.1 to 5 mM) of zinc or nickel ions were more potent than either calcium or magnesium in increasing channel lifetime, although they did not greatly affect channel conductance. The normal temperature and voltage sensitivity of channel lifetime was not altered by any of the divalent cations. Surface potential shifts arising from screening of membrane fixed surface charge by divalent cations cannot entirely explain the observed increases in channel lifetime, especially when taken together with the changes in channel conductance. Calcium may exert its effect by binding to

intrachannel sites, while zinc appears to directly affect the normal channel-closing mechanism.

The acetylcholine null potential was not changed by anion substitution. The sodium and potassium-dependence of the null potential was adequately described by the Goldman-Hodgkin-Katz formulation, except at high sodium concentrations. Channel lifetime and channel conductance were dependent on the external sodium concentration. The channel-closing rate constant and channel conductance appeared to 'saturate' with increasing sodium concentration. This sodium-dependence was altered by membrane voltage. The number of intrachannel ion-binding sites estimated from the apparent Michaelis constant is probably >1.

It was clear that the nature of permeant cations can markedly influence end-plate channel characteristics. The ion dependence of channel conductance appears to be explicable in terms of ion affinity for intrachannel binding sites, thus affecting the net mobility of permeant ions through end-plate channels. The effects of ions on channel lifetime are less easily explained, as the molecular details of the normal channel-closing mechanism remain unresolved. Models of ion permeation through end-plate channels that successfully account for the many and diverse characteristics so far observed will almost certainly differ from those proposed for the voltage-activated sodium and potassium channels found in nerve and muscle membrane.

TABLE OF CONTENTS

Page

LIST OF FIGURES

Page

LIST OF TABLES

ABBREVIATIONS AND SYMBOLS

C,pC,fC	coulomb, picocoulomb (10^{-12}C), femtocoulomb (10^{-15}C)
V,mV,μV	volt, millivolt (10^{-3}V), microvolt (10^{-6}V)
A,nA,pA	ampere, nonoampere (10^{-9}A), picoampere (10^{-12}A)
S,nS,pS	Siemen, nanosiemen (10^{-9}S), picosiemen (10^{-12}S)
m,μm,nm	metre, micrometre (10^{-6}m), nanometre (10^{-9}m)
Å	Angstrom (10^{-10}m)
Ω,kΩ,MΩ	ohm, kilohm (10^{3}Ω), megohm (10^{6}Ω)
s,ms,μs	second, millisecond (10^{-3}s), microsecond (10^{-6}s)
M,mM,μM	moles/litre, millimoles/litre, micromoles/litre
e.p.p.,e.p.c.	end-plate potential, current
m.e.p.p., m.e.p.c.	miniature end-plate potential, current
ACh	acetylcholine
AChe	acetylcholinesterase
τ	average open channel lifetime (see τ_D, τ_N)
τ_D	time constant of decay of e.p.c.s or m.e.p.c.s
τ_N	channel lifetime obtained from noise spectra
I_p,G_p	peak m.e.p.c. amplitude, conductance
Q_m,Q_c	charge transferred during a m.e.p.c. or through a single channel
H, volt constant	change in V_m required for an e-fold shift in τ
α,β	rate constants for channel closing, opening
γ	single channel conductance
$\gamma_{p.s.d.}$	γ estimated from noise spectra
γ_{var}	γ estimated from noise variance
σ_i^2	ACh-induced increase in noise variance
μ_i	mean ACh-induced e.p.c.
V,V_m,V_H	potential, membrane or holding potential
ε_o	ACh null potential
E_{Na},E_K	Nernst equilibrium potentials for sodium, potassium
GHK	Goldman-Hodgkin-Katz type equation
NTR	normal toad Ringers (control solution)
f,Hz	frequency, Hertz
Q_{10}	increase in rate per 10°C increase in temperature
μ,K	neutral site model parameters: mobility, equilibrium constant
K_{Na}^m	Michaelis constant for sodium
SEM	standard error of the mean
e^-	electronic charge

LIST OF PUBLICATIONS

The following communications and papers have been published as a result of the research presented in this thesis.

1. BARRY, P.H. & TAKEDA, K. (1977). Salt leakage from microelectrodes. Proc. Austral. Physiol. Pharmacol. Soc. 8, 145P.
2. TAKEDA, K., DATYNER, N.B., BARRY, P.H. & GAGE, P.W. (1978). Post-synaptic effects of Zn^{2+} at the motor end-plate. Proc. Austral. Physiol. Pharmacol. Soc. 9, 126P.
3. TAKEDA, K., BARRY, P.H. & GAGE, P.W. (1979). Ammonium ions affect end-plate channel characteristics. Proc. Austral. Physiol. Pharmacol. Soc. 10, 185P.
4. BARRY, P.H., TAKEDA, K. & GAGE, P.W. (1979). NH_4^+ permeation through motor end-plate channels. Proc. Austral. Soc. Biophys. 3, 2A.
5. TAKEDA, K., BARRY, P.H. & GAGE, P.W. (1980a). Effects of ammonium ions on end-plate channels. J. Gen. Physiol. 75, 589-613.
6. TAKEDA, K., BARRY, P.H. & GAGE, P.W. (1980b). Divalent cations lengthen channel lifetime at the toad neuromuscular junction. Proc. Austral. Soc. Biophys. 4, 2A.
7. TAKEDA, K., GAGE, P.W. & BARRY, P.H. (1981a). Effects of divalent cations on toad end-plate channels. J. Membr. Biol. (in press).
8. TAKEDA, K., GAGE, P.W. & BARRY, P.H. (1981b). Surface charge potentials and the effects of divalent cations on end-plate channels. Proc. Austral. Physiol. Pharmacol. Soc. 12, 185P.
9. TAKEDA, K., BARRY, P.H. & GAGE, P.W. (1982). Effects of changes in external ion concentrations on toad end-plate channels. (in preparation).

CHAPTER ONE

GENERAL INTRODUCTION

The signalling capacity of excitable cells in the nervous system rests on the ability of these cells to regulate ion permeation across their surface membranes. This fundamental concept has roots that extend back almost to the very beginning of the discipline that has become neurophysiology. Brazier (1959) recounts how, in the late 1700's, Galvani focussed attention on the relationship between electrical phenomena and living things. The work of Du Bois-Reymond and Helmholtz in the 19th century produced further advancement in electrophysiology, with the electrical stimulation of tissues and the production of electrical currents by injury and activity. The development of the cable equation by Kelvin at this time proved important in the later description of the electrical characteristics of nerve axons. With the understanding of electrolyte and solution behaviour by Nernst and Boltzmann, the stage was set early this century for Bernstein's (1902) classic membrane hypothesis on the role of potassium ions. Bernstein believed that the membrane potential was set by potassium ions and that during excitation, a non-specific increase in membrane permeability to small ions led to the abolition of the resting potential. Although now known to be inadequate, the idea that electrical activity involves changes in ion permeabilities remains with us. It is interesting to note that Overton's experiments (1902) foreshadowed the key role sodium ions play in action potential propagation.

The demonstration of the all-or-none behaviour of muscle and nerve by Lucas (1909) and Adrian (1912) and the work of Blinks (1930) and Osterhout (1931) that showed an increase in membrane conductivity coincident with activity in plant cells provided the background for the pioneering studies of Cole, Hodgkin, Huxley and Katz. The development of local circuit theory (Hodgkin, 1937a,b) and the observation (Hodgkin &

Huxley, 1939; Curtis & Cole, 1942) that nerve excitation resulted in a transient reversal (or 'overshoot') of membrane potential (rather than Bernstein's predicted zero potential) were the foundations for the sodium hypothesis. The power of the voltage clamp technique developed by Cole (1949) and Marmont (1949) was amply demonstrated in the elegant and now classical work of Hodgkin and Huxley on squid giant axons (see Hodgkin, 1964; Cole, 1972). The sodium hypothesis depends on voltage-sensitive changes in the membrane permeabilities of sodium and potassium ions in accounting for the conduction of regenerative action potentials in nerve.

It is now accepted that the generation of post-synaptic potentials following release of chemical transmitter substances from presynaptic nerve terminals arises from specific increases in membrane ion permeabilities. Historically, Newton's vitalistic speculation on the role of the ubiquitous aether ("exceedingly more rare and subtle than air") led to much confusion concerning the essential electrical nature of nervous activity. The idea of electrical transmission between nerve and muscle may then have its origin in a complete refutation of vitalism by later physiologists (see Brazier, 1959). Following on Sherrington's conception of a synapse and the development of the neuron theory by Ramón y Cajal (using Golgi's silver staining technique), it was not until early this century that chemically mediated synaptic transmission was formally proposed. Elliot (1904) is credited with initially suggesting that "adrenaline might then be the chemical stimulant liberated on each occasion when the (nerve) impulse arrives at the periphery", expanding on the earlier observations of Langley on the effects of sympathetic nerve stimulation. Langley (1905) first deduced the need for agonist receptors ("a receptive substance") in muscle interposed between the active agent and the contractile mechanism when he showed that nicotine and curare could block acetylcholine (ACh)-induced contractions in

denervated muscle while the response of the muscle to direct electrical stimulation remained unaltered. Dale (1914) subsequently provided pharmacological evidence for the separation of ACh-receptors into nicotinic and muscarinic types. The discovery of "Vagusstoff" by Loewi (1921) reawakened interest in the chemical hypothesis with the elegant demonstration that a transmitter was released following nerve stimulation.

However, at the neuromuscular junction, in spite of the rigorous conclusion of Dale, Feldberg & Vogt (1936) that ACh was liberated in response to motor nerve activation, it was argued that transmission was too fast to be chemically mediated and thus, some continuous electrical process was responsible. The controversy persisted until the advent of the intracellular microelectrode (Ling & Gerard, 1949) enabled Katz and his co-workers to confirm the chemical nature of neuromuscular transmission in the 1950's. It should be noted that electrical (or electrotonic) synapses do exist (Furshpan & Potter, 1959) in most organisms (in the form of gap junctions), and that they are of considerable importance where speed and coupling of many cells is required (for review, see Bennett, 1966, 1974).

The end-plate potential was shown to be a transmitter-induced depolarization, which in turn could generate a muscle action potential if it reached a critical size (Eccles, Katz & Kuffler, 1941). In isolated single nerve-muscle fibre preparations, direct applications of low concentrations of ACh caused specific depolarization of end-plate regions, followed by muscle spikes (Kuffler, 1942, 1943). The presence of a specific acetylcholinesterase concentrated at the neuromuscular junction was demonstrated histochemically (Koelle, 1950; Couteaux, 1951).

The original explanation of ACh-mediated postsynaptic conductance changes was that "the end-plate membrane suffers a transient insulation

breakdown of the kind postulated by Bernstein" (Fatt & Katz, 1951). This local short-circuiting of active muscle membrane by transmitter was postulated to arise from a non-selective increase in ion permeabilities at the end-plate region. The null[1], or zero-current potential was measured in two ways (Fatt & Katz, 1951). End-plate potentials were recorded intracellularly and a second electrode was used to displace membrane potential by passing different constant currents. The null potential was found to lie between 0 and -20 mV (Fig. 1.1A), although the method suffers because of the necessity to extrapolate, as end-plate potentials were obtained over the voltage range -90 to -270 mV. The second method utilized the directly evoked muscle action potential to change membrane potential. The motor nerve was stimulated at varying times in relation to the muscle action potential so that transmitter was released at different membrane potentials. Recordings from end-plate regions showed that transmitter release decreased the amplitude of the muscle action potential and introduced a characteristic 'bump' (Fig. 1.1B), which tended to shunt the membrane to -10 to -20 mV (see also Del Castillo & Katz, 1954). The observed null potential was close to the value expected for a free diffusion (or liquid junction) potential between the myoplasm and the surrounding Ringer's, and was thus advanced as in support of the 'short-circuit' hypothesis.

Nastuk (1953) concluded that the depolarizing action of ACh at the end-plate was primarily due to an increase in sodium permeability. However, Del Castillo & Katz (1955) showed that ACh caused increases in membrane conductance in depolarized preparations exposed to isotonic K_2SO_4 (i.e. zero NaCl), confirming that ions other than sodium pass

---

[1] As Gage (1976) has pointed out, the use of the terms ACh equilibrium potential or reversal potential can be misleading - none of the individual ionic currents flowing through end-plate channels have zero amplitude nor do they reverse direction at the null potential. Furthermore ACh is obviously not "in equilibrium".

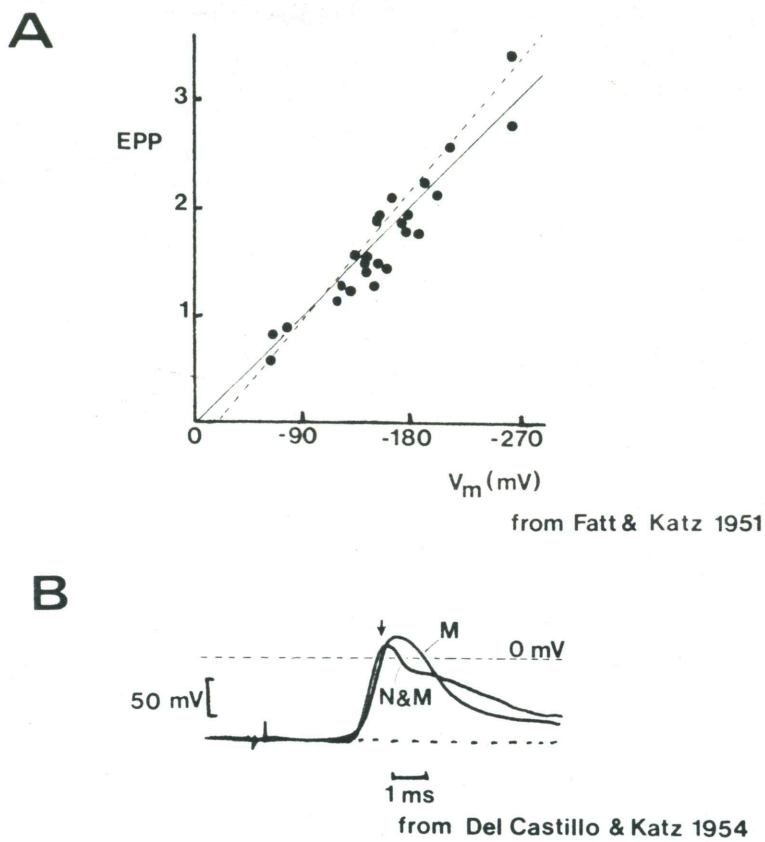

Figure 1.1 Early estimates of the ACh null potential in frog sartorius muscles. A. Normalized end-plate potential peak amplitude plotted as a function of the membrane potential. The solid line indicates proportionality and the broken line is drawn to intersect the abscissa at -14 mV, (which is the theoretical junctional potential between the myoplasm and external solution). The membrane potential was displaced by passing current. Redrawn from Fatt & Katz (1951). B. Directly elicited muscle action potentials (M) were used to control the membrane potential. Nerve stimulation (arrow) resulted in ACh shunting the active response (N+M) towards a plateau (null) potential. Temperature 19°C. Redrawn from Del Castillo & Katz (1954).

through ACh-activated channels. The results could be explained by an increased flux of potassium ions. The possibility that other ions (e.g. chloride) are permeant was considered unlikely, in view of the washing out of internal sodium and chloride that occurs in K_2SO_4 solutions.

Several groups reported that ACh-induced depolarizations could be recorded when sodium ions were replaced by a variety of ammonium-based organic cations (Furukawa,Furukawa & Takagi, 1957; Furukawa & Furukawa, 1959; Nastuk, 1959; Koketsu & Nishi, 1959). It was observed that ammonium ions gave a larger depolarization than sodium ions (Furukawa et al., 1957) and that the decay of end-plate potentials was prolonged by hydrazinium ions (Koketsu & Nishi, 1959).

The two microelectrode voltage clamp technique was first used by Takeuchi & Takeuchi (1959) to record the synaptic current underlying the end-plate potential (see also Oomura & Tomita, 1960). The null potential for end-plate currents (e.p.c.s) was found to be -10 to -20 mV. Two criticisms can be made: firstly, a fairly small voltage range (-70 to -120 mV) was used so that the null potential was found by linear extrapolation and secondly, imperfect spatial control of voltage (due to the extended nature of amphibian end-plates) may have resulted in spurious contributions to the e.p.c. The Takeuchis noted that the decay phase of an e.p.c. was 'approximately exponential', and was apparently lengthened at hyperpolarized potentials. In further studies, the Takeuchis (1960) confirmed that increases in the permeability of sodium and potassium, but not chloride ions occurred during the e.p.c. However, they observed that the null potential did not obey the Goldman (1943) - Hodgkin-Katz (1949) Constant Field Equation when the external sodium or potassium ion concentrations were changed (Fig. 1.2A). An empirical description was given based on the simple equivalent circuit shown in Fig. 1.2B. It was necessary to assume that the conductance ratio

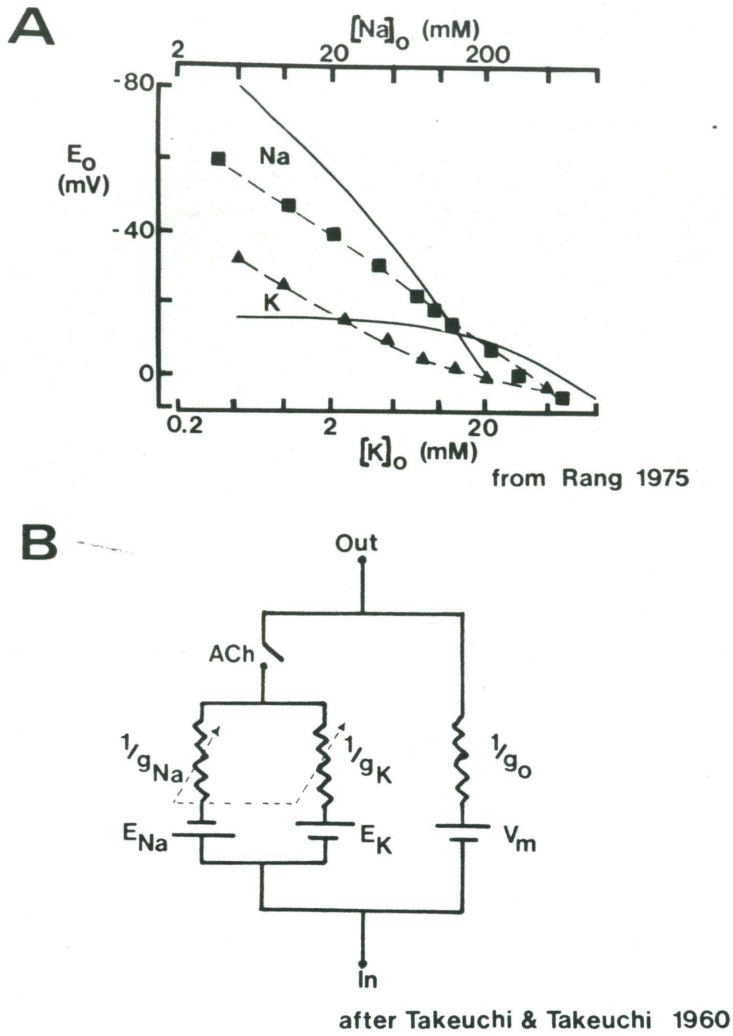

Figure 1.2. The Takeuchi & Takeuchi (1960) results. A. Null potentials (ε_o) as a function of external Na (■) and K (▲) concentrations, determined using linear extrapolation. The solid lines are the Goldman (Constant Field) Equation predictions assuming $P_{Na}/P_K = 0.64$ (which gives their observed ε_o of -15 mV). Internal Na and K concentrations assumed were 15.5 and 126 mM respectively. Redrawn from Rang (1975). B. Schematic electrical equivalent circuit used by Takeuchi & Takeuchi (1960) to explain the observed shifts in ε_o with changes in external Na and K concentrations. The increase in end-plate conductance for Na and K, $\Delta g_{Na}/\Delta g_K$, caused by ACh was assumed to be constant. Redrawn after Takeuchi & Takeuchi (1960).

g_{Na}/g_K did not change with sodium or potassium ion concentrations, but that the shifts in null potential arose from changes in the Nernst equilibrium potentials for these ions. It was later reported (Takeuchi, 1963a,b) that g_{Na}/g_K was decreased in high external potassium and calcium solutions. Calcium ions were shown to be permeant as ACh-induced depolarizations could be demonstrated for isotonic calcium (zero Na) solutions.

Extensive discussion of the validity of the Takeuchis' constant conductance ratio approach exists in several excellent reviews (Ginsborg, 1967, 1973; Rang, 1975; Gage, 1976). As pointed out initially by Finkelstein & Mauro (1963), the separation of end-plate conductance into distinct sodium and potassium components has no physical meaning unless separate conductance pathways exist for the ions (see Jaffe, 1974). Some support has been advanced for the proposal of separate sodium and potassium ionophores at the end-plate (Maeno, 1966; Gage & Armstrong, 1968; Deguchi & Narahashi, 1971). The evidence was based on the biphasic e.p.c. and miniature end-plate current (m.e.p.c.) decay phases produced by procaine, and on the voltage dependence of m.e.p.c. decay. Kordaš (1969) has argued that the effect of membrane potential on the decay phase of e.p.c.s does not arise from separate ionic components with differing time courses. Rather, because the e.p.c. 'reverses' quite clearly at -1 to -10 mV (without becoming diphasic), it was concluded that membrane potential could be affecting ACh loss from the synaptic cleft, the interaction of ACh with its receptor or the inactivation of the ionophore. The work of Kordaš (1972a,b) and Magleby & Stevens (1972a,b) has favoured the view that the voltage-dependence of e.p.c. decay arises because the channel closing mechanism is voltage dependent. The monotonic, exponential decay of end-plate current (e.g. Magleby & Stevens, 1972a,b; Gage & McBurney, 1972), the minimum in

variance of end-plate current fluctuations at the null potential (Dionne & Ruff, 1977), taken together with the observations of Kordaš (1969) showing a single 'reversal' potential strongly support the conclusion that both sodium and potassium ions permeate through a common ACh-activated channel at the end-plate. Also, to date, no pharmacological separation of end-plate sodium and potassium conductances has been reported, unlike the situation in nerve and muscle, where distinct sodium and potassium channels exist (e.g. Hille, 1970).

It is apparent that the null potential is now agreed by weight of evidence to lie between 0 and -5 mV, contrary to the earlier observation of -10 to -20 mV (see Table 1.1). Quite clearly the (linear) extrapolation technique is unsatisfactory when the current-voltage relationship is known to be non-linear (e.g. Dionne & Stevens, 1975). Interpolation of the zero-current potential using e.p.c.s and especially m.e.p.c.s appears to be the method of choice. Possible lack of voltage control when recording e.p.c.s or iontophoretically applied ACh-induced responses from distributed end-plates found in amphibian preparations can be avoided by the use of m.e.p.c.s. Also, it is relevant to point out the importance of the glycerol-treatment procedure (Fujino, Yamaguchi & Suzuki, 1961; Krolenko, Adamjan & Shvinka, 1967; Howell & Jenden, 1967; Gage & Eisenberg, 1967) in defining the null potential - that is, currents can be recorded at depolarized potentials without the activation of the contractile machinery of the muscle. However, glycerol treatment has been suggested to alter internal ion concentrations (e.g. Steinbach & Stevens, 1976), although null potentials determined directly are not different in normal and glycerol treated fibres (e.g. Colquhoun et al., 1975; Katz & Miledi, 1977; this laboratory).

Several recent studies (Magazanik & Potopova, 1969; Ritchie & Fambrough, 1975; Steinbach, 1975; Lassignal & Martin, 1977; Linder &

TABLE 1.1. The acetylcholine null potential, ε_o.

REFERENCE	ε_o (mV)	PREPARATION
Albuquerque & Thesleff (1967)	-7 to -20	cat denervated
Steinbach (1968)	-5 to -15	frog EDL, sartorius
Kordaš (1969)	-1 to -11	frog sartorius
Magazanik & Potapova (1969)	-15	rat diaphragm & denervated
Dunin-Barkovskii et al.(1969)	-15	frog sartorius
Deguchi & Narahashi (1971)	-4	frog sartorius
Maeno, Edwards & Hashimura (1971)	0	frog sartorius
Feltz & Mallart (1971a,b)	-14,(-42)	frog sartorius,(extrajunct)
Gage & McBurney (1972)	+5 to -5	toad sartorius
Magleby & Stevens (1972a,b)	0	frog sartorius
Kordaš (1972a)	-5	frog sartorius
Bregestovski et al. (1972)	-17	frog sartorius
Anderson & Stevens (1973	0	frog sartorius
Mallart & Trautmann (1973)	-45	frog denervated,(high pH)
Steinbach (1975)	-2	rat myoball
Dionne & Stevens (1975)	0	frog cutaneous pectoris
Ritchie & Fambrough (1975)	-3	rat myoball
Kuffler & Yoshikami (1975)	-15	snake, frog
Colquhoun et al. (1975)	0	frog cutaneous pectoris
Scuka (1975)	0	frog sartorius
Neher & Sakmann (1976b)	0	frog c.pectoris & denervated
Mallart, Dreyer & Peper (1976)	0	frog c.pectoris & extrajunct.
Trautmann & Zilber-Gachelin (1976)	0	frog sartorius & denervated
Kuba, Chikazawa & Koketsu (1976)	0	frog sartorius
Van Helden, Gage & Hamill (1977)	-3	toad sartorius
Kordaš (1977)	-1	frog EDL
Sachs & Lecar (1977)	-3	chick myoball
Lassignal & Martin (1977)	0	eel electroplaque
Dionne & Ruff (1977)	0	frog cutaneous pectoris
Colquhoun, Large & Rang (1977)	-5	rat diaphragm
Lambert et al. (1977)	-2	frog sartorius
Katz & Miledi (1977)	0 to -8	frog sartorius
Feltz, Large & Trautmann (1977)	0 to -10	frog cutaneous pectoris
Brenner & Sakmann (1978)	0 to -5	frog sartorius, ectopic
Fischbach & Lass (1978)	-5	chick myoball
Terrar (1978)	0	frog cutaneous pectoris
Adler, Albuquerque & Lebeda (1978)	0	frog sartorius
Gage, McBurney & Van Helden (1978)	-4	toad sartorius
Linder & Quastel (1978)	0	mouse diaphragm
Lewis (1979)	-4	frog cutaneous pectoris
Kuba & Nishi (1979)	-10	frog sympath. ganglia
Ascher, Large & Rang (1979)	-10	rat parasympath. ganglia
Gage, Hamill & Van Helden (1979)	-3	toad sartorius
Cull-Candy, Miledi & Trautmann (1979)	+1	human intercostal
Tsai et al. (1979)	-3	frog sartorius
Adler et al. (1979)	0	frog sartorius
Watanabe & Narahashi (1979)	-7	frog sartorius
Gage & Van Helden (1979)	-3	toad sartorius
Colquhoun, Dreyer & Sheridan (1979)	0	frog cutaneous pectoris
Glavinovic (1979)	0 to -7	cut rat diaphragm
Spivak et al. (1980)	~0	frog sartorius

..../2

(Table 1.1 - cont.)

REFERENCE	ε_o (mV)	PREPARATION
Fiekers et al. (1980)	-5	frog sartorius
Horn & Brodwick (1980)	0	rat myoball
Gage & Hamill (1980)	-4	toad denervated
MacDermott et al. (1980)	-5	frog sympath. ganglia
Lambert et al. (1980)	0 to -5	frog cutaneous pectoris
Takeda, Barry & Gage (1980)	-3	toad sartorius
Magleby & Weinstock (1980)	-5	frog cutaneous pectoris
Adams & Feltz (1980)	~0	frog cutaneous pectoris
Miledi & Parker (1980)	0	frog sartorius
Horn & Patlak (1980)	0	rat myoball
Dwyer, Adams & Hille (1980)	+1	frog semitendinosus
Adams, Dwyer & Hille (1980)	0	frog semitendinosus
McLachlan & Martin (1981)	0	frog EDL, mouse diaphragm
Dionne & Parsons (1981)	-5	snake, twitch & slow
Takeda, Gage & Barry (1981)	-2	toad sartorius
Miledi & Uchitel (1981)	~0	frog, twitch & slow
Alemà et al. (1981)	~0	rat diaphragm
Breitschmid & Brenner (1981)	0	frog, ectopic (autonomic)
Hamill et al. (1981)	0	rat myoball
Harvey & Van Helden (1981)	-2	chicken ALD,PLD
Rang (1981)	-10	rat submandib. ganglia
Boheim et al. (1981)	~0	reconstituted Torpedo AChR
Farley et al. (1981)	-5	frog sartorius
Landau et al. (1981)	-3	frog cutaneous pectoris

Quastel, 1978; Adams, Dwyer & Hille, 1980) have failed to demonstrate large shifts in the ACh null potential with changing external potassium ion concentrations as were observed by the Takeuchis (see Fig. 1.2A). Rather, the potassium-dependence of the null potential was well described by the Goldman-Hodgkin-Katz (GHK) type of equation. It should be noted that in the absence of any chloride permeability, the GHK equation is one of a series of different equations having the same form. Similarly, changes in the null potential with external sodium ion concentration have been observed to obey the GHK predictions (Steinbach, 1975; Lassignal & Martin, 1977; Linder & Quastel, 1978; Lewis, 1979; Barry, Gage & Van Helden, 1979a; Adams et al., 1980; Horn & Patlak, 1980; but see Ritchie & Fambrough, 1975). As pointed out by Barry et al. (1979a), the Takeuchis' constant conductance ratio equation is inappropriate in some ion substitution experiments, because in the presence of zero concentrations of cations on one side of the membrane, equilibrium potentials become infinite. Experiments to be presented here show that the null potential follows the GHK predictions for changes in external sodium and potassium ion concentrations.

It has been reported (Feltz & Mallart, 1971a,b; Mallart & Trautmann, 1973) that a marked negative shift in the null potential (from -15 to -42 mV) occurs in denervated muscle fibres (i.e. for extrajunctional ACh receptors), although earlier observations suggested that the null potential lay between -7 and -20 mV (Axelsson & Thesleff, 1959; Albuquerque & Thesleff, 1967; Magazanik & Potopova, 1969). More recent work has confirmed that the null potential in denervated fibres is close to 0 mV, and thus, not significantly different from the value found for junctional ACh receptors (Mallart, Dreyer & Peper, 1976; Trautmann & Zilber-Gachelin, 1976; Neher & Sakmann, 1976b;Gage & Hamill, 1980; see Table 1.1). Furthermore, similar estimates of 0.63 nm for the ACh-

activated channel diameter have been obtained from ion selectivity experiments at both junctional and extrajunctional receptors (Maeno, Edwards & Anraku, 1977; Guy, Dekin & Morello, 1977; see also Dwyer et al., 1980; Adams et al., 1980).

Increases in external pH were reported to shift the null potential to more negative values (Mallart & Trautmann, 1973). However, other workers (Ben-Haim, Landau & Silman, 1973; Trautmann & Zilber-Gachelin, 1975; Scuka, 1975; Ritchie & Fambrough, 1975) have failed to confirm this result, in agreement with observations from this laboratory (see later; Hamill, personal communication).

The ACh-induced increase in postjunctional sodium and potassium conductances is slowly reversed if the agonist application is sustained, a phenomenon known as desensitization (Del Castillo & Katz, 1957; Katz & Thesleff, 1957). The molecular mechanisms underlying desensitization remain unclear, in spite of considerable study (for review, see Magazanik & Vyskocil, 1973; Gage, 1976; Colquhoun, 1979). Several distinct classes of mechanisms have been postulated, although the commonly accepted model is based on a cyclic interconversion of active receptor-ionophore complexes to a desensitized ('non-conducting') state, which can then revert to the 'resting' receptor conformation (Katz & Thesleff, 1957; Rang & Ritter, 1970). Some support has been given to the view that desensitization arises from some change in the ionophore (e.g. Nastuk & Parsons, 1970), rather than in the ACh-receptors. It was reported that the null potential shifted to a more negative value at desensitized end-plates (Kuba & Koketsu, 1976), but subsequent work has shown a normal value for the desensitized null potential (Lambert, Spannbauer & Parsons, 1977; Katz & Miledi, 1977). Adams (1975) has proposed that agonists entering and blocking open end-plate channels in a sequential manner, result in desensitization, much as originally suggested by Del Castillo & Katz (1957). However, Sakmann, Patlak & Neher (1980) have recently

argued that desensitization does not occur by channel block on the basis of the observed agonist concentration dependence.

In the last decade, there has been an enormous increase in the number of publications relating to postsynaptic function. There can be little doubt that the primary impetus has been Katz & Miledi's (1970, 1971, 1972, 1973a,b) pioneering studies using fluctuation (noise) analysis as a molecular probe of agonist-activated channels. Verveen & Derksen (1965) first employed the technique of noise analysis to investigate the stochastic properties of ion conductance channels at the node of Ranvier (for review, see Verveen & DeFelice, 1974). The interest in ion channel research created by noise analysis is readily explained by the ability to characterize properties of individual channels and to deduce (quasi-) molecular mechanisms underlying single channel function from the ensemble behaviour of a population of channels using noise analysis. The technique has been applied using axon membranes and lipid bilayers (for reviews, see Fishman, 1975; Conti & Wanke, 1975; Ehrenstein & Lecar, 1977), photoreceptors (e.g. Hagins, 1965; Wong, 1978), epithelia (for review, see Lindemann, 1980), and perhaps most extensively, transmitter-activated synaptic channels (for reviews, see Gage, 1976; Neher & Stevens, 1977; Colquhoun & Hawkes, 1977; Stevens, 1977; Steinbach, 1980; Wray, 1980).

At the end-plate, the observation of the exponential decay of e.p.c.s and m.e.p.c.s (see Fig. 1.3) has lead to the suggestion that a first-order reaction rate-limits the decay of the conductance change (Magleby & Stevens, 1972a,b). An important conclusion was that the transient increase in ACh cleft concentration was short compared to the mean open time of a channel - i.e. the ACh concentration drops to zero before any channels close. The decay can be described as

$$I(t) = I(0)\exp(-t/\tau_D)$$

where I(t) is the current t ms after the peak current at 0 time, I(0), and τ_D is the time constant of decay. It has been shown that τ_D is both temperature and voltage sensitive (Takeuchi & Takeuchi, 1959; Gage & Armstrong, 1968; Kordaš, 1969; 1972b; Gage & McBurney, 1972, 1975; Magleby & Stevens, 1972a,b; Anderson & Stevens, 1973). The increase in fluctuations in the focally-recorded voltage noise coincident with the steady depolarization caused by ACh were analyzed by Katz & Miledi assuming that the fluctuations represented moment-to-moment variations in the number of open channels. It was possible to estimate the amplitude of a single channel and the average open channel lifetime (τ_N) assuming Poisson statistics. Values of τ_N were found to be in reasonable agreement with values of τ_D obtained from extracellularly recorded m.e.p.c.s.

Anderson & Stevens (1973) utilized the voltage clamp technique to extend Katz & Miledi's observations on ACh-noise. They also obtained conductance power density spectra which were well described by single Lorentzian curves (i.e. consistent with a first order process; for a definition, see General Methods). A two-state model of channel conductance (i.e. single channels have zero conductance when closed, and a fixed conductance, γ, when open; Stevens, 1972) was assumed, along with the applicability of Poisson statistics. A population of channels could then be described which had an exponential distribution of lifetimes. Single channels then have average open times, τ_N and average conductance, γ. Anderson & Stevens found that τ_N was in excellent agreement with τ_D. Moreover, τ_N and τ_D exhibited identical voltage and temperature sensitivity. The results supported the kinetic model proposed by Magleby & Stevens (1972b) where τ_N was rate-limited by a first order process involving a conformational change in a membrane protein (for review, see Steinbach & Stevens, 1976).

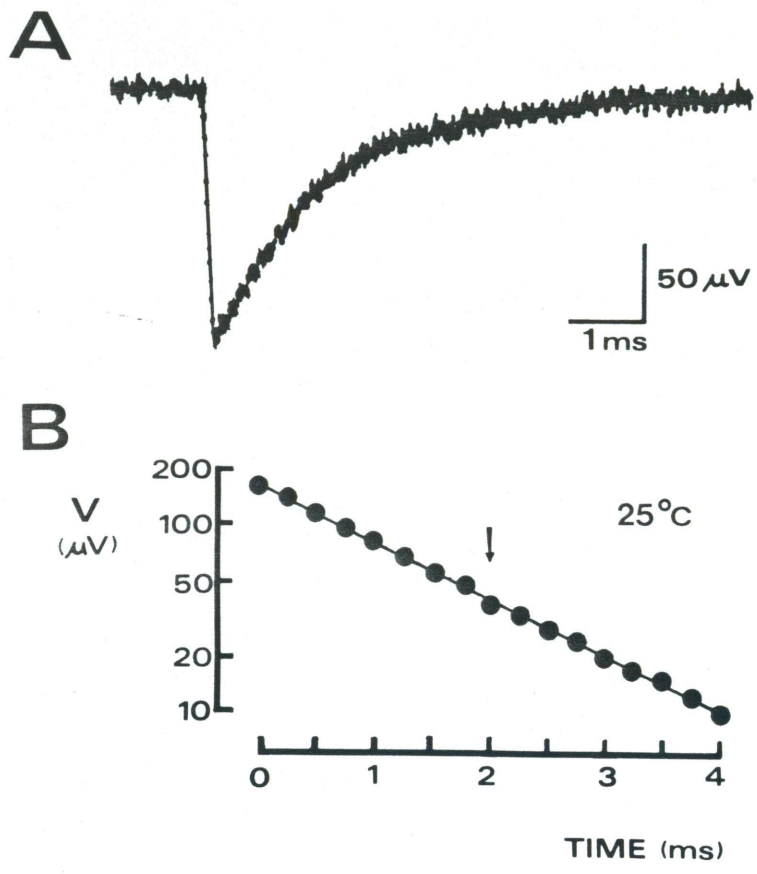

Figure 1.3. The exponential decay of a miniature end-plate current. A. Extracellularly recorded m.e.p.c. from a toad sartorius muscle at 25°C. Inward membrane current is shown as a downward deflection in this and all subsequent figures. B. The decay of the current amplitude is plotted semilogarithmically against time and is well-described by the equation: $I(t) = I(0)\exp(-t/\tau_D)$. The time constant of decay (τ_D, arrow) is 2.05 ms.

Many simple chemicals and drugs have been found to affect τ, although there is no conclusive or even persuasive evidence that allows the determination of the normal rate-limiting step for channel closure. The commonly accepted explanation for the kinetics underlying agonist-induced conductance changes at the end-plate is that following an agonist molecule(s) (A) binding to the ACh-receptor (R), an inactive agonist-receptor complex (associated with a closed ionophore; AR) is rapidly formed which then undergoes a subsequent slower conformational change to the active agonist-receptor complex (AR*) containing an open ionophore (Del Castillo & Katz, 1957; Magleby & Stevens, 1972a,b). This can be represented as:

$$A + R \underset{k_{-1}}{\overset{k_1}{\rightleftharpoons}} AR \underset{\alpha}{\overset{\beta}{\rightleftharpoons}} AR^*$$

where k_1 and k_{-1} are the forward and backward rate constants for agonist binding, and β and α are the channel opening and closing rate constants, respectively. The key assumption in this scheme is that the binding reaction is very rapid, so that the rate-limiting step is the closed $\rightleftharpoons$ open conformation change. This is based on the analogy between the agonist-receptor mechanism and the initial steps in enzyme-substrate reactions (Magleby & Stevens, 1972b; for review, see Gage, 1976; Colquhoun, 1979).

The voltage dependence of τ was postulated to arise from the effect of membrane potential on the change in dipole moment of the agonist-receptor protein complex as it undergoes the closed $\rightleftharpoons$ open conformational change (Magleby & Stevens, 1972b). The properties of the lipid surrounding membrane proteins may influence channel behaviour, as has been inferred from the effects of the aliphatic alcohols on τ (Gage McBurney & Van Helden, 1974, 1978; Gage, McBurney & Schneider, 1975). Further molecular clues to the mechanisms regulating normal end-plate channel function has come from the study of local anaesthetic action on

channel lifetime. For example, some local anaesthetics and partial agonists appear to enter and block open end-plate channels by binding to a critical intrachannel site (Adams, 1976b,1977b,Ruff, 1977; Adams & Sakmann, 1978a;Neher & Steinbach, 1978).

Much attention has recently been focussed on the characterization of the molecular dimensions of end-plate channels using ion selectivity experiments. There seems little reason to doubt that the end-plate channel forms a large aqueous pore. A wealth of evidence supports this assertion: permeability ratios calculated from null (zero-current) potentials have been compiled for an exhaustive list of cations, both organic and metal, monovalent and divalent (Van Helden, Hamill & Gage, 1977; Lassignal & Martin, 1977; Linder & Quastel, 1978; Lewis, 1979; Gage & Van Helden, 1979; Bregestovski, Miledi & Parker, 1979; Watanabe & Narahashi, 1980; Takeda, Barry & Gage, 1980; Dwyer, Adams & Hille, 1980; Adams, Dwyer & Hille, 1980; see Rang , 1975 for a review of earlier work). What is the basis for this selectivity? The most plausible suggestion is the end-plate channel contains at least one negatively charged site with which cations interact and which excludes anions from crossing the channel. The strongest evidence for this hypothesis is that anions have zero permeability through end-plate channels (Takeuchi & Takeuchi, 1960). Also, it has recently been observed that the single channel conductance γ, depends on the nature of the permeating cation both at the end-plate (Van Helden et al., 1977; Gage & Van Helden, 1979; Lewis, 1979; Bregestovski et al., 1979; Takeda et al., 1980) and for ACh-activated, cation selective channels in Aplysia neurones (Ascher, Marty & Neild, 1978; Marchais & Marty, 1979). The observed voltage dependence of conductance and its dependence on the major ions present on both sides of the membrane (e.g. Van Helden, Gage & Hamill, 1979), together with the concentration dependence of γ has been accounted for by Barry, Gage &

Van Helden (1979a) in a model which proposes that the end-plate channel contains 'neutral' sites that bear net negative charge (e.g. the negative end of a dipole). The ion and voltage dependent effects on γ can then be explained in terms of the ease with which ions partition into or enter the channel (thus determining the equilibrium ion concentration within) and the mobility of ions inside the channel (largely determined by considerations of attractive site energy and ion hydration energy). Relative ion permeabilities can then be separated into two components: relative partition coefficients (or equilibrium constants) and relative mobilities. For the alkali cations, the observed equilibrium constant sequence of Li>Na>K>Cs (Barry et al., 1979a; Gage & Van Helden, 1979) is in fact a high field strength sequence (Eisenman, 1962). It should be noted that, although the end-plate channel exhibits relatively weak selectivity for the alkali cations (which in fact follow their free solution mobilities; e.g. Van Helden et al., 1977; Adams et al., 1980) compared to Na and K channels in nerve and muscle membranes, any model which explains cation selectivity requires some negative membrane groups to account for the observed differences in equilibrium constants.

In spite of considerable investigation at the end-plate channel, no complete description of the molecular mechanisms underlying channel behaviour has been possible. Moreover, modelling of ion permeation through end-plate channels has resulted in the realization that the basic physical properties of the channel are different from those inferred for the well-studied Na and K channels in nerve and the Gramicidin A channel in artificial lipid bilayers (e.g. see Barry et al., 1979a; Adams, et al., 1980). The relationship between the agonist-receptor interaction and the actual ionophore mechanism is unclear, and remains of central interest. Certainly, both the nature of the agonist (and receptor) and of the permeant cations can influence end-plate channel characteristics

(e.g. Colquhoun et al., 1975; Van Helden et al., 1977), a fundamental difference compared to the voltage-activated Na and K channels in nerve (although Swenson & Armstrong (1981) have recently reported that the lifetime of K channels in squid axons can be modulated by the presence of certain permeant cations).

The general aim of this thesis is to further characterize ion permeation through ACh-activated end-plate channels. Specifically, the results obtained are divided into three sections. The first deals with the effects of an 'organic' cation , ammonium, on channel characteristics and its compatibility with the 'neutral' site model of Barry et al. (1979a). The second section examines the effects of some divalent cations on both channel lifetime and conductance, and the role played by surface charge potentials in determining these effects. Finally, concentration-dependent changes in the null potential and channel characteristics are presented along with a discussion of ionic strength and saturation effects. A description of general methods and materials common to all the Results chapters is given in Chapter Two. Brief accounts of necessary protocol relating to specific experiments can be found at the beginning of each of the Results chapters. An attempt to pinpoint specific questions and to provide useful speculation concerning end-plate channel function is made in Chapter Six.

CHAPTER TWO

GENERAL METHODS AND MATERIALS

Preparation

In all experiments sartorius muscles from the toad, *Bufo marinus* were used. Toads, 6-8 cm in length, were obtained from a Queensland supplier (P. Krauss, Atherton, Qld.) every 1-2 months and were maintained in a terrarium in the laboratory. Fresh water was provided daily. Toads were killed by decapitation and usually both sartorius muscles were removed. Muscles were pinned out, dorsal side up, at ~1.2 times their rest length on a Sylgard base in a Perspex bath and were fine-dissected under a Wild Stereomicroscope. Care was taken in removing adhering connective tissue and in obtaining a parallel alignment of muscle fibres, as this greatly facilitated visualization of fine nerve endings and insertion of microelectrodes. Muscles were transilluminated from below.

Tissue Bath

The thin-walled bath was fitted tightly into a Perspex jacket through which a methanol-water mixture at constant temperature (Lauda, K2RD) was circulated. The temperature could be controlled anywhere from 4 to 40°C (±0.2°C) and was monitored with a thermistor placed close to the muscle. The bath had a volume of 3-4 ml and was connected via small diameter holes to inlet and outlet chambers (thus minimizing solution flow artifacts).

Solutions

Solutions were aerated and flowed continuously (gravity feed) through the bath at a rate of 2-3 ml/min. The solutions were pre-cooled (or warmed) before entry to the bath by passing them through a large brass block in series with the methanol-water circulation. Excess solution was removed by suction in order to maintain a constant solution depth. Normal toad Ringer (NTR, the control solution) contained (mM): NaCl, 115; KCl, 2.5; $CaCl_2$, 1.8; NaHEPES buffer, 2, and had a pH of

7.1-7.2. Monovalent cations were substituted for Na by equimolar replacement of NaCl with the chloride salt of the test cation. Divalent cations were added directly (to 1 mM); NaCl concentration was reduced appropriately to maintain osmotic strength with higher divalent cation concentrations. When the ionic strength of the solution was decreased, mannitol was added so that the solution remained isosmotic. Glucosamine-HCl was used as a (relatively) impermeant substitute for NaCl when ionic strength was to be kept constant. In experiments where pH was altered, HCl or NaOH was added to the HEPES buffered solution. Details of different solution compositions are given in the text. Stock solutions were filtered and kept refrigerated. Normal toad Ringer was usually freshly made up on the morning of experiments.

Glycerol-treatment

When muscle fibres are depolarized under voltage clamp or when ACh is applied iontophoretically, activation of the contractile machinery often occurs. Muscle fibres were therefore routinely glycerol-treated, effectively decoupling the surface membrane from the transverse tubular system (Howell & Jenden, 1967; Gage & Eisenberg, 1967). Glycerol was added to normal toad Ringer to give concentrations of 400-670 mM and fine-dissected muscles were incubated in this solution for 60-70 min. The glycerol-containing solution was usually refreshed after 5 and 30 min. The muscles were then transferred to a modified Ringer (containing 5 mM $CaCl_2$ and 5 mM $MgCl_2$) for 20 min (Eisenberg, Howell & Vaughan, 1971). Glycerol-treatment was instrumental in allowing data (both m.e.p.c.s and ACh-induced current fluctuations) to be collected from individual fibres voltage-clamped over wide ranges of membrane potential in both control and test solutions.

Viable preparations could be maintained for as long as 10 hours after glycerol-treatment. Resting membrane potential sometimes was

decreased following glycerol-treatment, but no systematic quantification was undertaken. More importantly, null potentials measured in glycerol-treated fibres (ε_o = -2.1 ± 0.4 mV, n=20) were not significantly different from those in non-glycerol-treated fibres (ε_o = -3.5 ± 1.2 mV, n=4). In normal fibres, contraction was avoided by slowly changing the holding potential, thereby presumably inactivating the contractile apparatus. Some seasonal variation was also apparent - 'summer' toads were harder to glycerol-treat successfully and thus, required higher glycerol concentrations (see also Dulhunty & Gage, 1973).

Data Recording

A number of standard methods were employed to optimize the recording of the small electrical signals of interest. Firstly, the tissue bath, amplifiers and micromanipulators were mounted on a heavy steel plate. The table supporting the plate was protected from vibration using sand-filled boxes mounted on closed-cell foam and a layer of heavy felt decoupled the table from the plate. Secondly, a Faraday cage enclosed the table to minimize noise pickup from mains operated equipment. Thirdly, a careful grounding system minimized loops - all amplifiers were grounded to one central point and 'on-board' grounds(either actually required by the operational amplifier or used in decoupling the power supplies) utilized this point rather than the power supply return. Leads entering the cage were shielded, solution bottles were placed inside the cage, and the external, thermal water jacket surrounding the tissue bath was grounded. Noise levels were typically $\lesssim$ 100 μV r.m.s. for a 10 MΩ electrode (5 kHz bandwidth).

Electrodes

Two techniques were used to record electrical activity and each required different types of microelectrodes. Focal extracellular recording was often the method of choice when m.e.p.c.s were to be

studied over a prolonged period of time, for example as a function of temperature, as fibre deterioration was minimal. More importantly, the low resistance of extracellular electrodes resulted in an increased signal bandwidth and thus, a more faithful representation of high frequency components. Electrodes were pulled from 0.7 mm I.D. - 1.0 mm O.D. glass (No. 46485, Kimble Products, U.S.A.) on a horizontal Narishige puller and were broken by hand to give tip diameters of 10-20 μm. Wide tip electrodes were sometimes made by prolonged bevelling followed by heat polishing on a microforge. Electrodes were backfilled with normal toad Ringer (or 200 mM NaCl) in a 1% agar gel, and typically had resistances of ~1 MΩ.

For voltage clamp work, a number of criteria were important for optimal microelectrodes. Firstly, ease of multi-electrode penetration (thus avoiding excess damage and high leakage currents) required sharp, fine-tipped (high resistance) electrodes. However, voltage-recording electrodes ideally should have low noise and current-passing electrodes should not rectify, both characteristics of low resistance microelectrodes. Secondly, the overall clamp speed was enhanced by low resistance electrodes. Initially, batches of 12 microelectrodes were pulled from the Kimble glass on a Narishige puller, and were first filled with a methanol-water solution under negative pressure at ~80°C. The electrodes were then backfilled with 2 M KCl (voltage electrodes) or a 2 M K citrate-0.8 M KCl mixture (current electrodes) and left overnight immersed in their respective electrolytes. Microelectrodes were then broken 'on the job' to give resistances of 3-8 MΩ and tip diameters of $\lesssim$0.2 μm. Microelectrodes were sometimes bevelled, but in the end, breaking to suitable resistances proved most efficient. More recently, filament-containing microelectrodes (Clark Electromedical) were used and had the considerable advantage of immediate use, as they could be pulled and

backfilled in less than a minute. With not a little serendipity, ~5 MΩ microelectrodes (after filling) could be pulled directly and this was the near ideal situation.

When ACh was applied iontophoretically, microelectrodes containing 2 M AChCl with resistances of 20-30 MΩ were used. This proved more suitable in providing stable, reproducible concentrations of agonist than local microjet perfusion from wide tip micropipettes.

Ground electrodes were made using 2.5 mm I.D. glass tubing filled with a 2 M KCl-3% agar gel. To prevent contamination due to diffusion of KCl out of the electrode, the electrodes were always placed 'down-stream' in the bath. Electrical contact with the electrolyte was via a coiled Ag/AgCl wire. Resistances were ≤1000Ω, and paired grounds showed <200 μV difference. Grounds were stored connected together in 2 M KCl in the refrigerator.

Fine Ag/AgCl wire provided electrical connection from a micro-electrode to the input lead of an amplifier. The Ag wire was carefully cleaned by sanding with fine wet and dry paper, followed by nitric acid and distilled water rinses before being chlorided in 0.1 M HCl at a DC current of 1 mA/cm^2 for ~10 min. Internal wires were re-chlorided at regular intervals.

Prior to pulling, all microelectrode glass was cleaned in chromic acid, followed by methanol and distilled water rinses. The glass was then oven dried and stored in a sealed container. Electrolytes for filling microelectrodes were routinely filtered through 0.1 μm Millipore filters before use in order to minimize 'clogging' of the fine tips, and were stored refrigerated.

Electronic Equipment

A block diagram of the circuitry used for voltage clamp experiments is given in Fig. 2.1. Voltage followers were made using high input

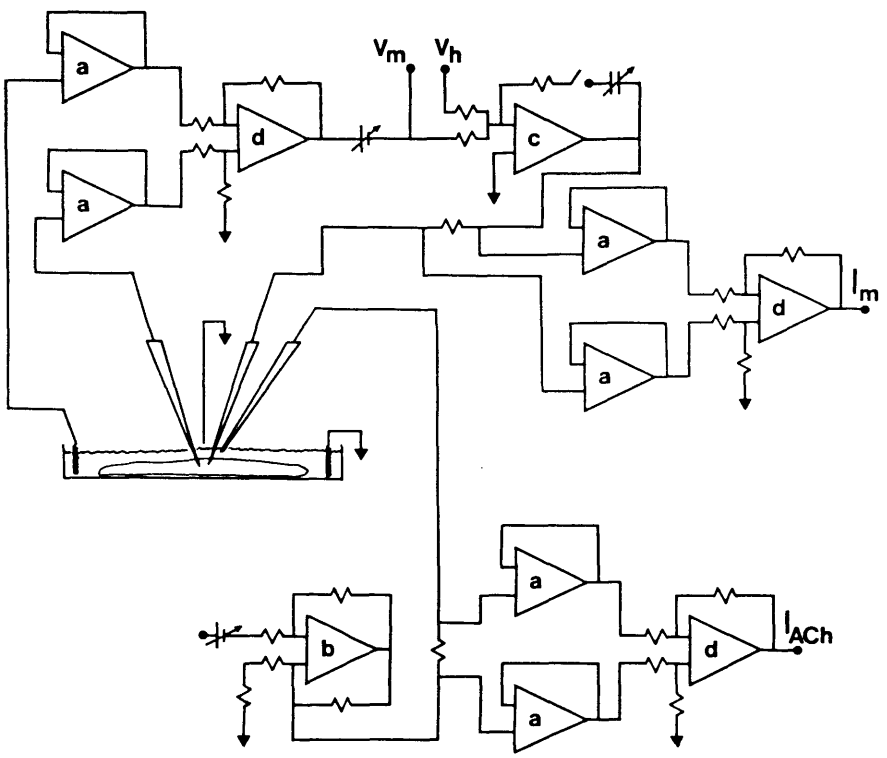

Figure 2.1. Schematic block diagram of voltage clamp circuitry. Membrane potential (V_m) was recorded differentially. The command or holding potential (V_H) was derived from a battery. The clamp current (I_m) was monitored differentially across 100 kΩ. A constant current generator (b) was used for ACh iontophoresis. The iontophoretic current (I_{ACh}) was also monitored differentially across 100 kΩ. a, voltage followers (Philbrick 1026, or Datel 406-2); b, constant current generator (Philbrick 1026); c, clamp amplifier (Philbrick 1026); d, differential amplifiers (Philbrick 1026).

impedance, FET amplifiers (1026, Philbrick) with driven shields and variable capacity neutralization. DC voltages (e.g. arising from micro-electrode tip potentials) were backed-off using batteries. A conventional voltage clamp circuit was used and the amplifier gain/bandwidth product could be selected by switching various capacitances into the feedback loop. Command voltages were derived from a battery. Clamp currents were monitored in two ways. Initially, a virtual earth circuit with a 1 MΩ feedback resistor (in parallel with 10 pF) was used. However, this arrangement had the disadvantage of measuring all current (irrespective of source) flowing to ground. For noise analysis, it was important to obtain an accurate measurement of the mean, ACh-induced, DC end-plate current and this was often complicated by the ACh iontophoretic current also flowing to ground. To overcome this problem, clamp current was monitored differentially across 100 kΩ in series with current-passing microelectrode using FET followers (Datel 406-2). This signal was appropriately filtered to match the current electrode RC characteristic. There was no difference in m.e.p.c.s or noise monitored with the different amplifiers. A constant-current 'pump' was used for iontophoresis of ACh. Iontophoretic current was also monitored differentially across 100 kΩ in series with the ACh electrode.

Digital panel meters (initially, AD 2001, Analog Devices) were used to read membrane potential and command voltages, clamp and iontophoretic current, and thermistor output. However, the multiplexing of the high current LED's in these DPM's introduced significant noise so battery powered, low current LCD's (Intersil ICL 7106) were used. All the voltages measured by the amplifiers within the cage were usually in the mV range (and in retrospect, a gain of 10 for all amplifiers would have been preferable). Further signal amplification was provided by rack mounted modular units consisting of a fixed X10 DC gain first stage followed by a variable gain (1,2,5,10 or 100x) second stage with AC

coupling time constants of 1 or 6 s and simple 1 pole low pass filters with 5,20 or 100 μs time constants. Membrane voltages were also audio monitored by a voltage to frequency conversion unit.

All the amplifiers used here were driven by a ± 15 V DC power supply designed and constructed within the School. The power supply was well regulated (using current sense) and had ripple of <500 μV under load (maximum output current 1A).

High gain, AC coupled membrane voltages and clamp current were displayed on an oscilloscope (Tektronix 365, 3A3 and 3A9 differential amplifiers). ACh-induced end-plate current and ACh-iontophoretic current were recorded (DC coupled) on a chart recorder (HP 7402A). The amplified end-plate current and membrane voltage signals were also recorded on tape (Sony TC377) after frequency modulation (Electrodata Associates, Sydney). The use of FM modules and an analog tape deck resulted in a 2 channel FM recording system (bandwidth DC - 2.5 kHz, 3dB point) at considerably less cost than a comparable commercial unit. Experimental protocol was also recorded on tape as voice over the membrane potential channel.

Voltage Clamp Procedure

End-plate regions were located by determining where a rapid depolarization was caused by iontophoretically applied ACh and by the presence of miniature end-plate potentials (m.e.p.p.s) having fast rise times ($\lesssim$1 ms) and amplitudes of at least 0.5 mV. In some experiments, focal extracellular m.e.p.c.s were recorded before the clamping electrodes were inserted. Following penetration of a fibre with two microelectrodes (which were 1 fibre diameter apart or $\lesssim$50 μm), it was often possible to assess electrode positioning with respect to the end-plate by using the 3A3 differential amplifier to record the difference between m.e.p.p.s from the two electrodes. If both electrodes recorded

m.e.p.p.s of equal size, the displayed difference voltage trace was flat and one assumed that the electrodes were roughly equidistant from the current source. This was of some importance in obtaining well-clamped m.e.p.c.s, although with the distributed nature of amphibian end-plates it was possible to record both well and poorly-clamped m.e.p.c.s simultaneously. The overall clamp speed was optimized by introducing a grounded metal shield between the clamping electrodes (thus reducing interelectrode capacitative coupling), by maintaining a low solution level over the end-plate ($\lesssim$2 mm) as this minimised the microelectrode capacitance (which amounts to ~1pF/mm of solution depth; Nastuk & Hodgkin, 1951) and by increasing the capacity compensation until both voltage and current traces just started to ring. The leads connecting the microelectrodes to the circuitry were also carefully shielded. In tests of the overall clamp circuitry, 20 mV command steps applied to a model membrane via simulated microelectrodes (5 MΩ in parallel with 3.3. pF) were established $\lesssim$50 μs after the step. A transient recorder (N3, Neurograph, or one built and kindly lent by N.B. Datyner) was used to 'capture' m.e.p.c.s (minimal sampling speeds of 50 μs per point) and the m.e.p.c.s were used to judge the quality of the clamp. Poorly clamped m.e.p.c.s were 'peaky' and often had a distinct overshoot coincident with a 'kick' on the voltage trace. The decay of these m.e.p.c.s did not follow a single exponential time course.

When ACh-induced current fluctuations were generated, the iontophoretic electrode was positioned so that with a reverse (bucking) current of 5-15 nA no noise was observable. Iontophoretic currents of 5-20 nA gave mean end-plate currents of 30-70 nA. At different voltages in any one cell, the iontophoretic current was always kept constant. Because of the requirement of stationarity for noise analysis, some care was exercised in obtaining a stable ACh-induced end-plate current. One of the main problems here was the rapid onset of

desensitization that often occurred with a too focal placement of the iontophoretic electrode. Also, it was important not to exceed the low concentration limit for ACh (see later) - mean end-plate currents were usually never >100 nA.

The general experimental protocol was to record m.e.p.c.s and/or noise in normal toad Ringer at 15°C at a series of potentials in one cell, before changing temperature or introducing test solutions. Usually, data from paired cells was obtained (i.e. in both control and test solutions).

A typical example of ACh-induced end-plate current is shown in Fig. 2.2A and the associated fluctuations can be compared to a control baseline record (in the absence of agonist) in Fig. 2.2B.

Data Analysis

Initially, m.e.p.c.s were photographed with an oscilloscope camera (Nihon Kohden PC-2A) and measured after projection onto calibrated graph paper. Peak m.e.p.c. amplitude and 20-80% growth time were obtained directly and a semilogarithmic plot of the decay phase allowed calculation of τ_D, the time constant of decay. With tape recorded data, m.e.p.c.s were captured using the transient recorder and then transferred directly to a minicomputer (PDP8E, DEC). The growth phase (20-80% rise time, fitted by linear regression), peak amplitude and τ_D (85-5% decay phase slope obtained by linear regression of the logarithm of m.e.p.c. amplitude against time) were calculated for each m.e.p.c., along with correlation coefficients for the regression analysis. M.e.p.c.s were also averaged after normalizing amplitudes and here, the peak of m.e.p.c.s was used for synchronizing m.e.p.c.s. A more automated system was used later, and differed only in the acquisition of m.e.p.c.s. The analog-to-digital converter of a PDP 11-34 minicomputer (DEC) was set up with a circular buffer to sample at 50 or 100 μs per point. All m.e.p.c.s crossing a pre-set threshold were stored (with some preceding

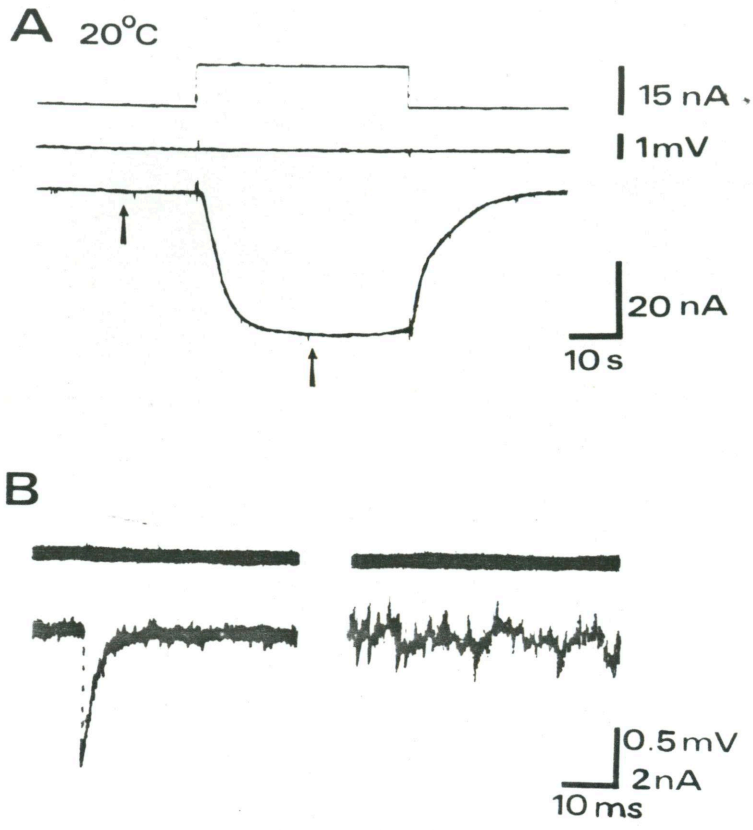

Figure 2.2. ACh-induced end-plate current noise. A. The increase in membrane current caused by iontophoresis of ACh (upper trace) can be seen in the lower trace (DC-coupled, recorded on a chart recorder). Downward deflections are m.e.p.c.s. The middle trace is the membrane voltage record. B. Upper traces are membrane voltage, lower traces are membrane current. Left hand panel shows a voltage-clamped m.e.p.c. and the baseline current noise level (in the absence of applied agonist). Right hand panel shows the increase in current fluctuations caused by the iontophoresis of ACh. The two records were obtained (arrows) from the cell shown above in A. Membrane potential, -100 mV; temperature, 20°C.

baseline; i.e. with negative delay). M.e.p.c.s were initially 'rough' edited automatically by the computer (using rise time and correlation to single exponential decay as criteria) and later, also edited manually by displaying captured m.e.p.c.s on a VDU (visual display unit; DEC VT55). As before, individual m.e.p.c. parameters were obtained and averaged, as well as normalized, averaged data.

Noise records stored on tape were filtered (2-pole cascaded Butterworth filter, 40 dB/decade roll-off, 800 Hz cutoff and later, using an8th order, elliptic filter; 160 dB/decade roll-off, ± 0.1 dB pass band ripple, adjustable cut-off) to prevent aliasing and were then digitalized at 2 kHz using the ADC of the PDP 11-34. A total of 8,192 or 16,384 data points were stored on RK05 disks in 512 point blocks (corresponding to 4 or 8 s of noise sampled at 2 kHz, in 16 or 32 blocks). In addition, 1 s of base line noise (in the absence of agonist) was stored. In order to exclude m.e.p.c.s and obvious artifacts, noise records were edited by displaying them in 250 ms segments on a graphics terminal (VT55) prior to transfer to disk. The variance of the stored noise blocks was calculated and averaged and spectral densities were determined by fast Fourier transformation. The data points in each block were reduced to differences from the mean and had a 0.1 cosine taper data window applied prior to transformation (Bendat & Piersol, 1971). The transformed base line noise was always subtracted from the agonist-induced noise before the final spectrum was calculated. Single-sided power density spectra (and standard errors) were determined from the ensemble average of 16 (or 32) transformed blocks. Spectral power values were calculated at 4 Hz intervals, and at higher frequencies, segment averages of adjacent values were determined at convenient frequencies.

The interpretation of the spectra obtained from the noise analysis

was based on the model and theory presented by Anderson & Stevens (1973; see also Katz & Miledi, 1972). A simple model of the underlying kinetics is :

$$nA + R \underset{k_{-1}}{\overset{k_1}{\rightleftharpoons}} A_nR \underset{\alpha}{\overset{\beta}{\rightleftharpoons}} A_nR^*$$

where n represents the number of agonist molecules, A, that must bind to the receptor, R before the channel can open. The closed agonist-receptor complex, A_nR undergoes a conformational change to the ionophore or open channel configuration, A_nR^*. The rate constants for the forward and backward agonist binding steps are k_1 and k_{-1} respectively, while β and α are the opening and closing rate constants. The power spectrum G(f) of ACh-induced current noise (resulting from fluctuations in the number of open channels) will have a single Lorentzian form:

$$G(f) = \frac{G(0)}{1+(2\pi f/\alpha)^2} \quad ,$$

where f is frequency, α is the closing rate constant and G(0) is the zero frequency asymptote. G(0) is defined for single-sided spectra as:

$$G(0) = 4\gamma \mu_i (V_m - \varepsilon_o)/\alpha \quad ,$$

where γ is the single channel conductance, μ_i is the mean ACh-induced current, V_m is the membrane potential, and ε_o is the null (or zero current) potential. Single Lorentzian curves were fitted to the transformed data points using G(0) and α as free parameters in a least squares search routine. Both G(f) and log G(f) values were used in the fitting process, and usually log G(f) values gave better 'eyeball' fits to the data although no statistical tests were applied. The single channel conductance, γ was calculated in two ways

$$\gamma_{psd} = \frac{G(0)\alpha}{4\mu_i (V_m - \varepsilon_o)}$$

and

$$\gamma_{var} = \frac{\sigma_i^2}{\mu_i (V_m - \varepsilon_o)} \quad ,$$

where σ_i^2 is the variance of the ACh-induced current fluctuations. (An equivalent method would be to find the area under the spectral density curve.) In practice, both methods gave excellent agreement, although γ_{var} was usually corrected for high-frequency loss using the correction factor $(2/\pi)\tan^{-1}(2\pi F\tau_N)$ where F is the filter cut-off frequency (see Colquhoun, Large & Rang, 1977). The single channel lifetime, τ_N was calculated as:

$$\tau_N = 1/\alpha = \frac{1}{2\pi f_{\frac{1}{2}}}$$

where $f_{\frac{1}{2}}$ is the frequency where G(0) was halved.

A number of assumptions apply to the interpretations outlined above: (1) the process under study is stationary, (2) agonist-induced noise and baseline (control) noise are independent of each other and can be subtracted, (3) open channels do not interact with each other, (4) each channel displays 2-state conductance behaviour, i.e. zero conductance when closed and a fixed conductance, γ when open, (5) the rate of the agonist binding reaction is very much faster than the subsequent, voltage-dependent conformational change (although formally, spectra are indistinguishable if the opposite is true; see Kordaš, 1969, 1972; Adams, 1976a, 1977a; Adams & Sakmann, 1978b) (6) the ACh concentration, [A] is constant, and sufficiently low so that only a very small fraction of the available channels (N) are open; thus N is essentially constant, and Poisson statistics apply, and it then follows that, (7) the open channel lifetime is exponentially distributed with a mean value of τ_N (see Magleby & Stevens, 1972a,b; Anderson & Stevens, 1973; Colquhoun & Hawkes, 1977; Neher & Stevens, 1977).

Recently, the elegant single channel patch clamp technique developed by Neher & Sakmann (1976a)has confirmed the 2-state conductance behaviour of ACh-activated channels (see Fig. 2.3A). It was also found that channel lifetimes were exponentially distributed (e.g. Neher & Sakmann,

1976a; but see Gration et al. (1981) who recently reported that glutamate channel lifetimes are concentration-dependent), although a better test of the low concentration limit (see assumptions 6 and 7 above) is the demonstration that σ_i^2 is linearly related to μ_i. In Fig. 2.3B, the variance of conductance fluctuations, σ_G^2 is plotted as a function of the mean conductance, μ_G for 3 different toad end-plates held at -90 mV. The slope of the regression line gives the single channel conductance, γ, which was 21.3 pS on average, for these 3 cells.

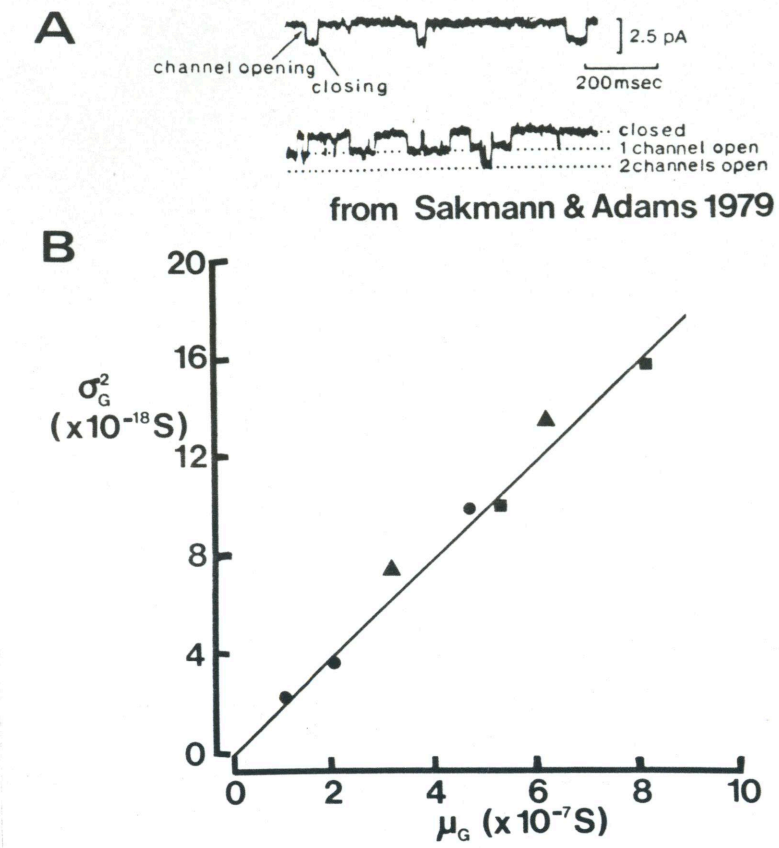

Figure 2.3. Evidence for some assumptions used in noise analysis. A. Two-state conductance behaviour of individual ACh-activated extra-junctional channels in denervated frog muscle. Single channel records were obtained with a Neher-Sakmann (1976a)patch clamp. Membrane potential, -120 mV; temprature, 8°C. Redrawn from Sakmann & Adams (1979). B. Variance of toad end-plate conductance fluctuations (σ_G^2) as a function of mean end-plate conductance increase (μ_G) induced by ACh. Data points are from 3 fibres voltage-clamped at -90 mV. The line fitted using linear regression passes through the origin and gives a single channel conductance (γ) of 21.3 pS. Mean values of γ calculated by the variance method and from power spectra were 20.2 ± 1.3 and 23.0 ± 1.8 pS, respectively. Temperature, 15°C.

CHAPTER THREE

EFFECTS OF AMMONIUM IONS ON END-PLATE CHANNELS

Introduction

Recent studies on the acetylcholine-activated channel at the amphibian motor end-plate have indicated that many simple chemicals and drugs can alter channel lifetime. Attempts to describe the physical nature of the ion permeation channel have revealed that channel lifetime is both voltage and temperature-sensitive (Anderson & Stevens, 1973) and that the nature of permeant cations affects both channel lifetime and conductance (Van Helden et al., 1977; Gage & Van Helden, 1979). Raising the divalent cation concentration prolongs the decay of miniature end-plate currents (Cohen & Van der Kloot, 1978), while lowering the extracellular pH has been reported to lengthen the decay of end-plate (Scuka, 1975) and miniature end-plate currents (Mallart & Molgó, 1978). Both of these effects have been attributed to a reduction in surface potential arising from screening of negative fixed surface charge (Van der Kloot & Cohen, 1979), although other divalent cations (e.g. zinc) also prolong channel lifetime in concentrations at which magnesium ions have no effect (Takeda, Datyner, Barry & Gage, 1978; See Chapter Four).

Earlier workers have shown that the acetylcholine channel at the end-plate is permeable not only to sodium, potassium and calcium ions (Takeuchi & Takeuchi, 1960; Takeuchi, 1963a,b) but also to a wide range of organic cations (e.g. Furukawa & Furukawa, 1959; Nastuk, 1959; Koketsu & Nishi, 1959; more recently, see also Maeno et al., 1977; Bregestovski et al., 1979; Dwyer et al., 1980; Adams et al., 1980). Classical approaches to the description of end-plate channel ion selectivity and concentration dependent behaviour have been shown to be largely unsatisfactory (Linder & Quastel, 1978; Lewis, 1979; Gage & Van Helden, 1979). The observation of the voltage dependence of single

channel conductance and the effects of the monovalent alkali cations on channel characteristics (Van Helden et al., 1979; Gage & Van Helden, 1979) have led to the proposal of a 'neutral site' channel model for the end-plate (Barry et al., 1979a,b). We were interested firstly, in obtaining more information about the molecular mechanisms determining effects of cations on channel conductance and lifetime, and secondly, in further testing the applicability of the neutral site channel model. Ammonium ions were investigated because they have a limiting equivalent conductivity in free solution similar to that of potassium ions, have the ability to form hydrogen bonds, unlike the alkali cations and also have the unusual property, like thallium ions, of being the only cations measurably permeant in both sodium and potassium channels of frog node of Ranvier and squid axon (for review, see Hille, 1975). We have found that substitution of NH_4Cl for extracellular NaCl increases channel conductance and lifetime.

Methods

The protocol for the experiments reported in this Chapter follows closely the detailed outline given in the General Methods and Materials (Chapter Two). Solutions in which ammonium ions were substituted for sodium ions were made by equimolar substitution of NH_4Cl (Merck, AR grade) for all the NaCl (NH_4 solution), or for half the NaCl (0.5 Na/0.5 NH_4Cl solution). The pH of these solutions was 6.9 to 7.1. In experiments where the pH was altered, HCl or NaOH (in Na solution) or NH_4OH (in NH_4 solution) were added to the HEPES-buffered solutions.

Measurements of single channel conductance (γ) were often made over a wide range of potentials in one cell, as illustrated in Fig. 3.1. It is true that, as the driving force decreases, the mean end-plate current also decreases (Fig. 3.1), so that the instrument plus background noise would represent a greater proportion of the total signal noise. However, this is very unlikely to lead to spuriously high estimates of γ close to the null potential because the baseline was always subtracted before the agonist-induced noise was analyzed, and large end-plate currents could be recorded on both sides of the null potential (Fig. 3.1).

In order to minimize cell to cell variability, conductance data were normalized relative to one potential (-50 mV, or in the case of the theoretical analyses, -70 mV) and the normalized data averaged. This resulted in two sets of errors arising from the raw data: relative S.E.M. for relative conductance values and absolute S.E.M. for the averaged absolute value of the conductance (measured experimentally at -50 mV). If for example, the relative conductance in Na-solution at -70 mV with respect to the -50 mV value was 0.915 ± 0.044 and the absolute value of conductance at -50 mV was 28.5 ± 1.63 pS, then the

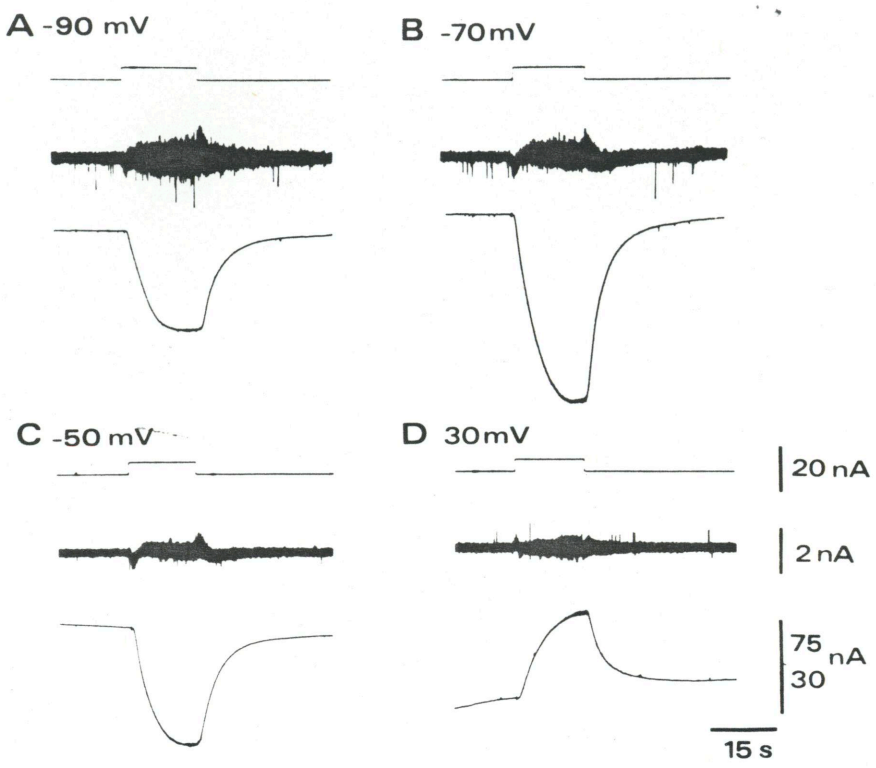

Figure 3.1. End-plate current fluctuations arising from iontophoresis of ACh in NH_4 solution, at -90, -70, -50 and 30 mV (A,B,C and D, respectively) in the same cell. In each of the four panels the upper trace is the iontophoretic current through the ACh electrode; the middle trace is the high-gain, AC-coupled record of the ACh-induced current fluctuations and the lower trace is the DC-coupled mean end-plate current. Note that the amplitude of the iontophoretic current was unchanged at each potential. Single channel conductance was 30.3, 34.9, 37.5 and 42.1 pS in A,B,C and D respectively. Temperature 15°C. Horizontal calibration 15 s, vertical 20 nA for ACh-iontophoretic current, 2 nA for AC-coupled noise, 75 nA (in A) and 30 nA (in B,C and D) for the DC-coupled mean end-plate current.

absolute conductance at -70 mV was calculated to 28.5 x 0.195 = 26.1 pS with relative S.E.M. given by 26.1 x 0.044/0.915 = 1.26. When the values normalized to -50 mV were now renormalized to -70 mV, for comparison with theoretical predictions, the relative S.E.M. of the conductance G_V, at another potential V, now became $G_V \times [(\bar{\sigma}_V/G_V)^2 + (1.26/26.1)^2]^{\frac{1}{2}}$ where $G_V \pm \bar{\sigma}_V$ is the value of the condutance (at that potential) ± the old relative S.E.M. (i.e. normalized to -50 mV). In the case of the -50 mV value, the old $\bar{\sigma}_V$ was zero. The errors considered so far have been for relative conductances in one particular cation solution. However, in order to compare conductance values in different solutions, it was necessary to correct for absolute errors. Since comparisons were done at -70 mV, the absolute error, $\bar{\sigma}_\gamma$, was calculated from the proportionate relative error at -70 mV (1.26/26.1) and the absolute proportionate error at -50 mV (1.63/28.5) to give $\bar{\sigma}_\gamma$ = $26.1\ [(1.26/26.1)^2 + (1.63/28.5)^2]^{\frac{1}{2}} = 2.0$, and thus, an absolute conductance value of 26.1 ± 2.0 pS. The effect of the S.E.M. of the null potential measurement was also allowed for in both the relative and absolute values to give the total S.E.M., $\bar{\sigma}_T$. In the case of the absolute conductance values for example, $\bar{\sigma}_T$ was calculated from

$$\bar{\sigma}_T = [(\bar{\sigma}_\gamma/G_V)^2 + (\bar{\sigma}_{\varepsilon_o}/(V-\varepsilon_o))^2]^{\frac{1}{2}}$$

where V = -70 mV and $\bar{\sigma}_{\varepsilon_o}$ is the S.E.M. of the null potential ε_o. In order to normalize conductances in NH_4 and 0.5 Na/0.5 NH_4 solutions with respect to the conductance in Na solution, a similar procedure was used to give corrected proportionate S.E.M.s, calculated as the square root of the sum of the squares of proportionate total absolute S.E.M.s (see also Barry et al., 1979a).

No explicit correction was made for changes in junction potentials occurring when ammonium solutions were introduced, as the calculated changes were small (≲0.8 mV). A more serious complication involves the

liquid junction potential between the microelectrode and the inside of the cell. This potential is not easily measurable and is difficult to calculate due to many unknown variables (e.g. intracellular anion conductance, mobility and activity of intracellular ions, nature of fixed charges in the cytoplasm, microelectrode tip potential; see also Cole & Moore, 1960; Barry & Diamond, 1970). However, preliminary calculations suggest that this junction potential $\lesssim 2$ mV, and would tend to make all the measured null potentials more negative. As no correction was made here, the absolute accuracy of the quantitative data presented in this study could be affected slightly. For example, making the null potentials 2 mV more negative would result in the equilibrium constants relative to potassium being reduced by less than 9% but the relative mobilities determined from the voltage sensitivity curve would essentially remain unchanged.

Results

End-plate regions of muscle fibres were localized by determining where a rapid depolarization was caused by iontophoretically applied ACh and by the presence of miniature end-plate potentials having fast rise times ($\lesssim$1 ms) and amplitudes of at least 0.5 mV (see Fig. 3.2). In normal solution miniature end-plate currents and ACh-induced current fluctuations (noise) were usually recorded at two or more potentials before changing to test solutions. Data from cells obtained only in ammonium-containing solutions always showed the same changes as were observed in paired cells (i.e. those from which data was recorded in both control and test solutions).

Miniature end-plate potentials and currents

When ammonium ions were substituted for sodium ions, the amplitude of m.e.p.c.s increased and their decay became slower. Similarly, miniature end-plate potentials (m.e.p.p.s) showed increases in both peak amplitude and time course of decay. In Fig. 3.2, simultaneous intracellularly-recorded m.e.p.p.s and extracellularly-recorded m.e.p.c.s are shown for the same cell in both control (Na) solution and in NH_4 solution. These effects were evident within 5 min of changing solutions. (The bath change-over time was kept slow so that cells could be readily held through solution changes.) As previously noted (Furukawa et al., 1957), m.e.p.c. frequency increased greatly, and after 40-50 min declined to almost normal levels (presumably due to depletion of transmitter). In Fig. 3.3A, an average of 20 m.e.p.c.s in the normal solution (Na solution) is shown on the left. The mean peak m.e.p.c. amplitude was 2.3 nA and the decay was exponential with a time constant of decay of 2.8 ms (clamp potential -50 mV, temperature 15°C). After 45 min in a solution containing NH_4Cl substituted for NaCl (NH_4 solution) the average peak amplitude of 20 m.e.p.c.s (recorded in the same cell at the same clamp

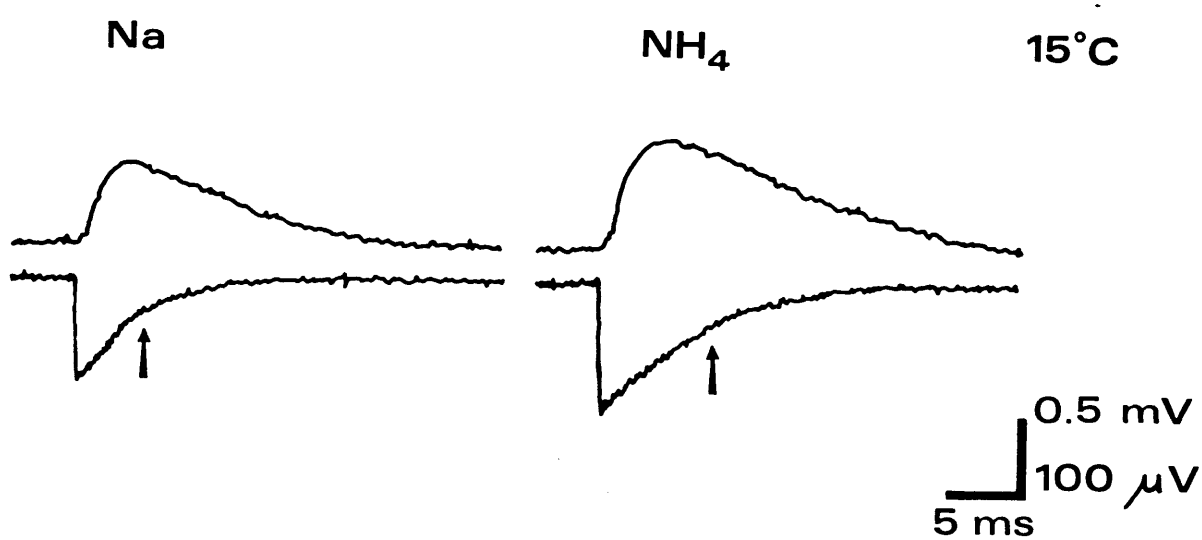

Figure 3.2 The effect of ammonium ions on m.e.p.p.s and m.e.p.c.s. Simultaneous intracellular (upper traces) and extracellular (lower traces) recording in control (Na) solution, and after 4 min in NH_4 solution. M.e.p.c. time constants of decay (τ_D; arrows) were 3.9 and 7.1 ms in Na and NH_4 solutions, respectively. The increase in m.e.p.p. amplitude in NH_4 solution results from both an increase in τ_D and an increase in m.e.p.c. peak amplitude. Vertical calibration: 0.5 mV for m.e.p.p.s, and 100 μV for m.e.p.c.s; horizontal calibration: 5 ms.

potential and temperature) was 3.2 nA. The decay of the average m.e.p.c. remained exponential as shown in the semilog plot of normalized current versus time in Fig. 3.3B (squares) and the time constant of decay increased to 5.0 ms.

Null potential

An increase in m.e.p.c. amplitude could be caused by a shift in the acetylcholine null potential to a more positive value. In fact, a positive shift was seen, but it was insufficient to account for more than a small fraction of the increase in m.e.p.c. amplitude. This is illustrated in Fig. 3.4A in which mean peak m.e.p.c. amplitude (I_p) is plotted against membrane potential. It can be seen that in Na solution (results from 12 fibres) the null potential was -3 mV whereas the null potential in NH_4 solution was 7 mV (results from 8 fibres). The estimate of null potential for m.e.p.c.s suffers from the limitation of a deteriorating signal-to-noise ratio at potentials close to the null potential. Therefore the null potential was also measured by determining the potential at which iontophoretic application of ACh generated no change in clamp current. The null potential determined in this way was -2.8 ± 0.8 mV (mean ± 1 S.E.M.) in Na solution (6 fibres) and 6.5 ± 1.3 mV in NH_4 solution (3 fibres).

However, this shift in null potential is obviously insufficient to account for the increase in m.e.p.c. amplitude in NH_4 solution. When peak m.e.p.c. amplitude was divided by $(V_m-\varepsilon_o)$, where V_m is the membrane potential and ε_o is the null potential, to give the peak conductance G_p, the value in Na solution was less than in NH_4 solution over a wide range of potentials (Fig. 3.4B, see also Table 3.1). As $G_p = n\gamma$, where n is the number of channels open at the peak of an m.e.p.c. and γ is the conductance of each channel, it seemed that either γ was increased or that the number of channels activated by a quantum of ACh was increased in NH_4

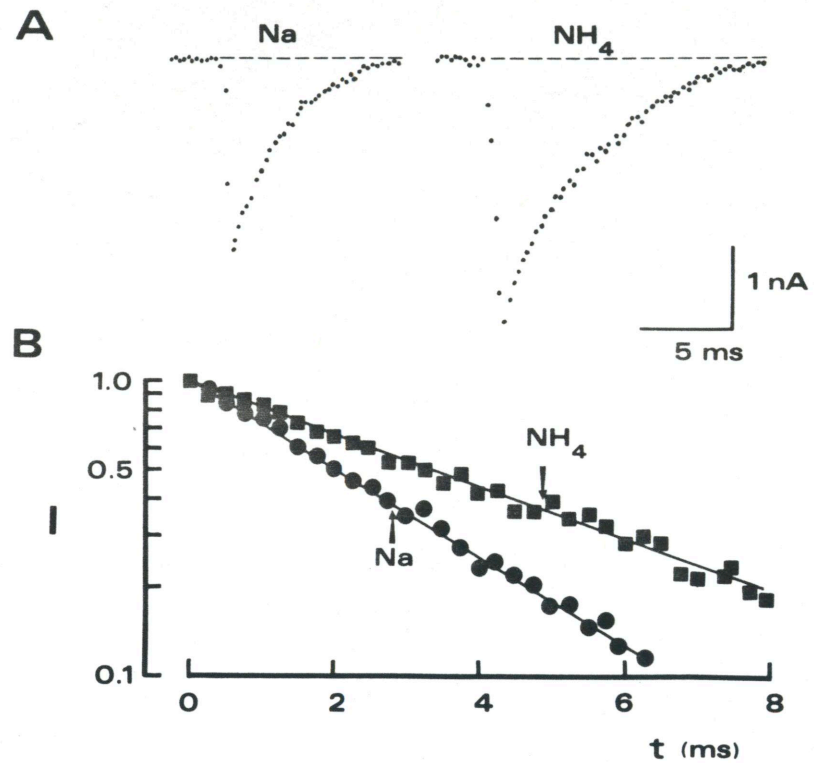

Figure 3.3. Voltage-clamped m.e.p.c.s in Na and NH_4 solutions. A. Averaged m.e.p.c.s (n=20) recorded at the same end-plate in Na solution and 45 min later in NH_4 solution. Clamp potential -50 mV, temperature 15°C. Horizontal calibration 5 ms, vertical 1 nA. B. The averaged m.e.p.c.s shown in A were normalized and their decay plotted semilogarithmically against time. M.e.p.c.s decayed exponentially with a single time constant (τ_D). In Na solution (●) τ_D was 2.8 ms. In NH_4 solution (■) τ_D was 5.0 ms (arrows).

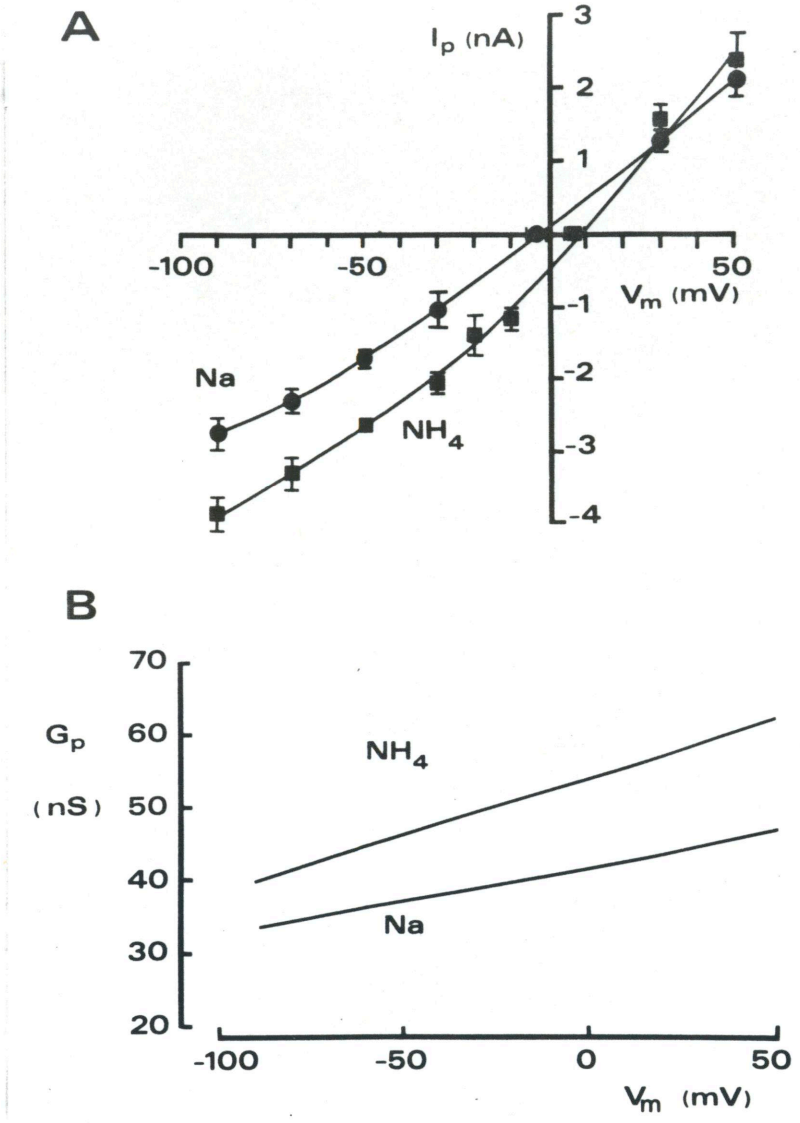

Figure 3.4. The effect of membrane potential on the peak amplitude (I_p) and peak conductance (G_p) of m.e.p.c.s. A. Averaged peak m.e.p.c. amplitudes plotted as a function of clamp potential for Na solution (● , 12 fibres) and for NH_4 solution (■ , 8 fibres). Error bars indicate ± 1 S.E.M. Curves were drawn by eye through the data points. Zero-current potentials plotted on the abscissa were determined from ACh-iontophoresis for Na solution, and from both ACh-iontophoresis and m.e.p.c. reversal for NH_4 solution. Temperature 15°C. B. Peak m.e.p.c. conductance-voltage relationship in Na (lower curve) and in NH_4 (upper curve) solutions. The curves were obtained from the I_p-voltage curves shown in A.

solution. In order to distinguish between these two possibilities, noise analysis (Katz & Miledi, 1970; Anderson & Stevens, 1973) was used to measure γ.

Channel characteristics

Mean end-plate current (μ_i) and current fluctuations in response to iontophoresis of ACh were increased in NH_4 solution. Noise data were usually obtained after 45 to 50 min in NH_4 solution. The increase in current fluctuations can be seen in Fig. 3.5A. The trace on the left shows the response to an iontophoretic current of 19 nA through the ACh electrode in Na solution while the trace on the right shows the response to an iontophoretic current of 9 nA in NH_4 solution in the same cell. The traces also show the characteristic increase in m.e.p.c. frequency in NH_4 solution (Furukawa et al., 1957).

Power spectral density curves of such current fluctuations in Na solution (circles) and in NH_4 solution (squares) were both well-fitted by single Lorentzians as shown in Fig. 3.5B. It can be seen that the half-power frequency (arrows) shifted to a lower frequency in NH_4 solution indicating that average channel lifetime was increased. Single channel conductance, whether calculated from the variance-to-mean ratio of end-plate current [γ(var.)], or from power spectra [γ(p.s.d.)] was found to be increased in NH_4 solution. Values of γ measured in several experiments are given in Table 3.1.

Half sodium/half ammonium solution

Characteristics of m.e.p.c.s and single channels were measured in solutions in which half the NaCl had been replaced with NH_4Cl (0.5 Na/ 0.5 NH_4 solution) in order to examine any possible sodium-ammonium ion interactions. Peak m.e.p.c. amplitude and τ_D were increased in this solution, but not as much as in NH_4 solution. The null potential determined using ACh iontophoresis shifted to 0.9 ± 1.6 mV (n=3), while

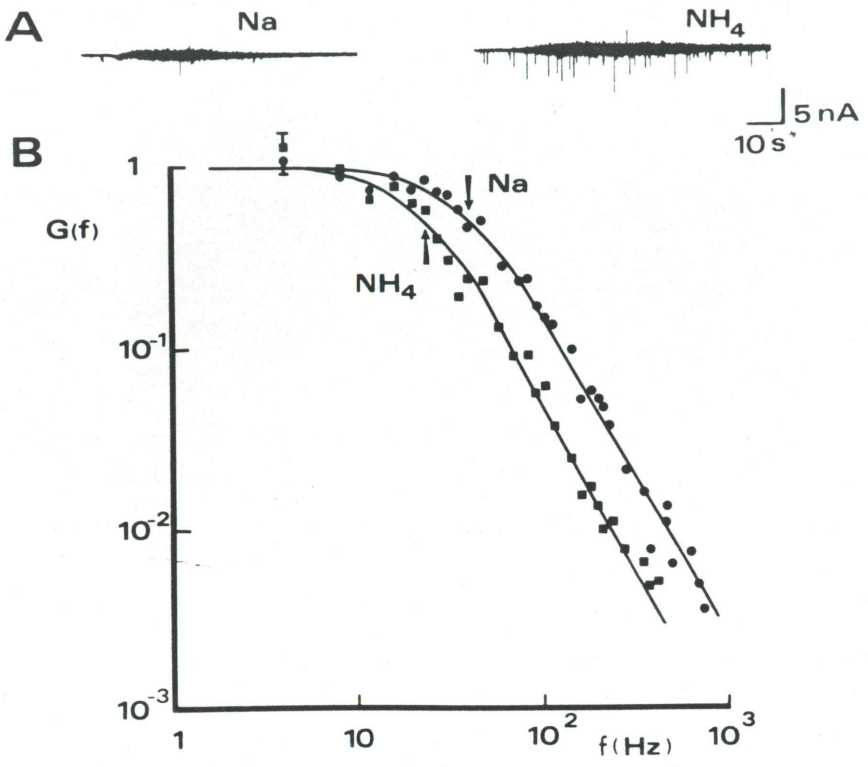

Figure 3.5. Channel lifetime and conductance are increased in NH_4 solution. A. End-plate current fluctuations evoked by ACh-iontophoresis in Na solution, and 50 min later in NH_4 solution at the same end-plate. Inward current is downwards. The large upward deflection is an artifact caused by switching off ACh-iontophoretic current, which was 19 nA in Na and 9 nA in NH_4 solution (backing current 5 nA). Note increase in m.e.p.c. frequency in NH_4 solution. Pen recorder bandwidth was 1.6 to 125 Hz. Membrane potential -70 mV, temperature 15°C. Horizontal calibration 10 s, vertical 5 nA. B. Normalized power spectra of the ACh-induced current fluctuations. The lines show the best (least squares) fits to single Lorentzian curves. Half-power frequencies (arrows) of 40 Hz in Na solution (•) and 22.5 Hz in NH_4 solution (■) gave mean channel lifetimes of 3.98 and 7.04 ms respectively. Asymptotic spectral densities were 2.05×10^{-21} and 4.04×10^{-21} A^2s for corresponding steady end-plate currents of 68 nA in Na solution and 55 nA in NH_4 solution. Single channel conductances determined in this case from power spectra [γ(p.s.d.)] were 28.3 pS and 33.0 pS respectively, while channel conductances determined from the current variance to mean ratio [γ(var.)] were 27.4 pS and 34.4 pS respectively for Na and NH_4 solutions. Note logarithmic axes. Error bars at 4 Hz indicate 1 S.E.M.

Table 3.1. Mean peak conductance during m.e.p.c.s (G_p) and mean channel conductance (γ) in Na, NH_4 and 0.5 Na/0.5 NH_4 solutions. Results are shown as mean ± S.E.M. appropriately corrected for the normalization procedure, with the number of fibres in parentheses. Values of γ(p.s.d.) were not significantly different from γ(var.) estimates, following correction for filtering. Temperature 15°C. The statistical significance of the increase in channel conductance (γ) in each of the solutions over the two voltages was calculated using the relative S.E.M. (e.g. see Table 3.5 for NH_4 values) rather than the absolute S.E.M. The superscripts *, **, and ***, given in the table imply that the increases in γ(p.s.d.) were significant with $P<0.1$, <0.025 and 0.005 respectively (Student's t test).

Solution	G_p (nS)		γ(p.s.d.) (pS)	
	-90 mV	50 mV	-90 mV	30 mV
Na	33 ± 3 (6)	45 ± 4 (5)	25.0 ± 2.3 (8)	35.1 ± 3.4 (4)**
NH_4	40 ± 2 (8)	54 ± 3 (4)	32.2 ± 2.1 (3)	40.9 ± 3.9 (3)*
0.5Na/0.5NH_4	35 ± 2 (9)	47 ± 3 (4)	31.5 ± 2.1 (9)	42.0 ± 4.0 (7)***

the interpolated value using averaged m.e.p.c. data was 1.5 mV. Single channel conductance data are given in Table 3.1 (see also Fig. 3.7).

Effect of membrane potential

Measurements of the time constant of decay of m.e.p.c.s (τ_D) recorded over a range of membrane potentials in a number of experiments are shown in Fig. 3.6A. In NH_4 solution (squares), a consistent increase in τ_D was seen. The slope of the exponential relationship between τ_D and membrane potential was not changed in NH_4 solution. The regression lines shown are described (Magleby & Stevens, 1972b;Anderson & Stevens, 1973; Gage & McBurney, 1975) by the equation

$$\tau(V) = \tau(0)\exp(-V/H)$$

where $\tau(V)$ is the average channel lifetime at membrane potential V, $\tau(0)$ is the average channel lifetime at zero membrane potential and H is the membrane potential change required for an e-fold change in τ. Similarly, average channel lifetimes measured from power spectra of ACh-induced current fluctuations (τ_N) were greater in NH_4 solution (squares) than in Na solution (Fig. 3.6B). It was also clear that the voltage-sensitivity of τ_N had not changed significantly in NH_4 solution. In 0.5 Na/0.5 NH_4 solution, both τ_N and τ_D were slightly greater than in Na solution, while the voltage-sensitivity was again unchanged. Values of $\tau(0)$ and H obtained from m.e.p.c.s and from noise analysis in Na, NH_4 and 0.5 Na/ 0.5 NH_4 solutions are listed in Table 3.2.

In NH_4 solution, the conductance change at the peak of m.e.p.c.s (G_p) was always larger than in Na solution. It was also apparent that G_p increased at depolarized potentials both in Na solution and in NH_4 solution (see Fig. 3.4B). Similarly, single channel conductance (γ) obtained from noise analysis was greater in NH_4 solution than in Na solution, and a slight increase in γ with membrane depolarization was observed (Fig. 3.7). This potential-dependent change in γ, which has been

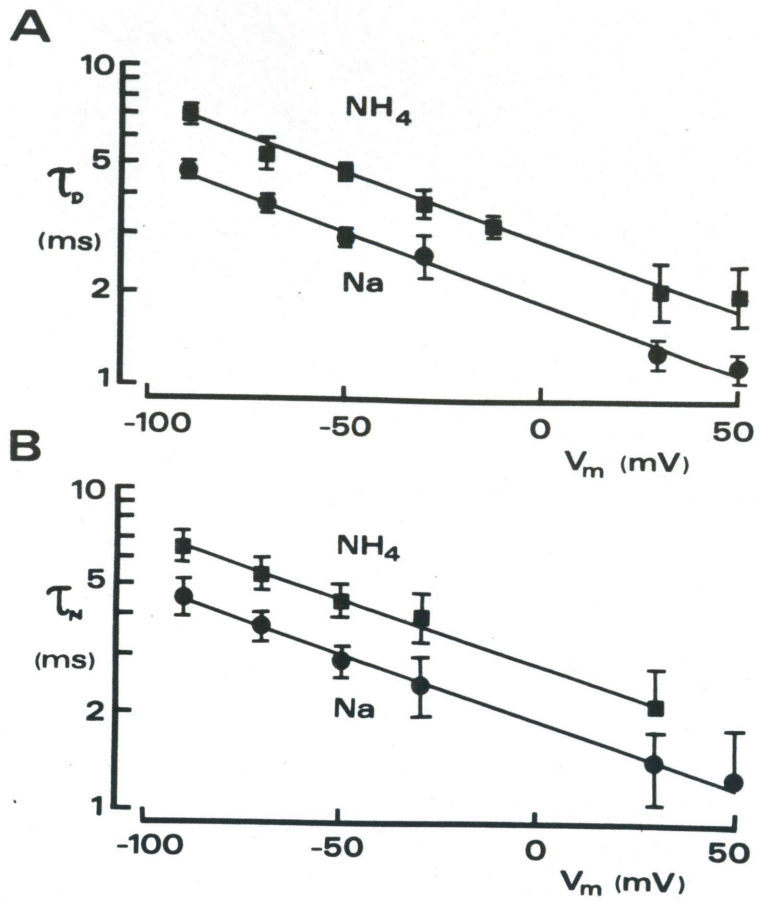

Figure 3.6. The effect of membrane potential on m.e.p.c. time constant of decay (τ_D) and on channel lifetime (τ_N). A. Voltage sensitivity of τ_D in Na solution (●, 12 experiments) and in NH_4 solution (■, 8 experiments). Each data point is the mean ± 1 S.E.M. of at least 45 m.e.p.c.s measured from a minimum of 3 cells. From the relationship $\tau(V) = \tau(0)\exp(-V/H)$, H values determined by linear regression were 102 mV for Na solution and 115 mV for NH_4 solution. B. Voltage sensitivity of τ_N in Na solution (●, 12 experiments) and in NH_4 solution (■, 7 experiments). Data points are mean ± 1 S.E.M. from at least 3 cells. H values for τ_N were 110 mV in Na solution and 128 mV in NH_4 solution. Temperature 15°C.

Table 3.2. Voltage sensitivity of m.e.p.c. time constant of decay (τ_D) and of channel lifetime (τ_N) in sodium and ammonium solutions. From linear regression lines fitted to the ln τ values as a function of V, $\tau(0)$ and H values were obtained using the equation $\tau(V) = \tau(0)\exp(-V/H)$. Results are presented as mean ± S.E.M. with the number of fibres in parentheses, (correlation coefficient, $\bar{r}$). Temperature, 15°C.

Solution	H(mV)		$\tau(0)$ (ms)		$\bar{r}$	
	M.e.p.c.	Channel	M.e.p.c.	Channel	M.e.p.c.	Channel
Na	103±9 (12)	110±7 (12)	1.9±.2	2.0±.1	-.99	-.98
NH_4	115±14 (8)	128±16 (7)	3.0±.3	3.1±.3	-.98	-.99
$0.5Na/0.5NH_4$	109±10(11)	117±12 (12)	2.7±.2	2.5±.3	-.98	-.99

previously reported for Na solution (Van Helden et al., 1979; Gage & Van Helden, 1979), was also quite clear in NH_4 solution. In 0.5 Na/ 0.5 NH_4 solution, γ values (Fig. 3.7, triangles) lay between those in Na and in NH_4 solution and had similar voltage-sensitivity (see also Table 3.1).

Net ion movements

In previous experiments in which monovalent alkali cations were substituted for sodium ions it was found that changes in both channel lifetime and the time constant of decay of m.e.p.c.s were accompanied by reciprocal changes in channel conductance and peak m.e.p.c. conductance respectively, so that charge transfer through a channel or during a m.e.p.c. tended to remain constant (Van Helden et al., 1977; Gage & Van Helden, 1979). Clearly this was not so with ammonium ions. Graphs of charge transfer during m.e.p.c.s ($Q_m = I_p \cdot \tau_D$) and through a single channel ($Q_c = \tau_N \cdot \gamma \cdot (V_m - \varepsilon_o)$) are shown over a range of potentials for Na solution (circles) and NH_4 solution (squares) in Fig. 3.8. Charge transfer both during a m.e.p.c and through a single channel was greater in NH_4 solution than in Na solution. Values of Q_m and Q_c in 0.5 Na/0.5 NH_4 solution were greater than in Na solution but were less than those measured in NH_4 solution (see Table 3.3).

Possible effects of pH

In ammonium solutions at pH ~6.9-7.1, a small proportion of ammonia will be present (assuming that the pK_a of ammonium ions ~9.5, Boron & De Weer, 1976). In squid axons and snail neurones, low concentrations (~10 mM) of ammonium ions cause rapid and reversible intracellular pH transients and these alkalinisations have been attributed to high ammonia fluxes followed by protonation to ammonium ions (Boron & De Weer, 1976; Thomas, 1976). Since pH effects on surface charge potentials are well-known (see e.g. Hille, Woodhull & Shapiro, 1975; Van der Kloot & Cohen,

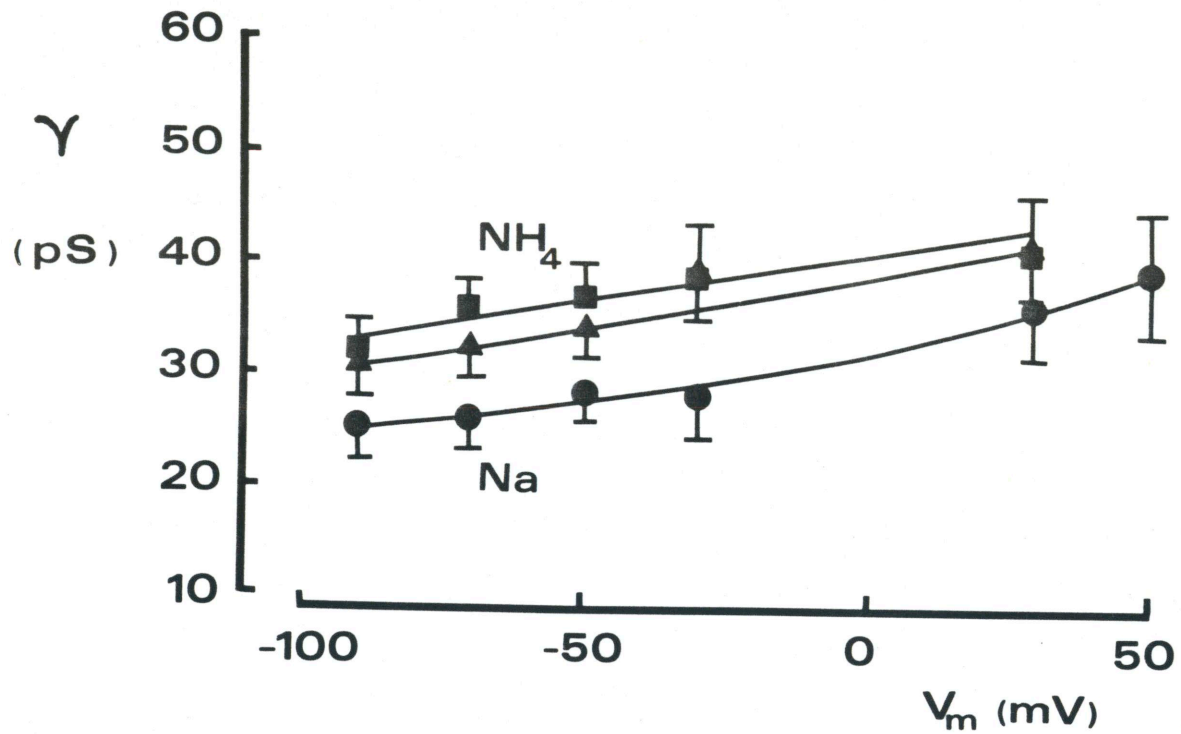

Figure 3.7. Voltage sensitivity of single channel conductance, γ. Curves were drawn by eye through the data points. Error bars for -50 mV data indicate 1 S.E.M.; in the other cases they represent the S.E.M. of the normalised conductance relative to the -50 mV value (see Methods). Each data point represents 3 to 12 estimates of γ(p.s.d.); Na solution (●, 12 fibres), NH_4 solution (■, 7 fibres), 0.5 Na/0.5 NH_4 solution (▲, 12 fibres). Temperature, 15°C.

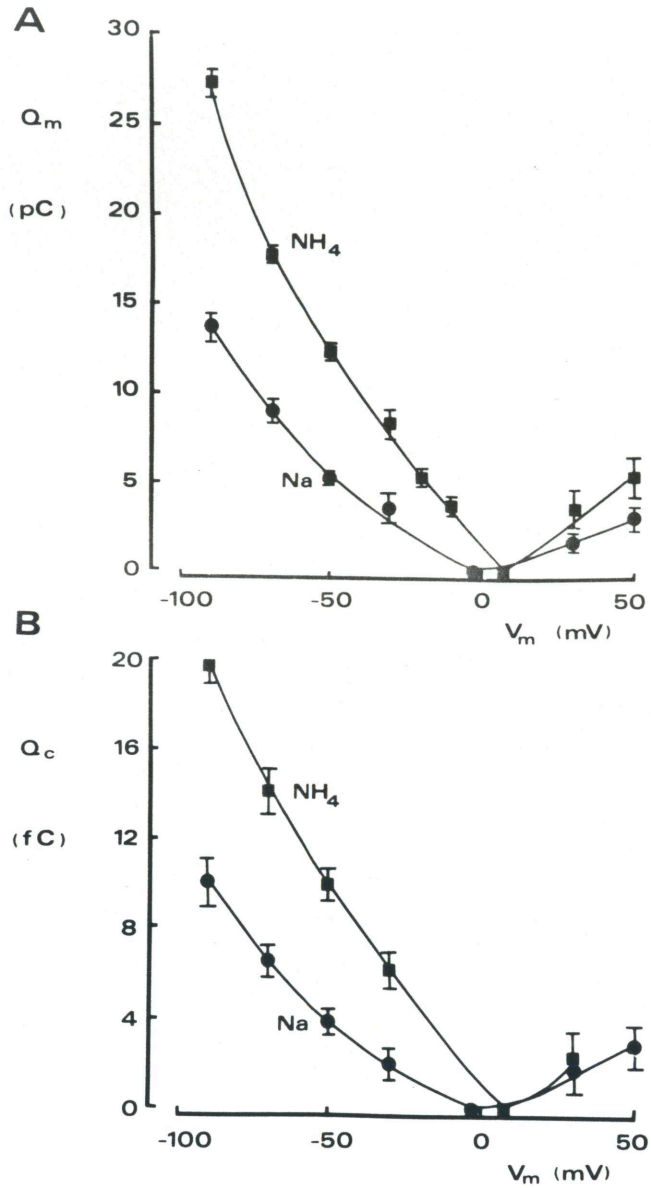

Figure 3.8. The effect of membrane potential on charge transfer during m.e.p.c.s (Q_m) and through a single channel (Q_c). A. Net ion movement for m.e.p.c.s in NH_4 solution (■, 8 fibres) was greater than in Na solution (●, 12 fibres). The curves were drawn by eye. Error bars indicate ± 1 S.E.M. B. Similarly net ion movement through a single channel in NH_4 solution (■, 7 fibres) was consistently greater than in Na solution (●, 12 fibres). Temperature 15°C.

Table 3.3. Net charge transfer during a m.e.p.c. (Q_m) or through a single channel (Q_c) in sodium and ammonium solutions at 15°C. Results are shown as mean ± S.E.M. with the number of fibres in parentheses.

Solution	Q_m (pC)		Q_c (fC)	
	-90 mV	50 mV	-90 mV	30 mV
Na	13.5±1.8 (6)	2.7±1.0 (5)	10.5±1.6 (8)	1.6±.6 (4)
NH_4	27.5±2.7 (8)	5.1±1.3 (3)	19.9±1.9 (3)	2.0±.4 (3)
$0.5Na/0.5NH_4$	17.9±2.5 (9)	3.3±1.2 (4)	15.4±1.8 (9)	2.1±.3 (7)

1979), and lowering the pH has been reported to lengthen the decay of e.p.c.s and m.e.p.c.s at frog end-plate (Scuka, 1975; Mallart & Molgó, 1978), we examined the effects of changing pH in Na solution. In a preliminary series of experiments, no large effects were found on the time constant of decay of m.e.p.c.s over the pH range 4-10. In 4 cells at pH 4, τ_D was 1.11±0.06 times the value at pH 7.1, while in 3 cells at pH 10 τ_D was 0.95±0.04 times the control value. As reported by Mallart & Molgó (1978), m.e.p.c. amplitude was unchanged over the pH range 4-10. Recently, similar observations have been made independently[1]. In one experiment, channel conductance and lifetime at -50 mV were obtained from noise analysis in Na solution at pH 5, and were not significantly different from values measured at pH 7. Attempts to modify the proportion of ammonia in NH_4 solution were made by raising the pH to 8.0, and m.e.p.c.s were not different from those seen in NH_4 solution at pH 7. We conclude that any long term effects of intracellular pH changes in ammonium solutions probably did not contribute greatly to the observations of increased channel conductance and lifetime. Furthermore, it is unlikely that significant accumulation of ammonium ions had occurred because even after long periods (>4 hr) in NH_4 solution, m.e.p.c. amplitude was always greater than in Na solution.

Replacement of $CaCl_2$ with $BaCl_2$

Activation of postsynaptic channels by ACh in an aplysia neurone can result in the development of late potassium current, presumably turned on by an influx of calcium ions (Ascher et al., 1978). The presence of a secondary calcium-activated potassium current could lead to overestimates of not only the null potential but also of single channel conductance. Replacement of extracellular calcium with cobalt or barium ions has been reported to block outward potassium currents in aplysia (Ascher et al.,

[1]Hamill, O.P., personal communication

1978; Adams, 1978). In two experiments, we found no significant change in the null potential in Na solution, when extracellular $CaCl_2$ was replaced with $BaCl_2$.

Discussion

It is clear from the results that when sodium ions are replaced by ammonium ions, the peak amplitude and time constant of decay of m.e.p.c.s are increased. The greater amplitude of m.e.p.c.s could not be explained by the shift in null potential seen in ammonium solutions, but is best accounted for by the observation of an increased single channel conductance. Increases in end-plate channel conductance have been recently reported when sodium ions are replaced by both caesium and potassium ions (Gage & Van Helden, 1979). Similarly, when sodium ions are replaced with caesium ions in an aplysia neurone, ACh-activated single channel conductance is increased, as is channel lifetime (Ascher et al., 1978). In lipid bilayers, gramicidin A channel conductance is also increased when caesium replaces sodium ions (Kolb & Bamberg, 1977). The increased channel conductance in ammonium solutions (compared to Na solution) is consistent with the observation that $P_{NH_4} > P_{Na}$, as is evident from the null potential measurements. For channel conductances estimated from noise analysis, we have assumed that all the current flowed through ACh-activated end-plate channels, and that secondary currents like the late calcium-activated potassium currents seen in aplysia (Ascher et al., 1978) were not present. Ammonium ions passing through open end-plate channels may turn on other currents through the muscle membrane, but the increased peak m.e.p.c. amplitude (assuming the number of channels activated is constant) in ammonium solutions and the high resting ammonium permeability of the muscle membrane (judging from the depolarizing action of ammonium ions) argue against this possibility.

Previously, it has been reported (Van Helden et al., 1977; Gage & Van Helden, 1979) that, for the alkali cations, channel lifetime and conductance appeared to be reciprocally related, so that charge transfer through a channel or during a m.e.p.c. tended to remain constant. Clearly,

this was not so for ammonium solutions. It is interesting to note that neither the voltage dependence of channel conductance nor the voltage dependence of channel lifetime was greatly different in ammonium solutions. If channel lifetime is determined by 'electrostatic stabilization' of the open conformation while an ion is bound to a site, then ions having high site affinities might tend to keep the channel open longer (see Kolb & Bamberg, 1977; Gage & Van Helden, 1979). Alternatively, ammonium ions hydrogen bonding to inter-site ligands may make the open conformation more favoured, and thus prolong channel lifetime.

From the known permeability of several large organic cations, the acetylcholine-activated channel at the end-plate could be thought of as a large, aqueous pore. However, the apparent absence of chloride permeability (Takeuchi & Takeuchi, 1960) strongly suggests the presence of at least one high resistance barrier to anions. There have been several recent studies on end-plate ion selectivity. For example, selectivity sequences for single channel conductance and null potential have been obtained for the alkali cations lithium, sodium, potassium and caesium (Van Helden et al., 1977; Gage & Van Helden, 1979). P_{NH_4}/P_{Na} values of 1.79 (Dwyer et al., 1979), ~1.1 (Linder & Quastel, 1978) and ~1.0 (Maeno et al., 1977) have been reported, which compare with the value 1.47 found in this study. Apart from the possible species difference, it should be noted that dissimilar techniques have been used to obtain the results. The relative permeability ratios obtained from null potential shifts can be predicted by not only the Goldman-Hodgkin-Katz equation (Goldman, 1943; Hodgkin & Katz, 1949) but also by both the neutral site and the charged site models (Barry et al., 1979a). However, it has been previously shown that single channel conductance is voltage dependent and that the nature of the alkali cation influences the voltage sensitivity of conductance (Van Helden et al., 1977; Van Helden et al., 1979; Gage & Van Helden, 1979). These observations together with

the concentration dependence of conductance can be predicted adequately only by the neutral site channel model (Barry et al., 1979a,b).

Neutral Site Channel Model

The model was based on the assumption that the channel length was much greater than the Debye length within it, and that there was at least one high resistance barrier for anions. The sites lining the channel were considered to be represented by the negative ends of polar groups and the analysis suggested that these sites were high field strength sites (Barry et al., 1979a).

We were interested in seeing whether single channel conductance measured in the presence of an 'organic' cation such as ammonium also fitted the predictions of the neutral site channel model or whether the hydrogen bonding capacity of the ammonium ion caused deviations from the model. The same technique of fitting the data was used here as reported before in detail (Barry et al., 1979a). The relative permeabilities P_{NH_4}/P_K and P_{Na}/P_K were obtained from measurements of the null potential ε_o, which was given by:

$$\varepsilon_o = \frac{RT}{F} \ln \left\{ \frac{[K]_o + (P_{Na}/P_K)\,[Na]_o + (P_{NH_4}/P_K)\,[NH_4]_o}{[K]_i + (P_{Na}/P_K)\,[Na]_i + (P_{NH_4}/P_K)\,[NH_4]_i} \right\} . \qquad (1)$$

In the absence of any significant anion permeation this equation is very similar in form to the Goldman-Hodgkin-Katz equation, where R, T and F have their usual significance. However, in the equation for the neutral site channel the relative permeability terms can be separated into two components: relative partition coefficients (K_{NH_4}/K_K) or equilibrium constants and relative mobilities (u_{NH_4}/u_K), which are related by:

$$\frac{P_{NH_4}}{P_K} = \frac{u_{NH_4}}{u_K} \cdot \frac{K_{NH_4}}{K_K} . \qquad (2)$$

Relative permeabilities were calculated from the null potential measurements using equation (1), but the individual relative mobility and

partition coefficient terms could not be determined separately from the null potentials alone. Nevertheless different combinations of relative mobilities and partition coefficients predicted by both neutral and charged site models did give rise to very different degrees of voltage sensitivity of conductance. Hence a given degree of voltage sensitivity implies a unique combination of relative mobilities and partition coefficients. The equation for single channel conductance γ is

$$\gamma = i/(V_m - \varepsilon_o) \tag{3}$$

where the single channel current i, is given by

$$i = B_1 \frac{\xi U'' - U'}{\xi C'' - C'} \quad (V_m - \varepsilon^*) \tag{4}$$

and

$$\xi = \exp\ (V_m F/RT) \tag{5}$$

$$U' = \sum_j u_j K_j a'_j \tag{6}$$

$$C' = \sum_j K_j a'_j \quad . \tag{7}$$

The summation is over all j, where j represents each of the cations sodium, potassium and ammonium. Superscript ' refers to the external solution and a is the activity of the cation. A similar set of equations arises for U" and C" where the superscript " now refers to the internal solution. ε^* is defined by

$$\varepsilon^* = \frac{RT}{F} \ln\ (C'/C") \ .$$

B_1 is a factor defined elsewhere (Barry et al., 1979a) and is dependent on both cation and anion concentrations and their partition coefficients, but is independent of their mobilities and the membrane potential.

The above procedure for obtaining permeation parameters is illustrated for NH_4 solution in Fig. 3.9A in which experimental values of single channel conductance plotted as a function of membrane potential are compared with neutral site channel predictions. Since a small concentration of sodium ions was present in NH_4 solution (see Methods)

and within the cell (assumed to be about 10 mM) it was necessary to use sodium parameters in these calculations. Initially, values of $K_{Na}/K_K = 2$ and $u_{Na}/u_K = 0.57$ (Barry et al., 1979a) based on the null potential and the voltage sensitivity measurements of Gage & Van Helden (1979) were used, although with so little sodium present, the curves were very insensitive to the particular value of K_{Na}/K_K chosen. A K_{NH_4}/K_K value of about 4 (with $u_{NH_4}/u_K = 0.42$) was considered to provide the best fit to the experimental data, although the value of 3 (with $u_{NH_4}/u_K = 0.56$) gave only a marginally worse fit.

From the null potential measurements in NH_4 and Na solutions, the predicted null potential in 0.5 Na/0.5 NH_4 solution is $2.3^{+0.4}_{-0.6}$ mV. This value is independent of the particular combination of mobilities and partition coefficients used and agrees within experimental error with the measured null potential of 0.9 ± 1.6 mV. Using the parameters that provided the best fit to the data in Fig. 3.9A, relative single channel conductance values were predicted and compared with those measured experimentally in 0.5 Na/0.5 NH_4 solution and the results are shown in Fig. 3.9B. In addition, the predicted curve for a higher K_{Na}/K_K of 4 is shown. This value was slightly more compatible with the Na solution data obtained here, although in view of the standard errors it was not significantly different from the value obtained previously (Barry et al., 1979a). Using these parameters and allowing for a range of uncertainty in K_{Na}/K_K the predicted absolute single channel conductances in NH_4 and 0.5 Na/0.5 NH_4 solutions at -70 mV (relative to the value in Na solution) were calculated and are compared with the experimental values in Table 3.4. Overall, a value of K_{NH_4}/K_K between 3 and 4 provided the best fit for both the absolute conductance data and for the voltage sensitivity data and suggest that $K_{NH_4} \gtrsim K_{Na} > K_K$.

For the four alkali cations in the previous study (Barry et al., 1979a,b), the product of the relative partitiion coefficient and mobility

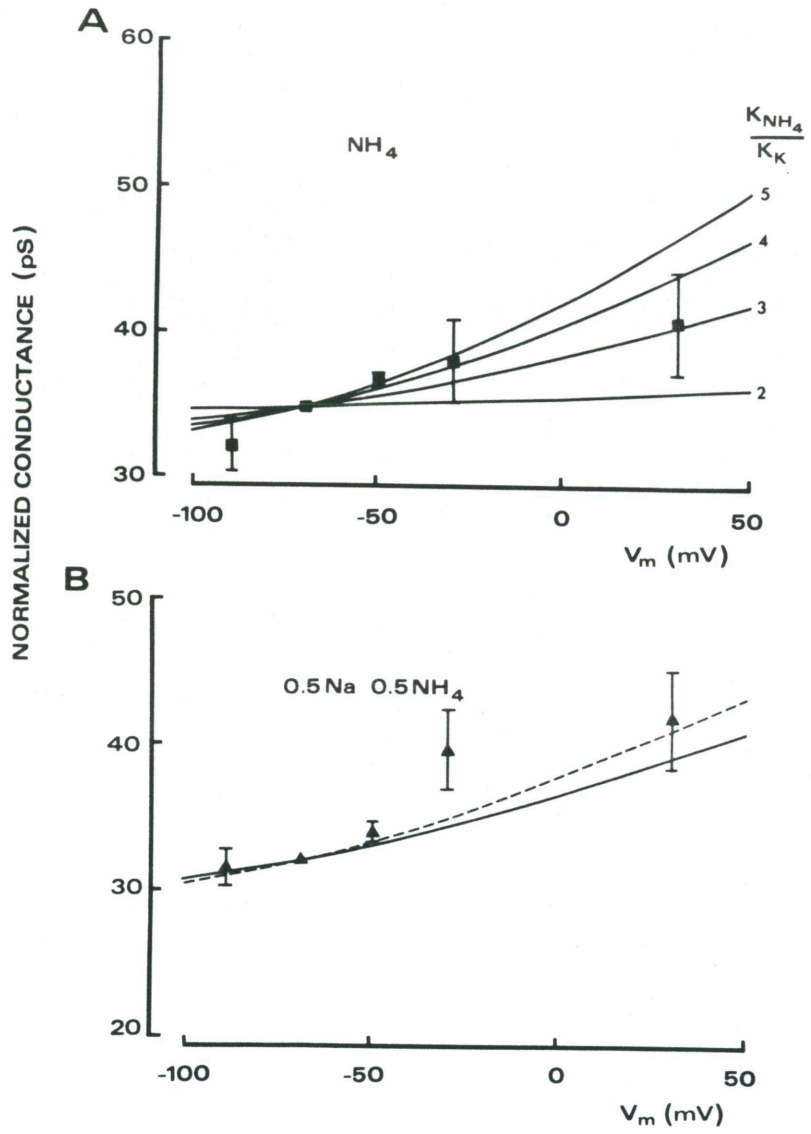

Figure 3.9. Single channel conductance [γ(p.s.d.)] measured as a function of membrane potential and compared with theoretical predictions. The experimental values (see Fig. 3.7) have now been normalized to the average value of conductance obtained at -70 mV. In each case the errors shown are the S.E.M. of the average conductance corrected for the normalization procedure and for the S.E.M. of the null potential measurement (see Methods). A. Results for NH_4 solution are compared with the theoretical curves predicted using the neutral site channel model. The values of K_{NH_4}/K_K used in each case are shown adjacent to each of the curves. Although a value of $K_{Na}/K_K = 2$ was used, the curves are very insensitive to the particular value chosen, since there is very little sodium present. A K_{NH_4}/K_K value of about 4 was considered to be the best fit, although the value of 3 is only marginally worse. B. Experimental results obtained in a 0.5 Na/0.5 NH_4 solution are compared with the theoretical curves predicted using $K_{NH_4}/K_K = 4$. The full curve is that obtained for a $K_{Na}/K_K = 2$ whereas the broken curve is for $K_{Na}/K_K = 4$.

Table 3.4. Experimental and predicted values of single-channel conductance in sodium and ammonium solutions.

Solution	Experimental γ(p.s.d.) (pS)	Theoretical predictions for γ(pS) $K_{Na}/K_K = 3\pm1$		
		$K_{NH_4}/K_K=3$	$K_{NH_4}/K_K=4$	$K_{NH_4}/K_K=5$
Na	26.1	26.1	26.1	26.1
NH_4	34.9±3.3	$34.1^{+4.3}_{-4.6}$	$30.3^{+3.8}_{-4.6}$	$27.5^{+3.5}_{-4.1}$
0.5Na/0.5NH_4	32.1±3.3	$30.2^{+1.7}_{-2.6}$	$28.3^{+1.9}_{-2.7}$	$26.8^{+2.0}_{-2.8}$

The experimental results in each case were based on the raw data obtained at -70 mV and used in Fig. 3.9. However, they now take into account absolute errors in each solution, and in the case of NH_4 and 0.5 Na/ 0.5 NH_4 solutions, were normalized to the experimental values in Na solution. The errors were appropriately corrected for the normalization procedure (see Methods). The theoretical conductance predictions were based on the neutral site channel model, and the +/- range given represents the upper and lower limit of K_{Na}/K_K respectively listed above.

for an individual cation was approximately constant, being equal to 1.07 ± 0.14 (S.D.). In contrast, for ammonium ions, the product (K_{NH_4}/K_K) x (u_{NH_4}/u_K) equals 1.68 ± 0.05 (S.E.M.). This implies a much higher mobility for ammonium ions than would have been predicted for an alkali cation having the same partition coefficient. Possibly this higher mobility arises from the ability of the ammonium ion to form hydrogen bonds with other inter-site ligands lining the channel. Since conductance is a function of both the equilibrium concentration and the mobility of cations within the channel, there may also be a contribution to the conductance from 'proton jumping' (Grotthus conductivity, see e.g. Moore, 1972), when the sites are occupied by ammonium ions, as this may appear as an increased u_{NH_4}/u_K.

From the data in this paper and the earlier data already mentioned (see Barry et al., 1979a) the equilibrium constant sequence appears to be $K_{Li} > K_{NH_4} \gtrsim K_{Na} > K_K > K_{Cs}$. This represents a high field strength sequence (Eisenman, 1965). The position of ammonium in the sequence would at first appear to be somewhat anomalous since it would suggest that the radius of the ammonium ion $\lesssim$ the radius of the sodium ion. In fact, the ammonium ion has an ionic radius 1.12 times that of the potassium ion and an almost identical free solution mobility (Robinson & Stokes, 1959). However, in other biological situations, ammonium ions behave as if they had a much smaller radius, and thus bind more strongly than potassium ions. This is true for the sodium channel in the frog node of Ranvier, where $P_{NH_4}/P_K \simeq 2$ (Hille, 1972) and is also true for the high field strength lithium aluminosilicate glass (LAS11-188) where both ammonium and sodium are more selected than potassium ions (Eisenman, 1967). In some cases, this enhanced binding of ammonium ions probably results from hydrogen bonding to suitably spaced oxygen ligands at the sites, since ammonium ion binding is very sensitive to the spatial configuration

of the site ligands (Szabo, Eisenman, Laprade, Ciani & Krasne, 1973). In gallbladder, some of the lower field strength ion selectivity data also indicate that ammonium ions bind more strongly than potassium and sometimes, even sodium ions (Moreno & Diamond, 1975). Ammonium, while not being as polarizable as thallium, is much more polarizable than the potassium ion, although the energy contribution due to polarization effects may not be significant in comparison to the contribution from hydrogen bonding.

Voltage sensitivity of conductance

The voltage sensitivity of single channel conductance in NH_4 solution is shown in Table 3.5 (see also Fig. 3.7) and is compared with Goldman-Hodgkin-Katz and neutral site predictions. Note that a reversed voltage dependence of conductance is predicted by the Goldman-Hodgkin-Katz equation. Other workers have indicated that single channel conductance is not very voltage sensitive in normal solutions (Anderson & Stevens, 1973; Lewis, 1979). However, the consistent increase in conductance with membrane depolarization is best seen at a single end-plate over a wide voltage range, as is illustrated in Fig. 3.1. Furthermore, variability in the conductance data obtained from different end-plates and measurement over a more limited voltage range make the voltage dependence difficult to detect. A linear relationship between variance and mean end-plate current and a more pronounced voltage dependence of conductance have been recently reported in denervated toad sartorius muscle fibres (Gage & Hamill, 1980).

Figure 3.10 illustrates the physical principles underlying the voltage sensitivity of conductance. The curve of single channel conductance has been replotted for the same parameters as used in Fig. 3.9A but now over an extended voltage range. The voltage sensitivity arises from the difference in mobility within the channel (and to some extent,

Table 3.5. Voltage sensitivity of single channel conductance in NH_4 solution. Temperature 15°C.

Vm (mV)	Experimental (pS)	Neutral Site (pS)	Goldman-Hodgkin-Katz (pS)
-90	32.2 ± 1.1	34.3	35.3
30	40.9 ± 3.2	40.0	32.2

Note that the Goldman-Hodgkin-Katz equation predicts the opposite voltage sensitivity compared to the experimental results and the neutral site predictions. The permeability ratios, $P_{NH_4}/P_K = 1.68$ and $P_{Na}/P_K = 1.15$, calculated from the observed null potentials, were used in the Goldman-Hodgkin-Katz predictions. For the neutral site channel model, these permeability ratios were separated into equilibrium constant and relative mobility terms (using the conductance voltage sensitivity data) and the following values were used: $K_{NH_4}/K_K = 3$, $u_{NH_4}/u_K = 0.56$; $K_{Na}/K_K = 3$, $u_{Na}/u_K = 0.38$.

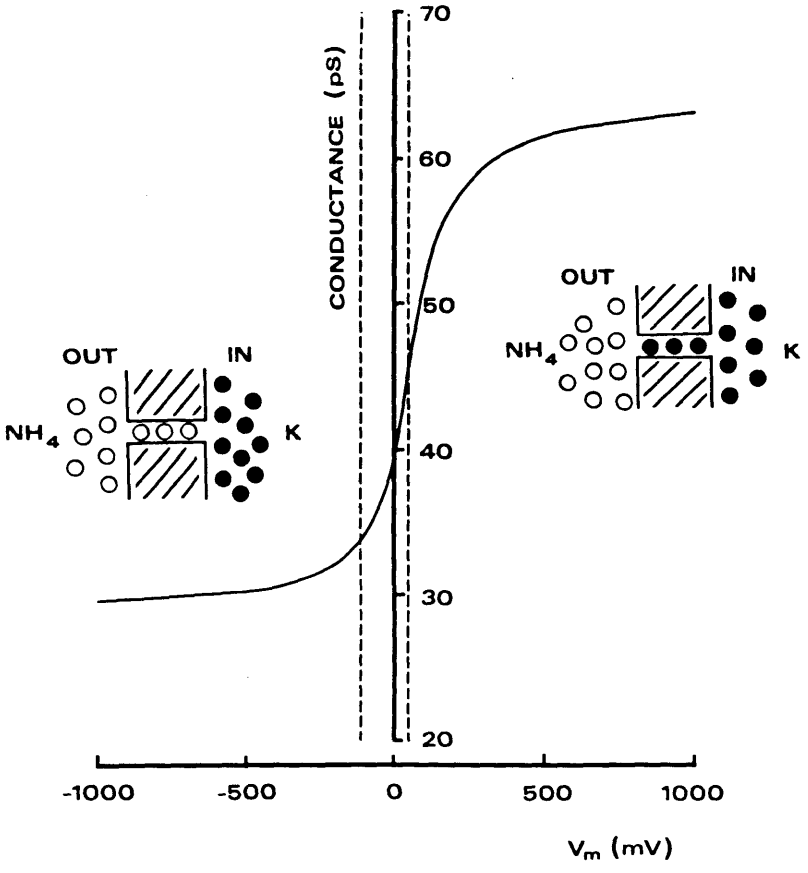

Figure 3.10. Single channel conductance predicted as a function of membrane potential for a neutral site channel model in NH_4 solution. The parameters used were the same as those used for the $K_{NH_4}/K_K = 4$ curve in Fig. 3.9A and normalized for the experimental value of conductance at -70 mV. The range from -110 mV to 50 mV considered in Fig. 3.9 is indicated by the two vertical broken lines. The extended voltage range shown here illustrates the physical principles underlying the voltage sensitivity of conductance predicted by the model. At extreme hyperpolarizing potentials, as illustrated schematically by the left inset, the neutral sites in the channel are predominantly occupied by ammonium ions: thus the conductance arises essentially from them alone. Because the ammonium ion has lower relative mobility (u_{NH_4}/u_K=0.42, estimated from the equilibrium constants and null potential measurements) the conductance at such hyperpolarizing voltages is relatively small. In contrast at extreme depolarizing potentials, as illustrated schematically by the right inset, the neutral sites in the channel are predominantly occupied by potassium ions: thus the conductance arises essentially from potassium ions alone. Since the potassium ion mobility is considerably greater than that of the ammonium ion, the conductance at such depolarizing voltages will be much larger.

differences in relative partition coefficients) for the different cations and from the asymmetrical nature of the external and internal solution composition (as depicted in the two schematic insets). At extreme hyperpolarizing potentials, the neutral sites in the channel would be predominantly occupied by ammonium rather than by potassium ions and hence, since ammonium ions have the lower mobility, the channel conductance would be minimal. In contrast, at extreme depolarizing potentials, the neutral sites in the channel would be predominantly occupied by potassium ions and the conductance would be maximal. Although the ratio of conductances at the two voltage extremes is determined essentially by the relative mobilities alone, the actual shape of the curve elsewhere is also dependent on the relative partition coefficients. It is interesting to note that the experimental voltage range occurs over part of the steepest section of the curve.

Two further points should be made about the applicability of the neutral site channel model. First of all, the mathematical model was derived earlier (Barry et al., 1979a) assuming that cation concentrations in the channel were well below site saturation levels. Allowing for the possibility of site saturation has shown that this was indeed a reasonable assumption (Barry, Gage & Van Helden, 1979c). Secondly, the model was originally derived using diffusion theory. However, virtually identical predictions can be made using a rate theory approach provided there are enough energy barriers (Barry et al., 1979c). Thus, single channel conductance and null potential measurements in NH_4 and 0.5 Na/0.5 NH_4 solutions appear to be compatible with an end-plate channel containing high field strength, neutral sites, and perhaps one or more high resistance barriers to anions. Furthermore, the ammonium ion permeation parameters would seem to imply some hydrogen bonding effects within these aqueous channels.

CHAPTER FOUR

EFFECTS OF DIVALENT CATIONS ON END-PLATE CHANNELS

Introduction

It has been known for some time that many cations, both monovalent and divalent, can pass through the ion channels activated by acetylcholine at the motor end-plate (Takeuchi & Takeuchi, 1960; for review see Rang, 1975). Furthermore, because end-plate channels are apparently impermeable to anions (Takeuchi & Takeuchi, 1959) and because single channel conductance depends on the nature of the permeating cation (Van Helden et al., 1977; Gage & Van Helden, 1979), it has been proposed that the channel contains negatively charged sites with which permeant cations interact (Barry et al., 1979a,b; Lewis & Stevens, 1979; Takeda, Barry & Gage, 1980). The observation of ion dependent, reciprocal changes in open channel lifetime and conductance at both the end-plate (Van Helden et al., 1977; Gage & Van Helden, 1979) and in aplysia neurones (Ascher et al., 1978) has led to the suggestion that ion binding to critical intrachannel sites influences channel lifetime. However, more recent reports (Takeda et al., 1980 ; Nonner, Adams, Dwyer & Hille, 1980) indicate that ion dependent changes in channel lifetime need not be reciprocally related to conductance changes, although the ion binding hypothesis would explain the increase in voltage sensitivity of channel lifetime seen in the presence of some divalent cations in aplysia neurones (Marchais & Marty, 1979).

When calcium ions are substituted for sodium ions in the external medium, single channel conductance is clearly reduced (Lewis, 1979; Bregestovski et al., 1979). However, there have been varying reports on the effects of high calcium ion concentrations on channel lifetime: in some experiments it was increased (Cohen & Van der Kloot, 1978) whereas in others, it was unchanged or decreased (Bregestovski et al., 1979; Magleby & Weinstock, 1980). Effects of calcium ions on channel characteristics could be related to their affinity for intrachannel sites

or to other effects on the channel or its close environment. Alternatively, it has been suggested that the increase in channel lifetime caused by elevated levels of calcium ions (and also hydrogen ions; Scuka, 1975; Mallart & Molgó, 1978) might be due to screening of membrane surface charge (Van der Kloot & Cohen, 1979). Our aim here was to investigate the effect of several divalent cations, particularly calcium ions, on the voltage and temperature dependent characteristics of end-plate channels in an attempt to obtain more information about what controls open channel lifetime and conductance.

Methods

The methods used here were essentially the same as those described in detail in Chapter Two. Briefly, toad (*Bufo marinus*) sartorius muscles were glycerol-treated to prevent contraction, and m.e.p.c.s were recorded extracellularly or in voltage-clamped fibres using conventional electrophysiological techniques. Extracellular electrodes were filled with normal toad Ringer (NTR:NaCl, 115 mM; KCl, 2.5 mM; $CaCl_2$, 1.8 mM; Na Hepes buffer, 2 mM; pH 7.2) and had resistances of 2-4 MΩ, while filament-containing microelectrodes (Clark Electromedical) filled with 2 M KCl for voltage recording or a 2 M KCl - 0.8 M K citrate mixture for current passing (resistance 4-8 MΩ) were used in voltage-clamp experiments. Analysis of end-plate current fluctuations (noise) produced by iontophoresis of ACh was based on the model and theory presented by Anderson & Stevens (1973). Experimental data were recorded on FM tape for off-line computer analysis (see Van Helden et al., 1977; Gage et al., 1978; Takeda et al., 1980 , for details). A minor change was the use of 16,384 data points for fluctuation analysis: i.e. 8 s of noise sampled at 2 kHz in 32 blocks. Base line noise in the absence of agonist was always subtracted. Usually, control data from several cells in each muscle were obtained in NTR at 15°C at a series of potentials before the temperature was changed or test solutions introduced. Solution changes were made by superfusing 3 to 5x bath volume (2-3 ml) of the test solution over a 5 min period - the bath changeover time was deliberately kept slow to facilitate holding cells through the solution change. Data then collected from cells in the test solutions always showed the same trends as data from the paired cells. Divalent cations

(up to 1 mM) were added directly to NTR; NaCl was reduced appropriately to maintain osmotic strength when greater divalent cation concentrations were used (20 mM divalent cation solutions also contained 90 mM NaCl, 2.5 mM KCl and 2 mM Na Hepes buffer; pH 7.2). Isotonic calcium solutions (80 Ca solution) contained 80 mM $CaCl_2$, 2.5 mM KCl and 2 mM K Hepes buffer; pH 7.2. Results are presented as means ± 1 S.E.M. unless otherwise noted.

Results

20 mM Ca and Mg

Isosmotic solutions containing 20 mM $CaCl_2$ (20 Ca solution) produced an increase in the time constant of decay (τ_D) of miniature end-plate currents (m.e.p.c.s), as illustrated in Figure 4.1. This increase in τ_D, though small, was regularly seen. In 5 paired cells, there was, on average, a 27.6 ± 4.3% (mean ± 1 S.E.M.) increase in τ_D in the 20 Ca solution (Table 4.1). This effect was not specific for calcium ions: an increase in τ_D of 36.6 ± 3.8% was also produced by solutions containing 20 mM $MgCl_2$ (20 Mg solution). In both 20 Ca and 20 Mg solutions, the decay of m.e.p.c.s remained exponential (Fig. 4.1B), and the increases in τ_D were fully reversible on return to control solution.

The voltage sensitivity of τ_D (Magleby & Stevens, 1972a) recorded in these solutions containing raised divalent ion concentrations was not significantly different from normal. Mean values of τ_D obtained from five cells in 20 Ca (squares) and 20 Mg solutions (open triangles) are plotted semilogarithmically against membrane potential (V_m) in Figure 4.1C. The straight lines are least squares fits to the equation $\tau_D(V_m) = \tau_D(0)\exp(-V_m/H)$, where $\tau_D(0)$ is the time constant of decay at zero membrane potential and H is the change in membrane potential for an e-fold change in τ_D (Magleby & Stevens, 1972b; Gage & McBurney, 1975). The H value (volt constant) obtained in this way in control solution was 98.4 mV: H values in 20 Ca and 20 Mg solution were 94.2 and 86.7 mV respectively. Values of H and $\tau_D(0)$ obtained in individual cells were also averaged and are given in Table 4.2.

80 mM Ca

Higher concentrations of calcium produced larger increases in τ_D. Changes in m.e.p.c.s recorded in an isotonic solution containing 80 mM

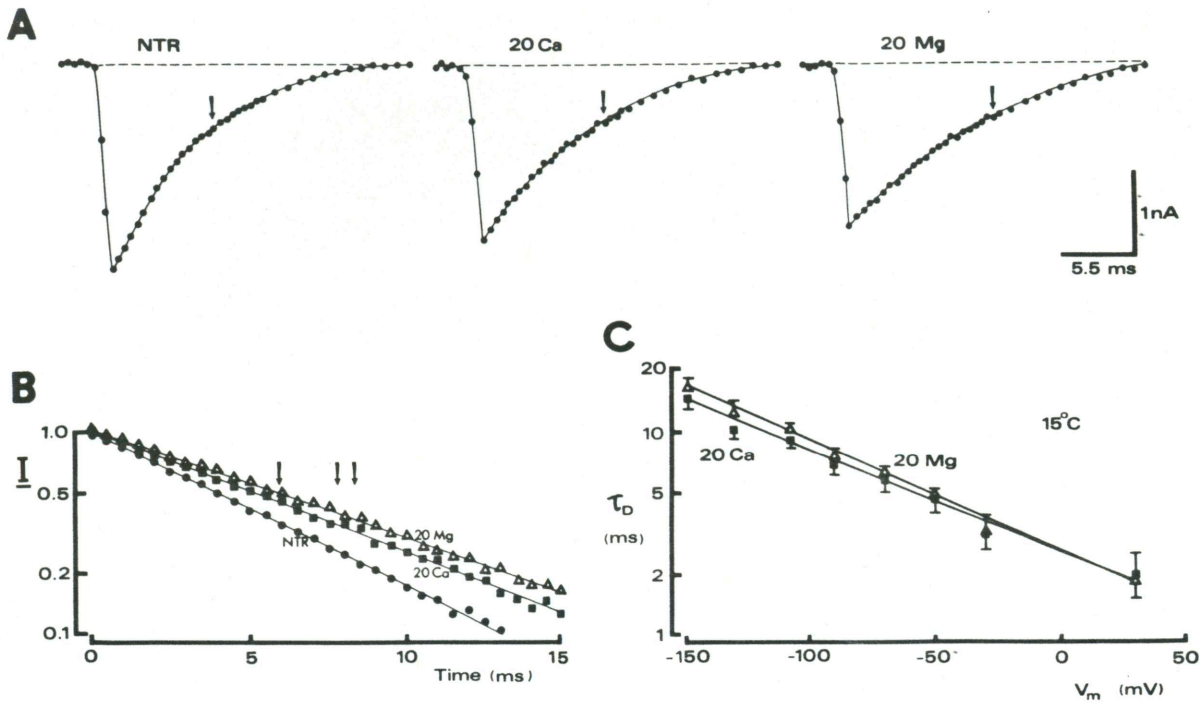

Figure 4.1. Addition of 20 mM Ca or Mg lengthens m.e.p.c. decay. A. Averaged m.e.p.c.s (n=20) recorded under voltage clamp at -90 mV in NTR, 20 Ca and 20 Mg solutions. M.e.p.c. time constants of decay (τ_D, arrows) were 6.0 (NTR), 7.13 (20 Ca) and 8.33 ms (20 Mg). Temperature, 15°C. B. The decay of the normalized m.e.p.c.s shown in A is well-fitted by a single exponential. C. Voltage dependence of τ_D. Averaged data at each potential from 5 cells in each solution were well described by the equation $\tau_D(V) = \tau_D(0) \exp(-V_m/H)$. H values were 94.2 and 86.7 mV, $\tau_D(0)$ values were 2.66 and 2.50 ms, and correlation co-efficients were 0.980 and 0.991 in 20 Ca (■) and 20 Mg (Δ) solutions, respectively, for each parameter. In this set of control experiments (NTR), H was 98.4 mV and $\tau_D(0)$ was 2.01 ms.

Table 4.1. Addition of 20 mM Ca or 20 mM Mg increases m.e.p.c. time constant of decay (τ_D). Data were obtained from paired cells under voltage clamp at -90 mV; temperature, 15°C.

Cell	τ_D(ms)		Cell	τ_D(ms)	
	NTR	20Ca		NTR	20 Mg
A	5.01	6.83	F	5.62	7.62
B	5.46	6.87	G	4.98	6.12
C	6.10	7.13	H	5.91	8.33
D	5.59	7.77	I	4.90	6.86
E	5.37	6.45	J	5.21	7.49

$CaCl_2$ and zero Na (80 Ca solution) are illustrated in Figure 4.2. M.e.p.c.s had a slower decay, which remained exponential, and were smaller in amplitude in 80 Ca than in control solution (Fig. 4.3). A large decrease in resting membrane conductance occurred in the 80 Ca solution and this facilitated the recording of m.e.p.c.s over large potential ranges, as less holding current was required to displace membrane potential. The voltage sensitivity of τ_D obtained using average values of τ_D from several cells showed little change in 80 Ca solution (Fig. 4.4; see Table 4.2 for averaged H values obtained from individual cells), and was not detectably different at 15°C and 25°C.

The reduction in peak m.e.p.c. amplitude in 80 Ca (Fig. 4.2B and 4.3A) was more pronounced at negative potentials, as is illustrated in Figure 4.5 in which mean m.e.p.c. amplitude is plotted against membrane potential (averaged data from eight cells). In fact, at positive potentials, there was no significant reduction in m.e.p.c. amplitude. A contributory factor to the decrease in m.e.p.c. amplitude was a negative shift in the null (zero-current) potential in 80 Ca. In normal toad Ringer, the null potential (ε_o) was -3.1 ± 1.2 mV (n=11) and in 80 Ca, ε_o was -34.3 ± 2.9 mV (n=4). The shift in ε_o in 80 Ca was not different at 15°C and 25°C (Fig. 4.5).

The shift in null potential in 80 Ca solutions was not sufficient to account for the whole of the reduction in m.e.p.c. amplitude. The magnitude of the conductance change produced by ACh was also reduced. This is illustrated in Figure 4.6 in which the conductance at the peak of a m.e.p.c. (G_p, calculated by dividing peak m.e.p.c. amplitude by the driving force, $V_m-\varepsilon_o$) is plotted against membrane potential. In 80 Ca, G_p was reduced at all potentials, but it is clear that the reduction at +50 mV was less than at -150 mV.

In order to test whether the increase in τ_D was caused by

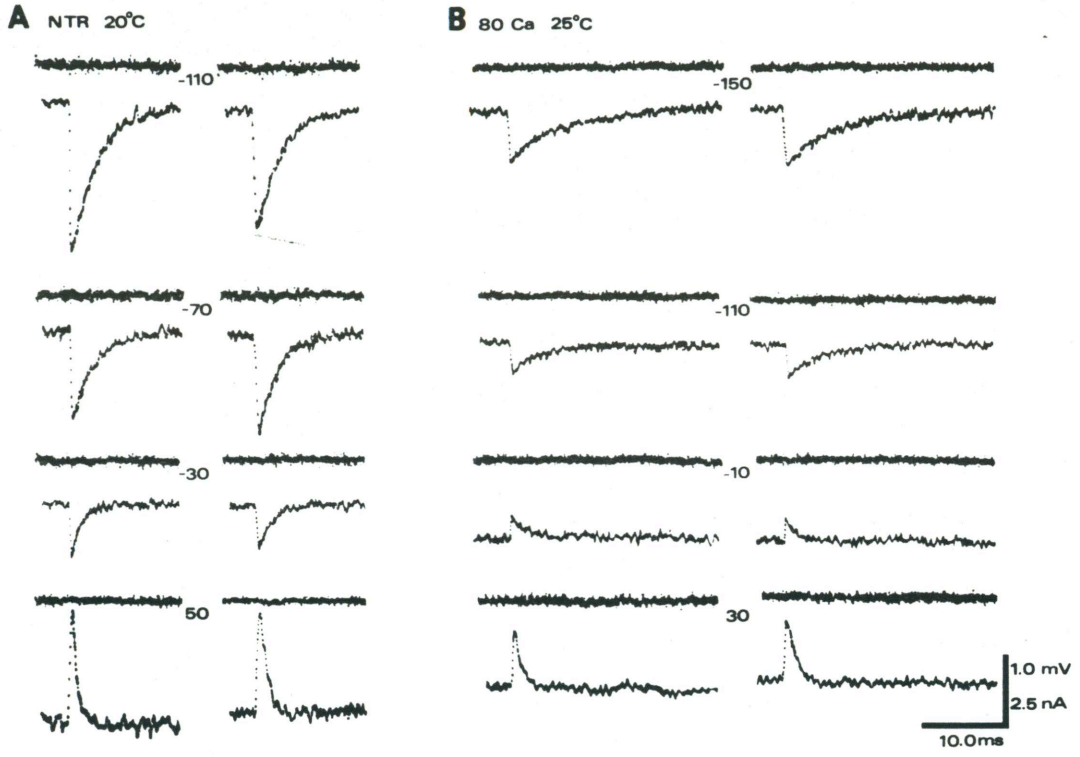

Figure 4.2. The effect of isotonic calcium solution. M.e.p.c.s recorded from a voltage clamped fibre in NTR (A) and 15 min later in 80 Ca solution (B). M.e.p.c.s were smaller, and decayed more slowly in 80 Ca solution at all potentials. Note the shift in null potential to a more negative value in the 80 Ca solution. The voltage trace is shown above each current trace.

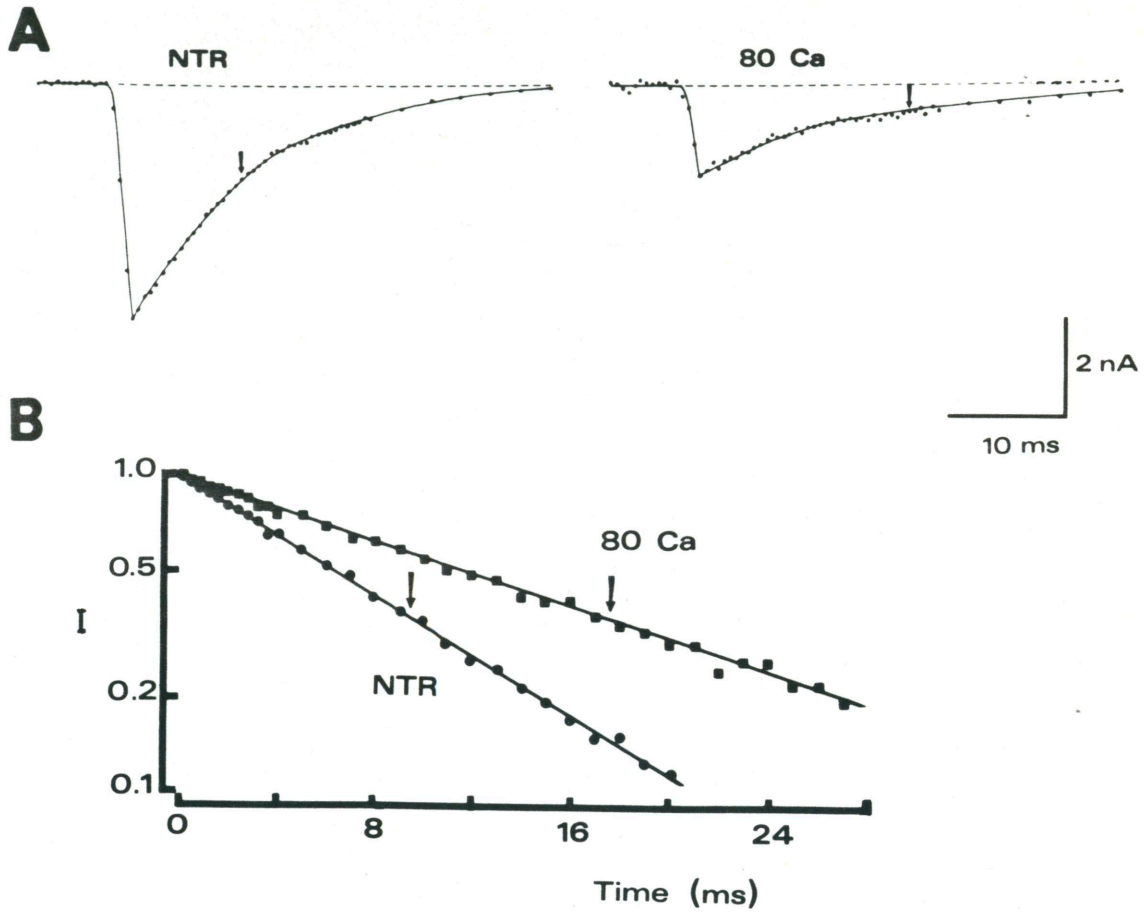

Figure 4.3. The decay of m.e.p.c.s remains exponential in 80 Ca solution. A. Averaged m.e.p.c.s recorded from one cell in NTR and 80 Ca solutions under voltage clamp. Holding potential, -150 mV; temperature, 14.5°C. B. The normalized amplitude of the m.e.p.c.s in A plotted semilogarithmically against time. Time constants of decay (τ_D; arrows) were 9.5 ms (NTR) and 17.6 ms (80 Ca).

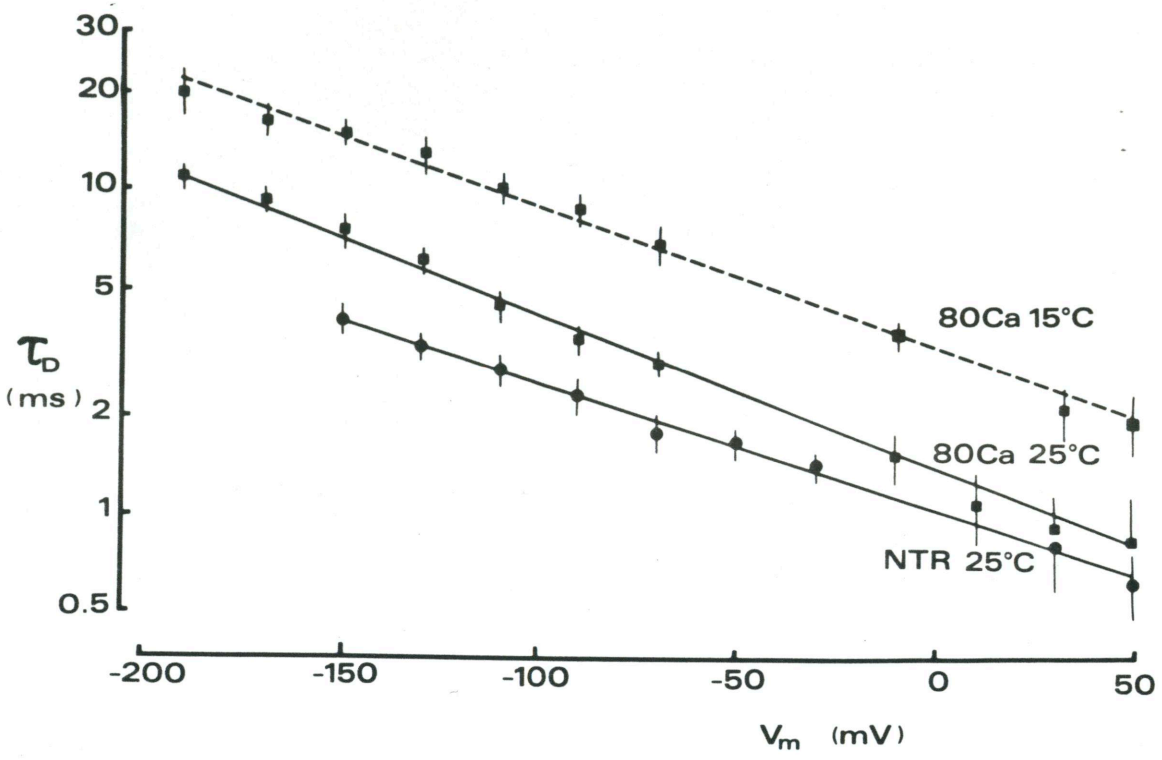

Figure 4.4. Voltage dependence of τ_D in control and 80 Ca solutions. Correlation coefficients for least squares fits to single exponentials were 0.980 (80 Ca, 25°C), 0.932 (80 Ca, 15°C) and 0.989 (NTR, 25°C). H values calculated were 101.4, 103.9 and 113.9 mV; $\tau_D(0)$ values were 1.49, 3.74 and 1.09 ms, respectively for 80 Ca (25°C), 80 Ca (15°C) and NTR (25°C). At each potential, the average τ_D from at least 6 cells is shown. See Table 4.2 for control data at 15°C.

Table 4.2. Voltage sensitivity of τ_D in normal toad Ringer (NTR) and in solutions containing added divalent cations. Data from single cells voltage clamped over wide ranges of potential were fitted (using least squares) by the equation: $\tau_D(V_m) = \tau_D(0)\exp(-V_m/H)$. Values of $\tau_D(0)$, H and $\bar{r}$ (correlation coefficient) are shown as mean ± 1 S.E.M. (n, number of fibres).

Solution	Temperature (°C)	H (mv)	$\tau_D(0)$ (ms)	$\bar{r}$	n
NTR	15	105.1 ± 4.2	2.02 ± .14	.994 ± .004	18
NTR	25	101.5 ± 10.8	0.98 ± .25	.992 ± .007	9
20Ca	15	89.8 ± 9.0	2.47 ± .30	.988 ± .005	5
20Mg	15	83.5 ± 11.7	2.40 ± .20	.989 ± .006	5
80Ca	15	104.6 ± 8.3	3.46 ± .40	.979 ± .018	6
80Ca	25	94.9 ± 7.9	1.68 ± .16	.982 ± .014	11
1Zn	15	92.7 ± 8.8	4.16 ± .36	.987 ± .009	7
1Ni	15	95.3 ± 6.6	3.61 ± .21	.981 ± .008	12

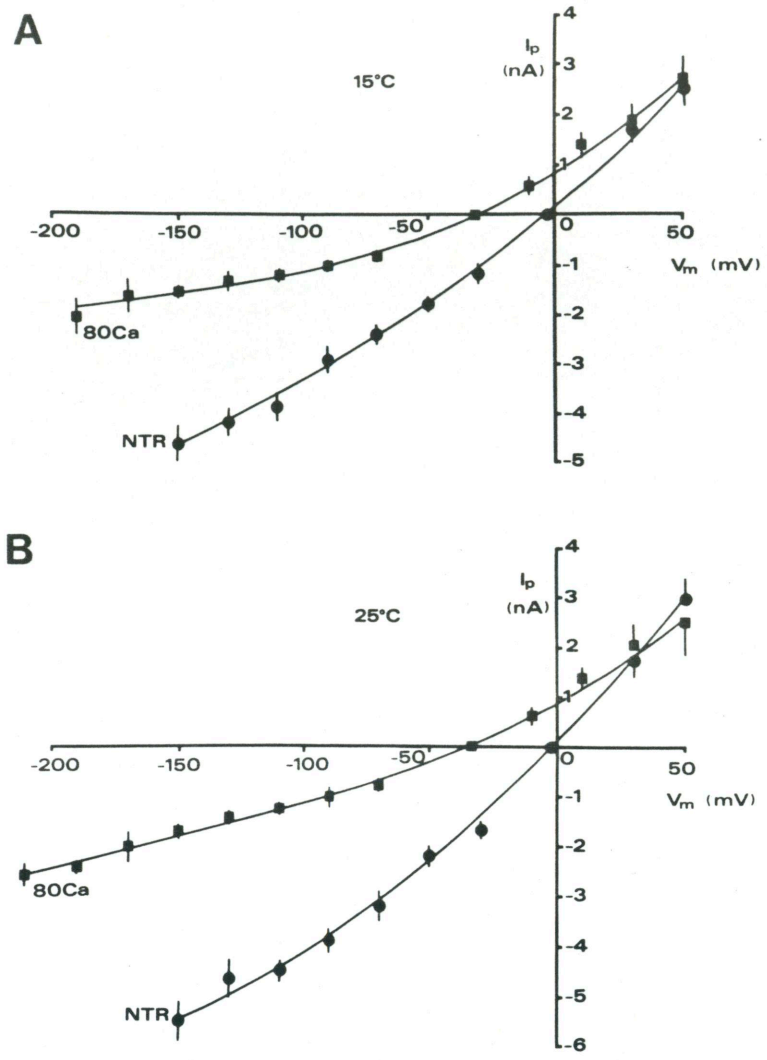

Figure 4.5. The effect of membrane potential on mean peak m.e.p.c. amplitude in NTR and 80 Ca. M.e.p.c.s had reduced amplitudes at negative potentials in 80 Ca at both 15°C (A) and 25°C (B), but were near normal-sized at positive potentials. The null potential shifted from -3 mV in NTR to -34 mV in 80 Ca, and was not affected by temperature. Data are averaged m.e.p.c. amplitudes ($n \geq 20$) from at least 8 cells.

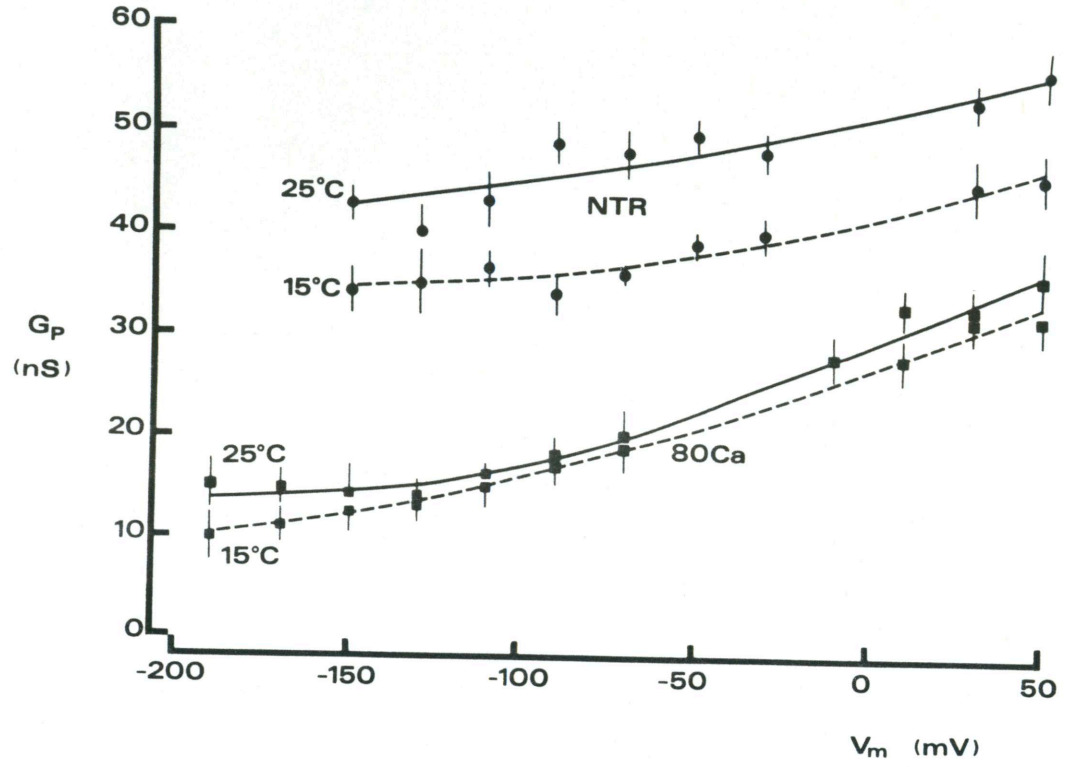

Figure 4.6. Voltage sensitivity of m.e.p.c. peak conductance in NTR and 80 Ca. Mean peak m.e.p.c. conductance was obtained by dividing the peak m.e.p.c. amplitude (see Fig. 4.5) by the driving force and the lines were fitted by eye. Note that G_p was always smaller in 80 Ca and that as the holding potential was made more positive, G_p increased slightly in both solutions.

inhibition of acetylcholinesterase in 80 Ca solution, the effectiveness of an anticholinesterase, prostigmine, was compared in normal toad Ringer and in 80 Ca. There should be little effect of prostigmine in 80 Ca if the latter had already significantly inhibited acetylcholinesterase. In Figure 4.7, it can be seen that addition of 3 μM prostigmine to normal toad Ringer produced an increase in τ_D from 7.0 to 11.2 ms, while in 80 Ca, 3 μM prostigmine resulted in τ_D increasing from 13.6 to 17.0 ms. Thus, prostigmine clearly caused an increase in τ_D in 80 Ca. However, the observation does not exclude the possibility that acetylcholinesterase was partially depressed, especially as the increase in τ_D caused by prostigmine was less than in the control solution. On the other hand, the increase in τ_D cannot be due wholly to inhibition of acetylcholinesterase, as 3 μM prostigmine had less effect than 80 Ca solution on τ_D (Fig. 4.7).

Further evidence against the idea that the increase in τ_D caused by 80 mM Ca might be due to inhibition of acetylcholinesterase came from comparison of channel open time in normal toad Ringer and in 80 Ca. Power density spectra of fluctuations in end-plate current generated by iontophoresis of ACh are presented in Figure 4.8 . Spectra recorded in normal toad Ringer and 10 min later in 80 Ca clearly show a shift to lower frequencies in 80 Ca, an effect not seen with anticholinesterases (Katz & Miledi, 1973b). Average channel lifetime (τ_N) calculated from the half-power frequency was 6.9 ms in normal toad Ringer and 13.7 ms in 80 Ca, an increase similar to the increase in τ_D caused by 80 Ca. Furthermore, m.e.p.c.s recorded in 80 Ca (Fig. 4.2B and 4.3A) showed no pronounced increase in rise time or rounding of the peak, features observed in prostigmine-containing solutions (Katz & Miledi, 1973b).

Another effect of the 80 Ca solution was to decrease single channel conductance (γ), as has been previously reported (Lewis, 1979; Bregestovski et al., 1979). Values of τ_N and γ obtained from noise analysis in NTR and

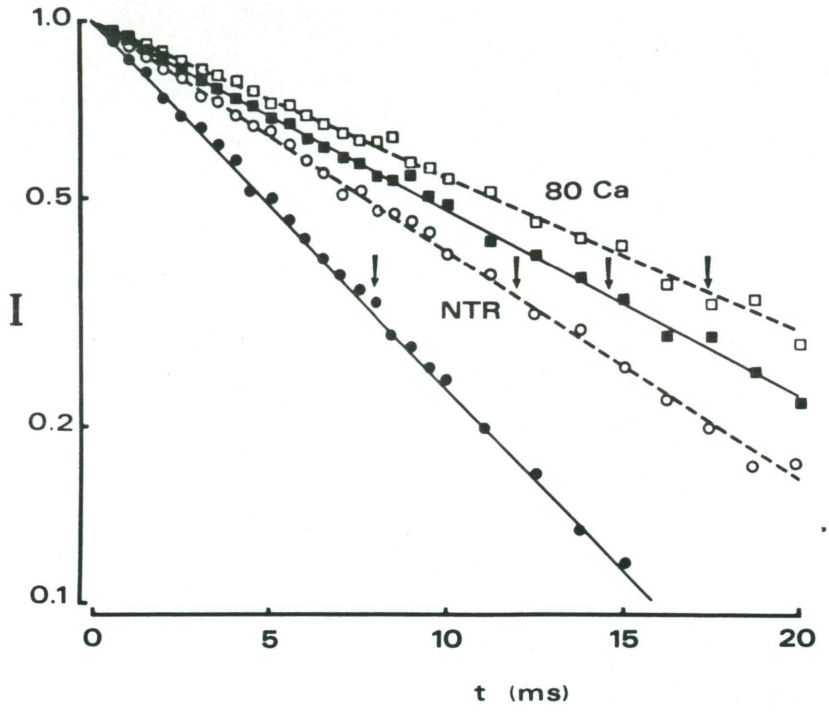

Figure 4.7. Addition of 3 μM prostigmine (broken lines) lengthens m.e.p.c.s in normal toad Ringer (NTR) and in 80 Ca solution. The decay of averaged (n=25), normalized m.e.p.c.s recorded under voltage clamp is shown plotted semilogarithmically. In NTR (●), τ_D (arrow) was 7.0 ms, and after addition of prostigmine (o), τ_D was increased to 11.2 ms. In 80 Ca (■), τ_D was 13.6 ms, and after addition of prostigmine (□), τ_D was increased to 17.0 ms. Holding potential, -130 mV; temperature, 15°C.

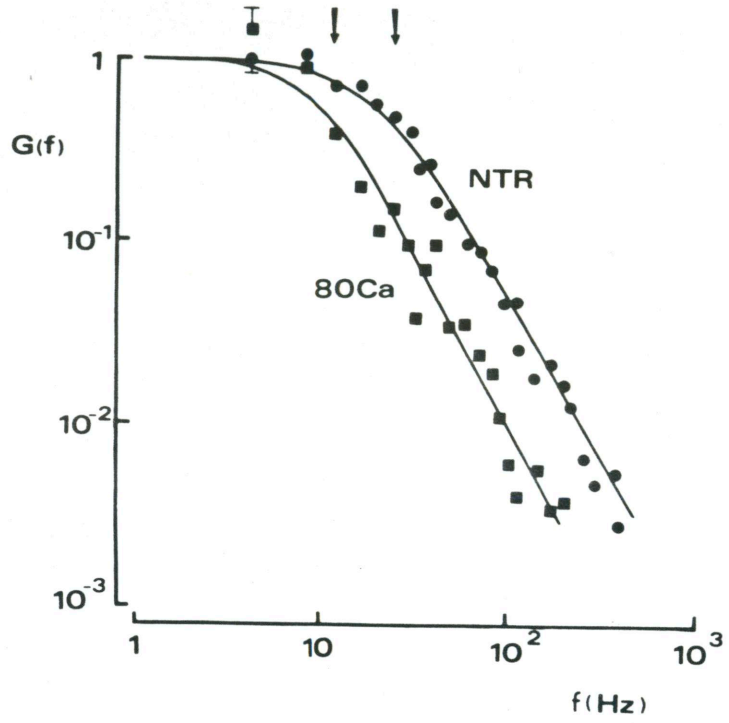

Figure 4.8. Power spectral density of ACh-induced fluctuations in NTR, and 10 min later in 80 Ca solution. Channel lifetime increased from 6.9 ms in NTR to 13.7 ms in 80 Ca, corresponding to half-power frequencies (arrows) of 23.1 and 11.6 Hz, respectively. Data were normalized and were well fitted (by least squares) to single Lorentzian curves. Channel conductances calculated from the spectra were 22.5 pS in NTR, and 4.7 pS in 80 Ca. Asymptotic spectral densities were 2.92×10^{-21} and 1.48×10^{-22} A^2s for steady-state currents of 37 and 6 nA, in NTR and 80 Ca, respectively, Membrane potential, -130 mV; temperature, 15°C.

80 Ca are given in Table 4.3.

Zinc and Nickel

Other divalent ions affected m.e.p.c.s in a similar way. Both zinc (Fig. 4.9) and nickel (Fig. 4.10) slowed the decay of m.e.p.c.s when added to normal toad Ringer at relatively low concentrations (0.1 to 5 mM). The effect of these ions on τ_D increased with concentration in this range, as can be seen in Figure 4.11, and were rapid in onset. Zinc was somewhat more potent than nickel and while the effects of nickel were largely reversible, those of zinc were less so. In the experiments illustrated in Figure 4.11, τ_D was doubled by a solution containing 0.1 mM Zn, whereas 1 mM Ni was required to produce a similar effect. There was no significant change in the growth phase of m.e.p.c.s in the presence of these ions and the decay phase remained exponential. No increase in τ_D was observed when 1 mM Mg was added to the control solution. The observations in Ni-containing solutions confirm those reported recently by Magleby & Weinstock (1980).

Although low concentrations of zinc and nickel had a greater effect than 80 Ca on τ_D, they caused much less depression of m.e.p.c. amplitude. The mean peak amplitude of m.e.p.c.s recorded from several cells under voltage clamp in normal toad Ringer, 1 mM Zn and 1 mM Ni is shown plotted against membrane potential in Figure 4.12A. It can be seen that there was only a slight decrease in m.e.p.c. amplitude in the presence of Zn or Ni. Furthermore, in contrast to the effects in 80 Ca, there was no appreciable shift in the null potential (Fig. 4.12A). Although Zn and Ni increased τ_D, they had no significant effect on the voltage dependence of τ_D, as illustrated in Figure 4.12B (see also Table 4.2).

Analysis of power density spectra of end-plate current fluctuations showed that both Zn and Ni increased average channel lifetime. This is illustrated for a 1 mM Zn solution in Figure 4.13. The half-power

Table 4.3. Single channel characteristics obtained from noise analysis. Mean channel lifetime (τ_N) was calculated using the equation $\tau_N = \frac{1}{2\pi f_{\frac{1}{2}}}$ where $f_{\frac{1}{2}}$ is the half-power frequency. Single channel conductance was calculated using the relationship $\gamma = \frac{G(0)}{4\mu_i (V_m - \varepsilon_o)\tau_N}$, where G(0) is the zero frequency asymptote and μ_i is the mean ACh-induced end-plate current. Estimates of γ obtained in this way were not different from values calculated using the equation $\gamma = \frac{\sigma_i^2}{\mu_i (V_m - \varepsilon_o)}$, where σ_i^2 is the variance of the current fluctuations. Temperature, 15°C; n, number of cells.

Solution	V_m (mV)	τ_N (ms)	γ (pS)	n
NTR	-130	7.1 ± 0.3	23.7 ± 2.0	5
80 Ca	-130	14.3 ± 0.5	5.2 ± 1.7	3
NTR	-90	5.9 ± 0.3	25.2 ± 0.9	7
1 mM Zn	-90	11.4 ± 0.9	20.4 ± 1.1	4
1 mM Ni	-90	9.0 ± 0.6	19.8 ± 1.0	6

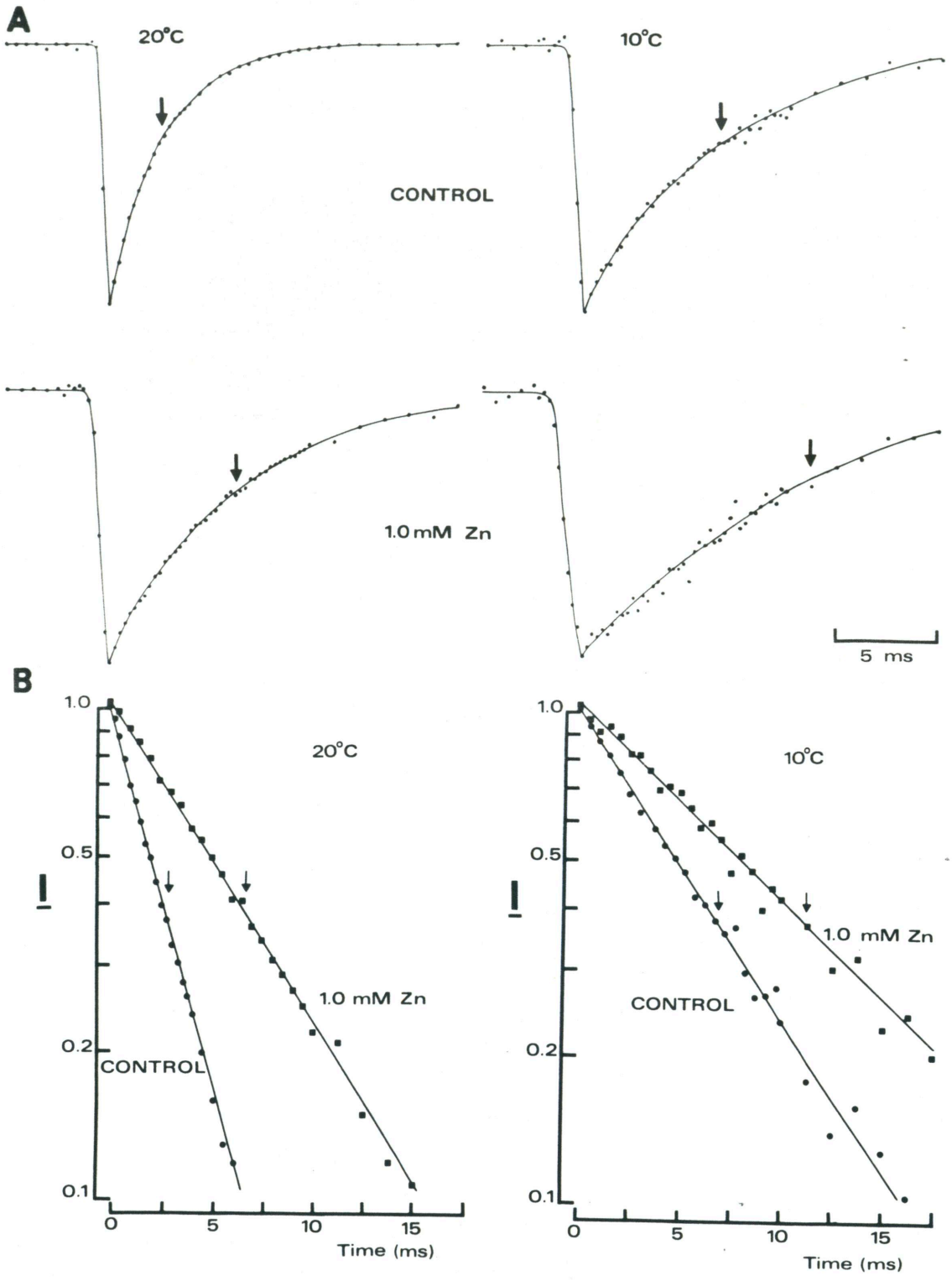

Figure 4.9. 1.0 mM Zn lengthens m.e.p.c.s. A. Normalized m.e.p.c.s recorded under voltage clamp in control and 1.0 mM Zn solutions. Averages were obtained from at least 20 m.e.p.c.s. Holding potential, -70 mV. B. The decay of the m.e.p.c.s shown in A is well-described by a single exponential. At 20°C, τ_D's were 4.3 and 7.8 ms for control and 1.0 mM Zn, respectively, and at 10°C τ_D's were 7.4 and 11.1 ms for control and 1.0 mM Zn solutions, respectively.

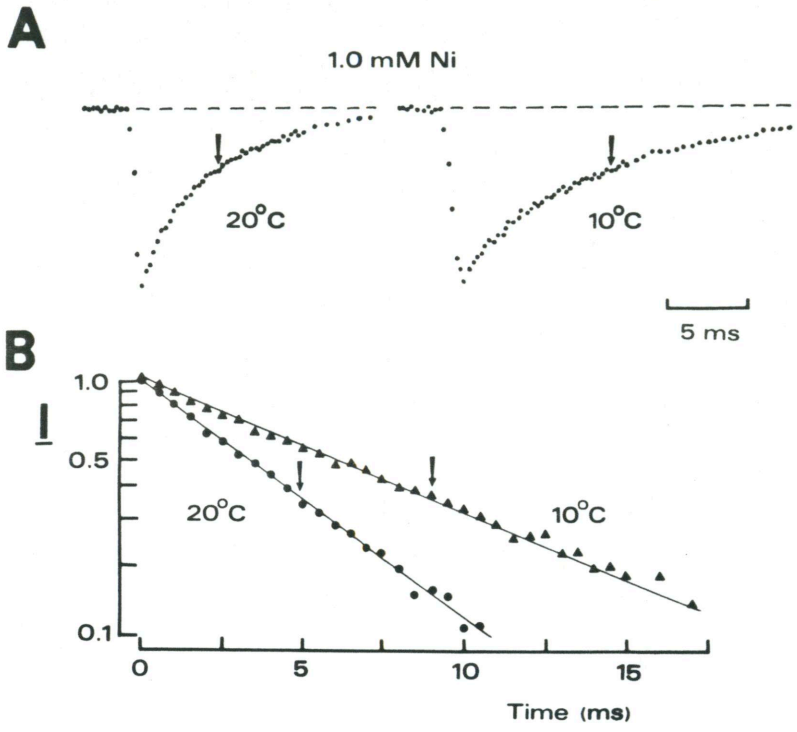

Figure 4.10. The effect of nickel on the time course of m.e.p.c. decay. A. Normalized averages (n≥20) of extracellularly recorded m.e.p.c.s in 1.0 mM Ni solution at 20°C and 10°C. B. The decay of the m.e.p.c.s shown in A is plotted semilogarithmically against time. τ_D's (arrows) were 5.1 and 9.3 ms at 10 and 20°C, respectively.

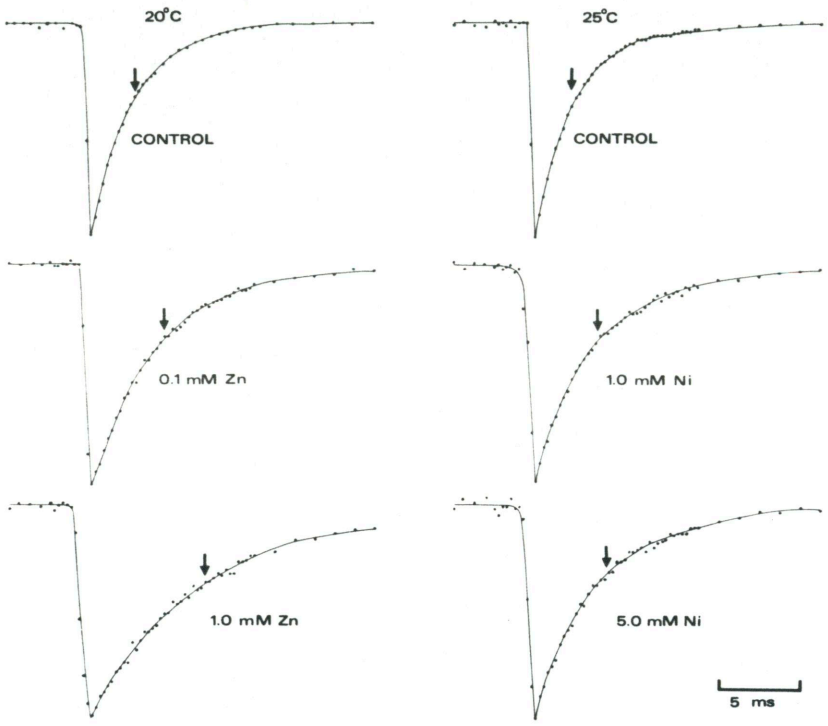

Figure 4.11. The increase in τ_D caused by zinc and nickel is concentration dependent. Left panel shows normalized averages (n=20) of m.e.p.c.s recorded extracellularly from the same cell in control solution, 0.1 mM and 1.0 mM Zn solutions (20°C). Arrows indicate time constants of decay which were 2.29 (control), 4.58 (0.1 mM Zn) and 7.29 ms (1.0 mM Zn). Right hand panel shows normalized averages of m.e.p.c.s recorded extracellularly from 1 cell in control and in nickel-containing solutions (25°C). τ_D's were 1.87 (control), 3.96 (1.0 mM Ni) and 4.79 ms (5.0 mM Ni).

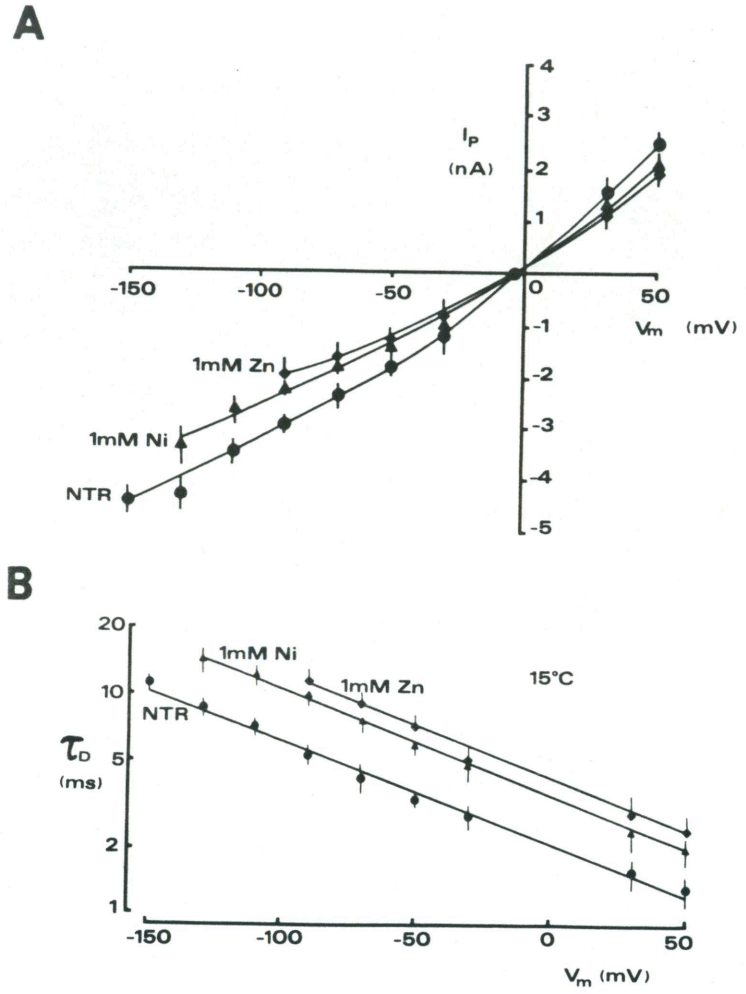

Figure 4.12. The effect of voltage on m.e.p.c. peak amplitude (I_p) and time constant of decay (τ_D). A. Current-voltage relationships for averaged m.e.p.c.s. ($n \geq 15$) recorded from at least 7 cells in NTR (●), 1 mM Ni (▲) and 1 mM Zn (◆) solutions (15°C). Peak m.e.p.c. amplitude was reduced slightly in the presence of the divalent cation, but no change in the null potential or in the overall shape of the I-V curve was apparent. B. Voltage sensitivity of τ_D. Averaged values of τ_D at each potential (at least 7 cells) were well fitted (least squares) by: $\tau_D(V_m) = \tau_D(0)\exp(-V_m/H)$. For normal toad Ringer, 1 mM Ni and 1 mM Zn solutions, H values were 99.8, 95.3 and 93.5 mV, $\tau_D(0)$ values were 2.06, 3.63 and 4.06 ms and correlation coefficients were 0.994, 0.989 and 0.992.

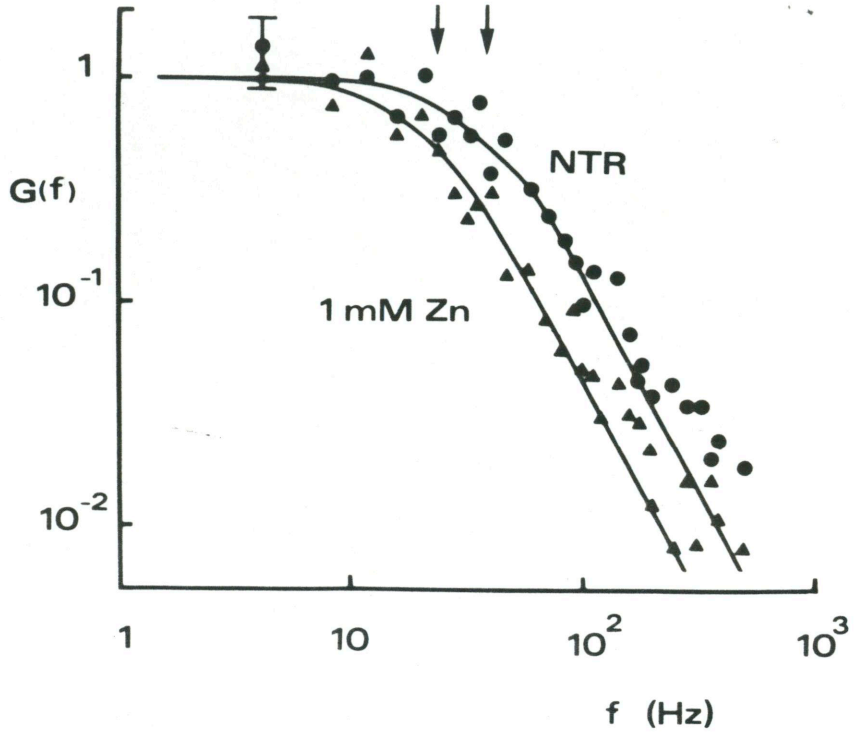

Figure 4.13. Channel lifetime (calculated from the half power frequency, arrow) increased from 4.17 ms in normal toad Ringer (NTR) to 7.03 ms in 1.0 mM Zn solution. Current fluctuations were recorded from the same cell in NTR, and after 5 min in 1.0 mM Zn. Holding potential, -70 mV, temperature 15°C. Spectra are shown normalized, and were well-fitted (by least squares using log G(f) values) to single Lorentzian curves. Asymptotic spectral densities were 9.1×10^{-22} and 1.1×10^{-21} A^2s, for mean end-plate currents of 32 and 28 nA in NTR and 1.0 mM Zn respectively. Single channel conductance values were 28.2 pS in control solution and 19.2 pS in 1.0 mM Zn. In 1.0 mM Ni (not shown), noise spectra gave channel lifetimes of 6.23 ms and conductances of 19.4 pS, under the same conditions.

frequency of 38.2 Hz in normal toad Ringer gave an average channel open time of 4.2 ms and the shift in half-power frequency to 22.6 Hz produced by 1 mM Zn gave a channel open time of 7.0 ms. In the same cell, average channel open time was 6.2 ms in a solution containing 1 mM Ni. Both Zn and Ni reduced single channel conductance, but to a lesser extent than 80 Ca. The effects of Zn and Ni on end-plate channels in several preparations can be seen in Table 4.3.

Effect of Temperature

If the divalent cations affect channel lifetime (τ) by changing the nature of the reaction that is normally rate-limiting, then a change in the temperature sensitivity of τ would be expected. Changes in τ_D with temperature in normal toad Ringer (circles), 1 mM Ni (triangles), 1 mM Zn (diamonds) and 80 Ca solution (squares) are shown in Figure 4.14. From the regression lines fitted to the points, Q_{10}'s of 2.60 in normal road Ringer, 2.55 in 1 mM Ni, 2.47 in 1 mM Zn and 2.20 in 80 Ca solution were obtained. Mean values of Q_{10} and activation energy obtained in several experiments are presented in Table 4.4.

Charge Movement

It has been reported previously (Van Helden et al., 1977; Gage & Van Helden, 1979) that some permeant monovalent cations have opposite effects on the amplitude and time constant of decay of m.e.p.c.s so that total charge movement during a m.e.p.c. is changed little when the cations are substituted for Na in the extracellular solution. The divalent cations, Zn and Ni, slowed the decay of m.e.p.c.s but caused only a small reduction in peak amplitude so that charge movement was greater than in normal toad Ringer (Fig. 4.15). In contrast, the decrease in m.e.p.c. amplitude in 80 Ca caused a decrease in charge movement compared to normal toad Ringer, in spite of the increase in τ_D (Fig. 4.15). For example,

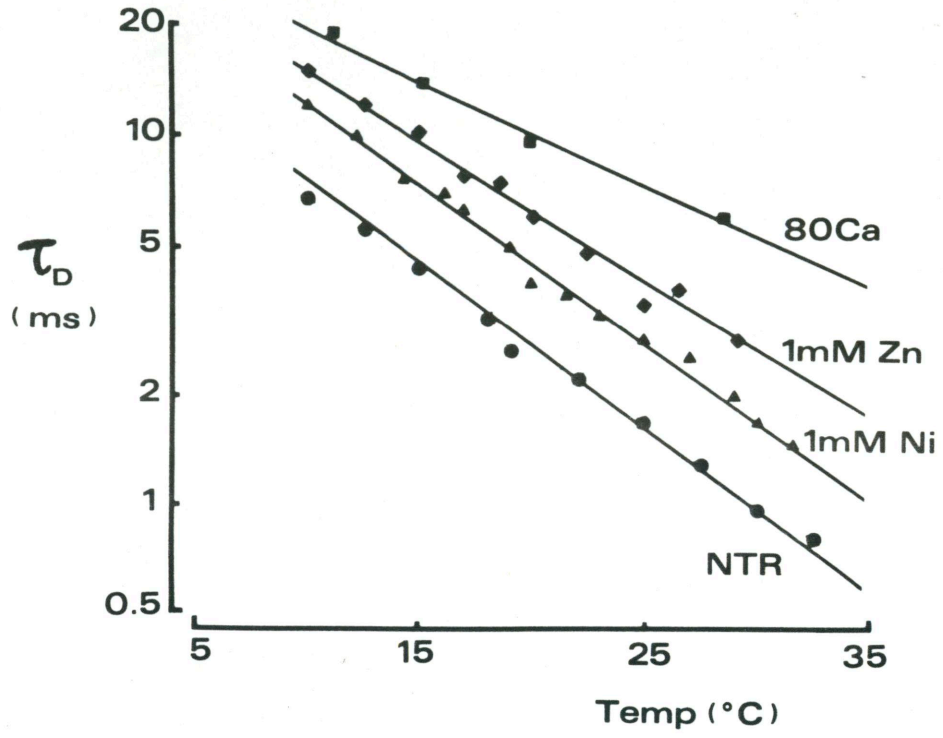

Figure 4.14. Temperature dependence of τ_D. M.e.p.c.s from single cells were recorded extracellularly in NTR, 1 mM Ni and 1 mM Zn solutions, and under voltage clamp in 80 Ca (holding potential, -130 mV). Data were also least squares fit to Arrhenius plots (not shown) and activation energies of 65.9, 64.5, 62.4 and 54.4 kJ/mol were calculated for NTR, 1 mM Ni, 1 mM Zn and 80 Ca solutions, respectively, corresponding to Q_{10}'s of 2.60, 2.55, 2.47 and 2.20.

Table 4.4. Effect of temperature on τ_D. M.e.p.c.s were recorded extracellularly (except in 80 Ca, where cells were voltage-clamped at -130 mV). Values of Q_{10} and activation energy for individual cells were obtained from least squares fits to Arrhenius plots, and are shown as mean ± 1 SEM. M.e.p.c.s were recorded at a minimum of 3 temperatures over at least a 15°C range. n, number of cells.

Solution	Activation Energy kJ/mol	Q_{10}	n
NTR	68.3 ± 3.0	2.66 ± 0.1	5
80 Ca	57.9 ± 4.9	2.33 ± 0.3	3
1 mM Zn	65.7 ± 3.8	2.60 ± 0.1	3
1 mM Ni	63.1 ± 3.7	2.50 ± 0.1	4

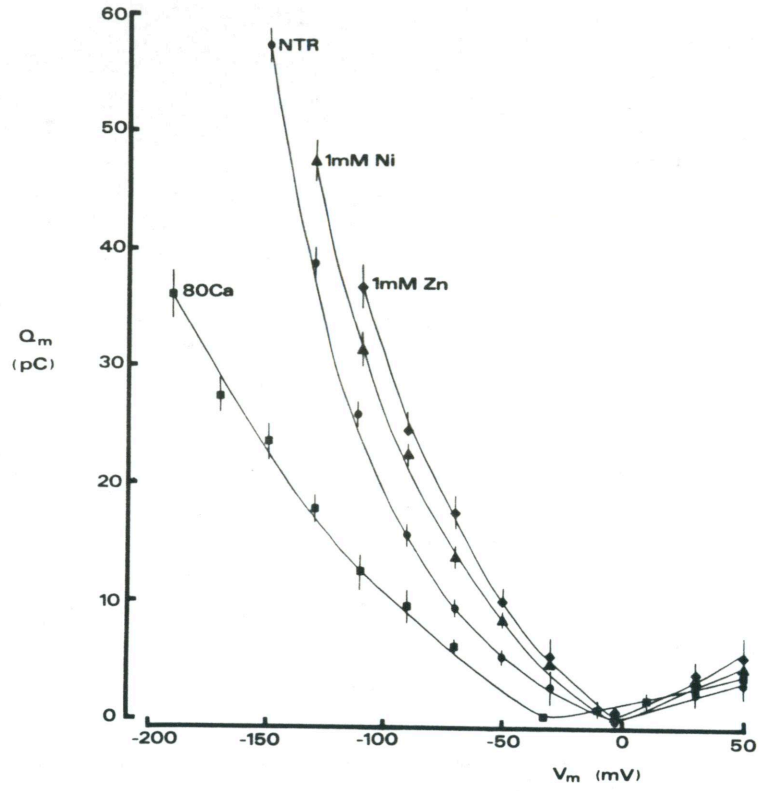

Figure 4.15. Voltage sensitivity of charge transfer during a m.e.p.c. Q_m (in pC) was calculated from $I_p \times \tau_D$. In 1 mM Ni or Zn, charge transfer was greater than in NTR, whereas in 80 Ca solution, Q_m was smaller. Temperature, 15°C.

charge movement (calculated using m.e.p.c. peak amplitude x τ_D) at -110 mV was 36.8 ± 1.5, 30.7 ± 0.9, 25.9 ± 0.7 and 12.2 ± 1.4 pC for 1 mM Zn, 1 mM Ni, normal toad Ringer and 80 Ca solutions, respectively (15°C).

Discussion

Channel lifetime, whether estimated from the time constant of decay of m.e.p.c.s or from fluctuation analysis, was clearly increased in the presence of the divalent cations and this is in agreement with some previous observations. Tenfold increases in Ca and Mg concentrations (from 1 to 10 mM) have been reported to cause increases in τ_D in frogs that would occur with hyperpolarizations of about 20 and 12 mV respectively (Cohen & Van der Kloot, 1978). It has also been found that end-plate currents recorded in solutions containing 8-10 mM Mg have a 50% greater time constant of decay than e.p.c.s recorded at curare-blocked (3 μM) end-plates (Mallart & Molgó, 1978). In both cases, the voltage sensitivity of τ_D was unchanged. In earlier experiments, it had been found that miniature end-plate potentials and end-plate potentials recorded in isotonic calcium (Na-free) solutions have very prolonged decay phases (Katz & Miledi, 1969). An increase in membrane resistance may partly account for this, but the decay of end-plate currents was probably prolonged also. In contrast, some workers have found that an increase in calcium concentration decreases or has little effect on the time constant of decay of end-plate currents. For example, Bregestovski et al. (1979) found that 10 mM Ca caused little change in τ_D, but that in isotonic Ca solution (82 mM $CaCl_2$, 0 NaCl) τ_N approximately halved, with no change in voltage sensitivity. Magleby & Weinstock (1980) reported a 17% decrease in τ_D and an 8% decrease in τ_N in 10 mM Ca solution but they did find that τ_D was increased by 80% and τ_N by 50% in the presence of 10 mM Ni. The voltage sensitivity of τ_D was unchanged either by Ca or Ni. We are unable to explain these divergent findings. A remote possibility is that there may be species differences: we used toads whereas most of the other work was done with frogs.

The increase in τ_D we have seen seems unlikely to have resulted from an anticholinesterase action of the divalent cations, as similar

increases in τ_N were observed (Table 4.3, Figs. 4.8 and 4.13), and 3 μM prostigmine caused a further increase in τ_D in 80 Ca solution (Fig. 4.7).

It has been suggested (Cohen & Van der Kloot, 1978; Van der Kloot & Cohen, 1979) that calcium ions may increase τ_D by reducing the surface charge potential (Hille, Woodhull & Shapiro, 1975). Our results are not completely compatible with this hypothesis. Raising Ca concentration from 1.8 to 20 mM increased $\tau_D(0)$ from 2.02 ± .14 to 2.47 ± .30 ms. Using an external surface charge density of 10^{-5} C/cm^2, similar to the value of 0.8×10^{-5} C/cm^2 used by Lewis (1979), the above change in ionic strength would be expected (Grahame, 1947)[1] to screen surface charge and result in a hyperpolarization, $\Delta\psi$, of 17 mV. Using the H value for NTR at 15°C (Table 4.2) and assuming that the change in τ_D as calcium concentration was increased could be explained solely in terms of surface charge screening, it can be calculated that $\tau_D(0)$ in the 20 Ca solution would be 2.38 ± 0.18 ms (experimental value, 2.47 ± 0.30 ms) and $\tau_D(0)$ in the 80 Ca solution would be 2.69 ± 0.22 ms (experimental value 3.46 ± 0.40 ms). It can be seen that the increase in $\tau_D(0)$ in the 20 Ca solution is consistent with simple screening of surface charge by the increased ionic strength. However, the increase in $\tau_D(0)$ in the 80 Ca solution is somewhat greater than predicted. This higher value in the 80 Ca solution may possibly be due to some specific binding of calcium to surface charge but it seems more likely that calcium ions have some other action that increases channel lifetime.

---

[1] These values were obtained by solving numerically for ψ in the surface charge equation (Grahame, 1947), which may be re-expressed as

$$\sigma = [2\ \varepsilon\ \varepsilon_o RT \sum_i m_i\ (e^{-ZF\psi/RT} - 1)]^{\frac{1}{2}}$$

where σ is the surface charge density in C.m^{-2}, ε is the relative dielectric constant, ε_o is the permittivity of free space (= 8.854×10^{-12} F.m^{-1}); R and T are the gas constant and temperature in °K so that $(2\ \varepsilon\ \varepsilon_o RT)^{\frac{1}{2}} = 1.86 \times 10^{-3}$ C.m$^{-\frac{1}{2}}$.mole$^{-\frac{1}{2}}$ and m_i is in moles.m^{-3}.

An alternative possibility is that the value of surface charge density assumed is too low. If a higher value of 1.6×10^{-5} C/cm^2 is used for surface charge density, as seems appropriate for the ion gating system of Na channels (Hille et al., 1975), then $\Delta\psi$ in 80 Ca solution (relative to NTR) becomes 35.7 mV and the predicted value of $\tau_D(0)$ is 2.84 ± .25 ms. However, this is still somewhat lower than the experimental value of 3.46 ± .40 ms. It should be noted that if a lower value of 0.2×10^{-5} C/cm^2 is chosen for surface charge density (Adams, Dwyer & Hille, 1980) then $\Delta\psi$ in 20 Ca solution would be 3.8 mV and the predicted value of $\tau_D(0)$ becomes 2.09 ± .15 ms, which is barely different from the value in NTR and is somewhat lower than the experimental value of 2.47 ± .30 ms. The deviation between observation and prediction is even greater with 80 Ca solution. The increases in $\tau_D(0)$ produced by Zn and Ni are even more difficult to explain in terms of screening of negative surface charges. For example, it can be calculated, (assuming a charge density of 10^{-5} C/cm^2) that the addition of 1 mM Zn would increase the actual transmembrane voltage by only 2 mV due to screening of negative fixed surface charge (see Fig. 4.16), yet Zn (and Ni) cause much greater lengthening than 20 Mg, 20 Ca or 80 Ca solutions. It may be that Zn and Ni bind specifically to membrane fixed charge and exert a much greater effect on surface potential than would be expected if they simply screened surface charge. Such an explanation was originally proposed by Huxley (in Frankenhaeuser & Hodgkin, 1957) to account for the shifts in voltage-dependent membrane characteristics produced by increases in external Ca concentration. Consistent with this hypothesis is the observation that both Zn and Ni are among the most potent divalent cations in shifting the voltage-dependence of Na activation curves in nerve membranes, and that Ca and Mg have much smaller effects (e.g. Hille et al., 1975; Blaustein & Goldman, 1968). However, for lipid bilayers, McLaughlin, Szabo &

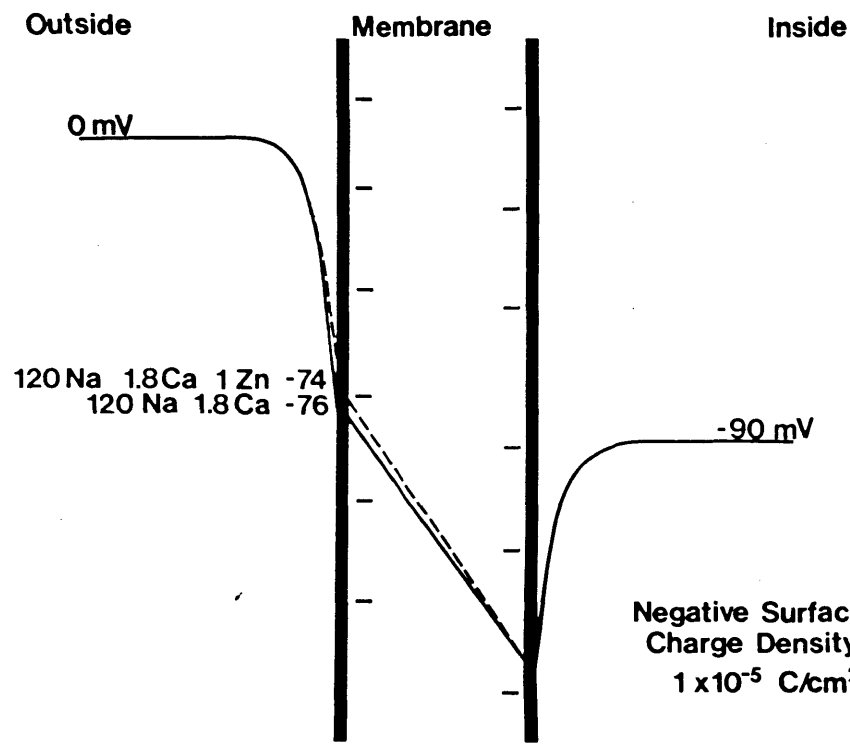

Figure 4.16. The effect of 1.0 mM Zn on the potential arising from fixed negative surface charges. Surface potential was calculated using the Grahame (1947) equation, with an average fixed charge density of $1x10^{-5}$ C/cm^2 (assuming that Zn simply screened and did not bind specifically to the fixed charges). An effective transmembrane hyperpolarization of only 2 mV results from the screening effects of 1.0 mM Zn on the surface charge potential.

Eisenman (1971) showed that the major effect of increasing divalent cation concentration (in the range 100 μM to 100 mM) on surface potential arises from a simple screening mechanism, irrespective of whether the ion exhibits pure screening or whether it both binds and screens. Cations that exhibit pure binding, like UO_2 (divalent) and Th (tetravalent) were effective at concentrations of 1-10 μM. In preliminary experiments, no lengthening of τ_D was seen when Th was added to normal toad Ringer to give final concentrations of 1 or 20 μM (Takeda, unpublished observations). On the other hand, surface potential calculations assume a uniform, 'smeared' fixed charge density. If the end-plate region has abnormally high fixed charge density, local potential changes may be much greater for cations like Zn and Ni, which have apparently higher association constants.

The effects of the divalent cations on m.e.p.c. peak conductance and on single channel conductance are not easily explained by surface potential changes. Certainly, negative surface charges may give membrane cation concentrations which are significantly greater than in the bulk solution. Assuming a fixed charge concentration of 10^{-5} C/cm^2, the surface concentration of monovalent cations in normal toad Ringer would be 20 times greater than in the bulk solution. In contrast, monovalent anions would be decreased to about one twentieth of their bulk solution values. A tenfold decrease in the surface charge would reduce this surface concentration ratio from 20 to 1.6. In these terms, cations causing the largest effective hyperpolarizations (and the greatest increases in τ_D) might be expected to reduce conductance the most. However, Zn and Ni, the most potent cations in prolonging τ, reduced both G_p and γ to a much smaller extent than 80 Ca solution. Of course, the conductance of end-plate channels may not be set solely by surface cation concentrations (although, the bulk concentration does affect γ;

Barry et al., 1979a; Lewis, 1979). In the neutral site end-plate channel model (Barry et al., 1979a), absolute values of conductance tend to be independent of surface potential because the conductance is influenced by both cation and anion concentrations, even though the anion mobility is considered to be small. Thus the reciprocal changes in surface concentrations of anions and cations (of the same absolute valency) caused by surface potential shifts would tend to balance each other with respect to the channel conductance. The possibility that the low anion permeability of end-plate channels is due to a very low surface anion concentration caused by negative surface charge seems unlikely because other ACh-activated channels can have a high chloride conductance (e.g. Kehoe, 1972), although presumably the surface membrane bears negative charges also. Finally, it should be noted that the normal voltage sensitivity of τ_D in the presence of the divalent cations is consistent with surface potential shifts.

A simple explanation for ion-dependent changes in τ is that permeant ions bind to intrachannel sites and create a favourable energy conformation for the open channel: thus, less mobile ions (producing a lower channel conductance) would give a longer channel open time (Van Helden et al., 1977; Ascher et al., 1978; Gage & Van Helden, 1979; Marchais & Marty, 1979). Similarly, Kolb & Bamberg (1977) originally proposed that, in lipid bilayers, the longer Gramicidin A channel lifetimes observed with increasing cation concentrations resulted from an 'electrostatic stabilization' of (open) channels containing permeating ions. For ACh-activated channels, the evidence rests on the reciprocal changes in τ and γ seen with monovalent alkali cations at the end-plate giving rise to constant charge transfer (Van Helden et al., 1977; Gage & Van Helden, 1979) and on the increased voltage sensitivity of τ observed in the presence of divalent cations in aplysia (Ascher et al., 1978;

Marchais & Marty, 1979). However, ion dependent increases in both τ and γ occur at the end-plate (Takeda et al., 1980 ; Nonner et al., 1980) and in aplysia (Ascher et al., 1978). Clearly, the divalent cations result in a total charge transfer different from normal. Marchais and Marty (1979) showed that, for divalent cations, surface potential shifts cannot account for both the prolonged τ, and for the increased voltage sensitivity of τ. Rather, they proposed that the voltage dependence of τ arises from the ions binding to intrachannel sites and encountering asymmetric energy barriers. A corollary would be that low temperatures should favour divalent cations binding and result in an increased voltage sensitivity of τ. The normal voltage and temperature sensitivity of τ observed here in the presence of divalent cations (see also Magleby & Weinstock, 1980; Miledi & Parker, 1980) is difficult to reconcile with the Marchais & Marty (1979) model. Other workers (Bregestovski et al., 1979; see also references in Marchais & Marty, 1979) have also observed normal voltage sensitivities of τ in isotonic Ca solutions.

Permeability ratios calculated from null (zero current) potentials have been compiled for an exhaustive list of cations, both organic and metal, monovalent and divalent (Van Helden et al., 1977; Linder & Quastel, 1978; Lewis, 1979; Gage & Van Helden, 1979; Watanabe & Narahashi, 1979; Dwyer, Adams & Hille, 1980; Adams et al., 1980). Some anomalies appear when these ratios are compared to conductance values obtained from noise analysis (Barry et al., 1979a; Takeda et al., 1980 ; Nonner et al., 1980). As permeability ratios obtained from null potential measurements using the Goldman-Hodgkin-Katz Constant Field Equation give good estimates of conductance ratios only in systems where the independence principle applies, it seems necessary to conclude that ion interaction occurs, which could give rise to competition, blocking or saturation effects. Values of P_{Ca}/P_K obtained from null potential measurements using the Constant Field Equation are dependent on the surface charge

density assumed (Lewis, 1979; Adams et al., 1980). In solutions containing only permeant monovalent cations, permeability ratios are independent of surface charge density, as the effects of surface potentials are exactly balanced by the changes in surface concentration of cations. If surface charge effects are ignored, $P_{Ca}/P_K = 0.14$. On the other hand, with a surface charge density of 10^{-5} C/cm^2, $P_{Ca}/P_K \simeq 0.04$.

The increase in m.e.p.c. peak conductance in 80 Ca solution with increasing membrane depolarization (Fig. 4.6) can be explained if Ca, like Li (Barry et al., 1979a)and NH_4 (Takeda et al., 1980), has a very much lower mobility than K. The voltage dependence of conductance then results from the asymmetrical nature of the solution composition. At depolarizing potentials the channel tends to be occupied by K ions with a reasonably high mobility and so the conductance is high, whereas at hyperpolarizing potentials the channel tends to be occupied by Ca ions with a much lower mobility and hence a resultant lower conductance. The actual slope of the conductance-voltage curve and the absolute value of conductance is dependent on the value of the Ca equilibrium constant. Quantitative fitting of the data to either neutral or charged site models was not undertaken because of the considerable theoretical complications arising from divalent and monovalent ions competing for sites in models where the independence principle is violated.

The blocking actions of some anaesthetics and partial agonists have been interpreted in terms of the blocking molecule entering open end-plate channels and binding to some critical intrachannel site, thereby presumably decreasing the flow of permeant ions (Adams, 1976b, 1977b;Ruff, 1977; Adams & Sakmann, 1978a;Neher & Steinbach, 1978). For Gramicidin A channels, Bamberg & Läuger (1977) have proposed that the blocking effects of Ca and Mg (which are impermeable) result not from binding to an intrachannel site, but rather to a site distinct from the main pathway for permeant ions, thus impeding the access of permeable

ions to the channel. Also by analogy with the effects of quaternary ammonium ions on K channels (Armstrong, 1975), blocking molecules could exert their actions from sites just outside the channel proper. However, the fact that Ca is permeant suggests, that in 80 Ca solution, the increased τ and smaller γ arises from interaction of Ca with intra-channel sites. On the other hand, although no experiments have been reported for isotonic Zn solutions, the high potency of 1 mM Zn in prolonging τ (without a corresponding decrease in γ) indicates that the mechanism of action for Zn might be different. It may be that blocking and permeant ions compete for the same site(s). A more likely explanation would be that Zn directly affects the 'gate' that controls channel life-time (Begenisich & Lynch, 1974; Armstrong & Gilly, 1979). The effects of Ni-containing solutions were similar to those reported by Magleby & Weinstock (1980). Moreover, Miledi & Parker (1980) have shown that strontium ions lengthen channel lifetime without greatly altering either the single channel conductance or the normal voltage sensitivity of τ.

In aplysia neurones, increases in both Ca and Mg concentrations result in marked increases in the average lifetime of ACh-activated (excitatory) synaptic channels (Ascher, Marty & Neild, 1978; Marchais & Marty, 1979; Marty, 1980), as judged from voltage-jump relaxation measurements and noise analysis. Similarly, Kuba & Nishi (1979) have also reported that small increases in Ca concentration (from 1.8 to 7.2 mM) cause significant lengthening of the half-decay time of the fast, (ACh-activated) excitatory postsynaptic current in bullfrog sympathetic ganglion cells, without altering the voltage-dependence of τ. It remains to be resolved whether or not the apparent discrepancy regarding the action of divalent cations (especially Ca and Mg) in prolonging τ is real, or whether it perhaps arises due to species-specific or technique-dependent differences.

CHAPTER FIVE

EFFECTS OF CHANGES IN EXTERNAL ION CONCENTRATIONS ON TOAD END-PLATE CHANNELS

Introduction

In a number of previous studies, the effects of varying the external sodium and potassium ion concentrations on the null potential of end-plate channels have been examined. The Takeuchis (1960; 1963a,b) first showed that marked shifts in the null potential (ε_o) occurred with decreases in external potassium concentration , and that these changes were not predicted by a Goldman-Hodgkin-Katz type of equation (GHK). The Takeuchis also reported that the sodium-dependence of ε_o was poorly described by a GHK formulation. However, subsequent investigations are not in agreement with the early observations, as they show that ε_o at ACh-activated end-plate channels essentially follows GHK predictions for changes in external concentrations of both sodium and potassium ions (e.g. Magazanik & Potopova, 1969; Steinbach, 1975; Ritchie & Fambrough, 1975; Linder & Quastel, 1978; Lewis, 1979; Barry, Gage & Van Helden, 1979a; Adams et al., 1980; see Chapter 1).

It is clear that single channel conductance depends on external sodium concentration at the end-plate (Linder & Quastel, 1978; Lewis, 1979; Barry et al., 1979a; Horn & Patlak, 1980; Redmann, 1980; Hamill, Marty, Neher, Sakmann & Sigworth, 1981; Adams, Nonner, Dwyer & Hille, 1981). On the other hand, relatively few observations of the effects of different external sodium concentrations on channel lifetime have been reported (but see Redmann, 1980; Adams et al., 1981). A more detailed study of concentration-dependent changes in end-plate channel characteristics was undertaken, as the nature of permeant monovalent and divalent cations is known to importantly influence both channel lifetime and conductance of ACh-activated channels (e.g. Van Helden, Hamill & Gage, 1977; Ascher, Marty & Neild, 1978; Bregestovski, Milèdi & Parker, 1979; Marchais & Marty, 1979; Gage & Van Helden, 1979; Takeda, Barry &

Gage, 1980; Takeda, Gage & Barry, 1981; Adams et al., 1981).

Ion-dependent changes in channel characteristics may be related to permeant ions binding to some critical intrachannel sites as they pass through the channel (Kolb & Bamberg, 1977; Marchais & Marty, 1979). Channel selectivity and conductance are then obviously affected by both the nature of the permeant ion and of the actual ion-binding site(s) (Barry et al., 1979a; Adams et al., 1980). Little is known about these sites or their numbers within the channel lumen. Also, it is not apparent how ion-binding is related to channel lifetime.

The experiments described here were firstly, to examine changes in ε_o at toad end-plate channels with varying external sodium and potassium concentrations and secondly, to measure single channel conductance and average channel lifetime in solutions containing a wide range of sodium ion concentrations. The overall goal was to gain further insight into the nature of ion permeation through end-plate channels and the underlying molecular mechanism which normally regulates channel lifetime.

Methods

As in the previous two Results Chapters, the experimental protocol followed was essentially that given in Chapter Two. M.e.p.c.s and noise were recorded from voltage-clamped, glycerol-treated sartorius muscle fibres from the toad. Decreased sodium solutions were made isosmotic with mannitol. In some cases, ionic strength was kept constant by substituting glucosamine HCl or $MgCl_2$ for NaCl, in order to minimize the effects of changes in surface charge potential (see Lewis, 1979). Hypertonic solutions contained added sodium glucuronate. In experiments with varying potassium concentrations, KCl was decreased or increased. No attempt was made to keep the [K]x[Cl] product constant (see Boyle & Conway, 1941; Hodgkin & Horowicz, 1959a,b). Details of solution compositions are listed in Table 5.1.

In solutions containing lowered sodium concentrations with glucosamine HCl, it was difficult to record m.e.p.c.s and noise. Glucosamine reduces channel conductance at frog end-plate (Adams et al., 1981) and in aplysia neurones (Marchais & Marty, 1980) by probably blocking the channel. End-plate currents (e.p.c.s) were evoked under voltage clamp by stimulating the sciatic nerve using a suction electrode in order to clarify the effects of low Na solutions on end-plate channel characteristics. Contraction was minimized by glycerol-treating the muscle and by adding 2 μM curare to the bathing solution.

Every attempt was made to obtain data from paired cells, that is in both control and test solutions. However, it was difficult to hold cells through some solution changes, especially when hypertonic solutions were introduced. Experiments were performed at 15°C. Data are presented as means ± one standard error of the mean (S.E.M.). Analysis of m.e.p.c.s and noise spectra were as outlined in detail in Chapter Two.

Table 5.1. Solution compositions (in mM). The pH of all solutions was 7.0-7.2. The osmolarity of the solutions was checked with a Fiske osmometer.

Solution	NaCl	KCl	$CaCl_2$	Na-HEPES	mannitol	(other)
4 Na	115	2.5	1.8	2	0	348 Na glucuronate
2 Na	115	2.5	1.8	2	0	116 Na glucuronate
Na (control)	115	2.5	1.8	2	0	-
3/4 Na	87	2.5	1.8	2	54	-
1/2 Na mannitol	58	2.5	1.8	2	112	-
1/2 Na glucosamine	54	2.5	1.8	6	0	58 glucosamine HCl
1/2 Na Mg	58	2.5	1.8	2	52	20 $MgCl_2$
1/4 Na mannitol	29	2.5	1.8	2	170	-
1/4 Na Mg	29	2.5	1.8	2	83	29 $MgCl_2$

Solutions with varying K concentrations were made by adding or deleting KCl directly. These solutions also contained 115 NaCl, 1.8 $CaCl_2$, 2 Na-HEPES.

It was necessary to calculate the internal ion concentrations in the various bathing solutions in fitting the ACh null potential data to the Goldman-Hodgkin-Katz equation. Estimates of control internal cation concentrations in glycerol-treated frog sartorius muscle fibres were obtained from Venosa & Horowicz (1973; Case (1): $[Na]_i$ = 17 mM, $[K]_i$ = 140 mM) and Henderson (1970; Case (2): $[Na]_i$ = 26.5 mM, $[K]_i$ = 114 mM). As previously noted (see Chapter 2), the membrane potential in glycerol-treated preparations was decreased to -60 to -70 mV, and for the estimation of the internal anion concentration in control solution, a value of -65 mV was assumed. The predictions for membrane potential in the other solutions were essentially independent (± 1 mV) of the initial internal concentrations chosen. When the external solution was changed, it was possible to calculate the new internal ion concentrations, assuming that, (1) Cl ions were in equilibrium with the membrane potential (e.g. Hodgkin & Horowicz, 1959a,b), (2) the membrane potential was set by the Na and K ion gradients and that P_{Na}/P_K was concentration independent, (3) osmotic equilibrium was maintained across the cell membrane, and (4) electroneutrality existed inside the cell. The calculated internal concentrations and the expected membrane potential for the different bathing solutions are given in Table 5.2.

The ACh null potential was predicted using the generalized current form of the Goldman (1943)-Hodgkin-Katz (1949) equation (e.g. Lassignal & Martin, 1977):

$$I = \sum_{j=1}^{n} \left[\frac{Z_j^2 \, \varepsilon_o P_j \, F^2}{RT} \left\{ \frac{(a_j^o - a_j^i)\exp(Z_j F \varepsilon_o / RT)}{(1-\exp(Z_j F \varepsilon_o / RT))} \right\} \right] ,$$

where Z is the valence, ε_o is the null (zero) current potential, P is the permeability, a^o and a^i are the outside and inside ion activities and F, R and T have their usual thermodynamic meanings. The equation was solved by setting I=0, summing over all ions (j) and calculating the value of ε_o using an iterative (Newton-Raphson) technique. Two types

of predictions were made: (1) the surface charge density was considered to be 0 on both membrane surfaces and (2) surface charge densities (σ) of 1.0×10^{-5} C/cm^2 and 0.5×10^{-5} C/cm^2 were assumed for the external and internal membrane surfaces, respectively (e.g. Hille et al., 1975; see Chapter 4, Discussion). Surface charge potential shifts ($\Delta\psi$) were calculated numerically, using the Grahame (1947) equation (see Chapter 4, Discussion). Surface membrane activities were obtained from the equation:

$$a_j^{o,i} = C_j^{o,i} \exp-(Z_j \Delta\psi^{o,i} F/RT),$$

where $C_j^{o,i}$ is the bulk ion (j) activity and o and i refer to the outside and inside, respectively. The value of ε_o was also corrected for the calculated $\Delta\psi$. For the divalent cations, it was assumed that $P_{Ca}/P_K \cong P_{Mg}/P_K \cong 0.15$ when $\sigma=0$, and 0.05 with the values of σ given above (see Chapter 4; Adams et al., 1980). Using the observed control ε_o (see Table 5.4) of -2.3 mV, it was possible to calculate 4 values of P_{Na}/P_K. For the Case (1) initial internal concentrations (see above), P_{Na}/P_K = 1.236 and 1.239 while for Case (2), P_{Na}/P_K = 1.092 and 1.098, with and without a correction for $\Delta\psi$, respectively. It can be seen (Table 5.4) that the uncertainty in P_{Na}/P_K does not significantly affect the predicted ε_o in the different bathing solutions, because of the compensating changes in the calculated internal ion concentrations (assuming, of course, that P_{Na}/P_K is concentration independent).

Table 5.2. Predicted internal ion concentrations and membrane potentials. See text for details of the method of calculation. Two estimates of internal concentrations are given (Case (1), initial $[K]_i$ = 140 mM, $[Na]_i$ = 17 mM and Case (2), initial $[K_i]$ = 114 mM, $[Na]_i$ = 26.5 mM in control) for the Na solutions. The effective valency of the internal indiffusible anions (A^-) is 1.91 (Case 1) and 1.40 (Case 2). For K, only Case (1) is considered. Concentrations are given in mM. Temperature, 15°C.

Solution		[K]	[Na]	[Cl]	[A^-]	V_m (mV)
	OUT	2.5	464	121.1		
4 Na	IN(1)	573.9	69.7	7.1	318.0	-70.6
	IN(2)	467.7	108.7	6.7	385.9	-71.9
	OUT	2.5	232	121.1		
2 Na	IN(1)	285.4	34.7	7.6	158.1	-68.7
	IN(2)	232.6	54.4	7.4	192.0	-69.5
	OUT	2.5	116	121.1		
Na (control)	IN(1)	140	17	8.8	77.6	-65
	IN(2)	114	26.5	8.8	94.1	-65
	OUT	2.5	88	93.1		
3/4 Na	IN(1)	144.3	17.5	5.4	79.9	-70.8
	IN(2)	117.4	27.3	5.5	96.9	-70.3
	OUT	2.5	59	64.1		
1/2 Na mannitol	IN(1)	147.5	17.9	2.8	81.7	-77.9
	IN(2)	120.0	27.9	2.9	99.0	-76.8
	OUT	2.5	59	118.1		
1/2 Na glucosamine	IN(1)	144.5	17.5	5.2	80.0	-77.3
	IN(2)	117.4	27.3	5.5	96.9	-76.3
	OUT	2.5	59	104.1		
1/2 Na Mg	IN(1)	145.3	17.6	4.6	80.5	-77.5
	IN(2)	118.1	27.5	4.8	97.4	-76.5
	OUT	2.5	30	35.1		
1/4 Na mannitol	IN(1)	149.7	18.2	1.1	82.9	-87.1
	IN(2)	121.8	28.3	1.2	100.5	-84.9
	OUT	2.5	30	93.1		
1/4 Na Mg	IN(1)	147.5	17.9	2.8	81.7	-86.8
	IN(2)	119.8	27.9	3.1	98.8	-84.5

..../2

(Table 5.2 - cont.)

Solution		[K]	[Na]	[Cl]	[A^-]	V_m (mV)
0.5 K	OUT	0.5	116	119.1		
	IN	139.8	17.0	7.0	77.4	-70.3
1.0 K	OUT	1.0	116	119.6		
	IN	139.8	17.0	7.5	77.5	-68.9
1.5 K	OUT	1.5	116	120.1		
	IN	139.9	17.0	7.9	77.5	-67.5
2.5 K (control)	OUT	2.5	116	121.1		
	IN	140	17	8.8	77.6	-65
5 K	OUT	5.0	116	123.6		
	IN	140.2	17.0	11.2	77.7	-59.6
10 K	OUT	10.0	116	128.6		
	IN	140.2	17.0	16.2	77.7	-51.4

It should be noted that the calculated internal concentrations in hypertonic solutions may well be in error due to the (presumed) increase in the activity of the Na/K pump. No correction factor was applied, as the predicted V_m in 4 Na solution when $[Na]_i$ was set to 17 mM became -72.6 mV (compared to the original prediction of -70.6 mV)

Results

Acetylcholine Null Potentials

Effects of Anions

The Takeuchis (1960, 1963a) originally observed that anions had no measurable permeability through end-plate channels (see also Oomura & Tomita, 1960). Later investigations have all supported this observation (e.g. Ritchie & Fambrough, 1975; Steinbach, 1975; Lassignal & Martin, 1977; Linder & Quastel, 1978; Adams et al., 1980). In the absence of any significant anion permeability, many theoretical descriptions of the zero-current potential reduce to a Goldman (1943)-Hodgkin-Katz (1949) type of equation (GHK), even though they often are more broadly-based than the original GHK formulation (see Barry & Diamond, 1971; Barry et al., 1979a). This important assumption was checked for toad end-plate channels in experiments where NaCl was replaced with equimolar amounts of the Na salt of various test anions (Table 5.3). There was no significant difference in the ACh null potential ($\mathcal{E}_o$) when tested with the following anions: Cl, Br, acetate, nitrate, sulphate, propionate and glucuronate (see Table 5.3). Null potentials were determined by measuring the potential at which the iontophoretically applied ACh-induced end-plate current "reversed" direction under voltage clamp in the various anion solutions.

Effects of Cations

Sodium

When the external sodium concentration was varied, marked shifts in the null potential occurred, as is illustrated in Fig. 5.1A. The values of the null potential in the various Na solutions are given in Table 5.4 and were calculated by averaging interpolated zero-current potentials obtained using m.e.p.c.s, nerve-evoked e.p.c.s and ACh-iontophoretic responses. As has been suggested previously by Barry et al. (1979a), null potentials measured in solutions with decreased ionic

Table 5.3. Anion substitution does not significantly change the ACh null potential. Chloride in the normal solution was replaced using equimolar amounts of the test anions; all solutions also contained (mM): KCl, 2.5; $CaCl_2$, 1.8; Na Hepes buffer, 2; pH ~ 7.2. Null potentials were determined directly using ACh-iontophoresis under voltage clamp.

Temperature, 15°C; n, number of cells.

Solution	ε_o (mV)	n
Chloride	-2.3 ± 0.4	23
Bromide	-2.9 ± 1.2	3
Acetate	-0.8 ± 2.1	3
Nitrate	-1.5 ± 1.7	4
Sulphate	-2.1 ± 1.1	2
Propionate	-3.1 ± 1.9	3
Glucuronate	-2.7 ± 0.9	3

strength (i.e. where NaCl was simply replaced by an isomotic quantity of mannitol) tended to be less negative than those observed in solutions where the ionic strength was kept constant (e.g. 1/2 Na Mg, 1/2 Na glucosamine solutions; see Table 5.1). The lines in Fig. 5.1 were drawn through the Goldman-Hodgkin-Katz predictions for ε_o presented in Table 5.4. At low Na concentrations, the experimental Na-dependence of ε_o is adequately fitted by the GHK equation. However, it is clear that the observed values of ε_o in 2 Na and 4 Na solutions deviate significantly from the calculated GHK values. One possible reason for the discrepancy is that the end-plate channel current may become saturated at these high external Na concentrations. Alternatively, the calculated internal ion concentrations may not accurately reflect the true internal concentrations in hypertonic solutions. Also, the predicted GHK values in solutions containing Mg ions are rather more positive than observed (Table 5.4). It may be that the assumed P_{Mg}/P_K ($\cong$ 0.05 or 0.15, with and without a surface charge potential correction, respectively; see Methods) is too high. For example, if $P_{Mg}/P_K = 0$, then the predicted value of ε_o becomes -19.4 and -35.4 mV, for 1/2 Na Mg and 1/4 Na Mg solutions, respectively (assuming no surface charge potential correction). Using the surface charge density given in the Methods, and assuming $P_{Mg}/P_K = 0$, the calculated ε_o then becomes -19.2 and -34.9 mV. It should be noted that the GHK predictions are quite insensitive to the calculated internal ion concentrations (except in hypertonic Na solutions) and to the presence or absence of a surface charge potential correction (except in Mg-containing solutions with a significant P_{Mg}/P_K; see Chapter 4, Discussion).

Potassium

In contrast to the changes observed in ε_o with Na concentration, no large changes in ε_o were apparent when the external K concentration

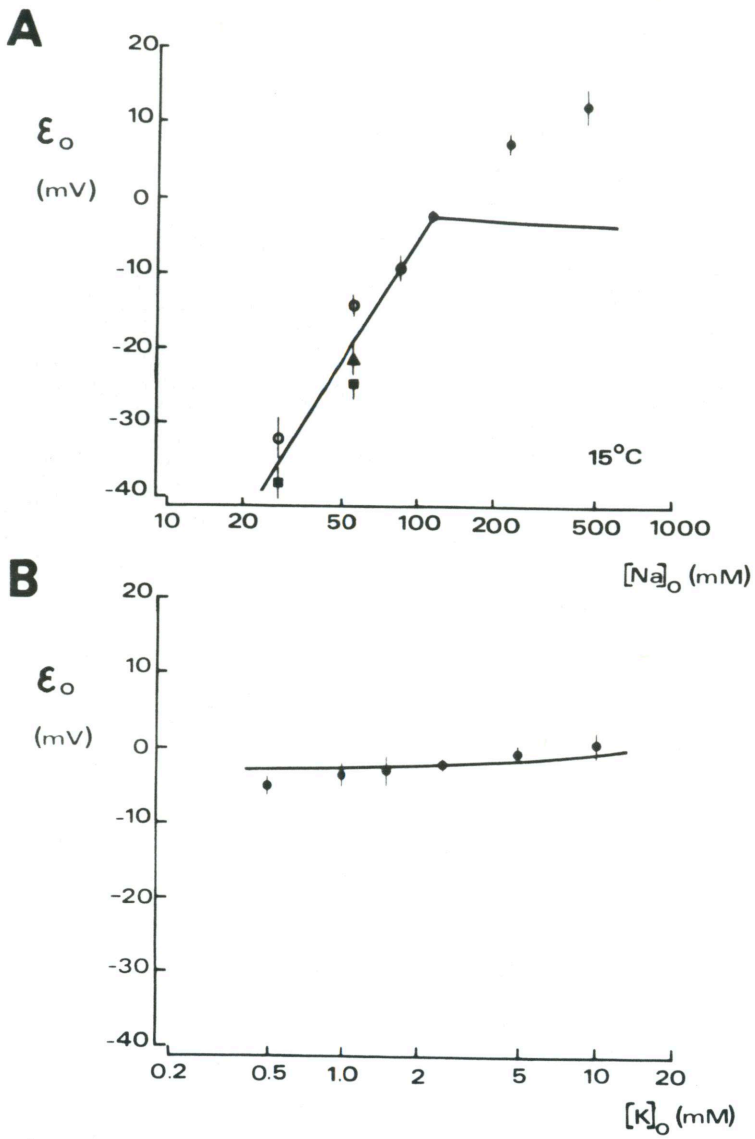

Figure 5.1. The sodium and potassium dependence of ε_o, the ACh null potential. A. The effect of changes in external Na concentration on ε_o. Hypertonic solutions contained added Na glucuronate. Low Na solutions were made isosmotic with mannitol (O) or also contained glucosamine HCl (▲) or $MgCl_2$ (■) as substitutes for NaCl when ionic strength was kept constant (see Table 5.1). B. The effect of changes in external K concentration on ε_o. The K concentration was varied by increasing or decreasing the KCl in the control solution. The lines were drawn through the calculated Goldman-Hodgkin-Katz values for ε_o in the different solutions ignoring the GHK predictions in Mg-containing solutions (see text). The thickness of the line represents the uncertainty in the GHK calculations (see Table 5.4). Temperature, 15°C.

Table 5.4. Comparison of the effects of sodium and potassium ion concentrations on the observed ACh null potential (ε_o) and the Goldman-Hodgkin-Katz predictions (GHK). The GHK values shown for varying $[Na]_o$ are the average values calculated for 4 cases (internal concentrations - cases (1) and (2) (see Methods; Table 5.2); with and without surface charge potential corrections). The uncertainties represent the range of the calculated values. For varying $[K]_o$, the GHK values are averages of 2 cases (internal concentration - case (1); with and without surface charge potential corrections).

Solution	$[Na]_o$ (mM)	Experimental		GHK
		ε_o (mV)	n	ε_o (mV)
4 Na	464	12.1 ± 2.8	4	-3.5 ± 0.2
2 Na	232	7.5 ± 2.1	3	-3.1 ± 0.1
Na (control)	116	-2.3 ± 0.4	23	-2.3
3/4 Na	88	-9.2 ± 1.8	3	-9.7 ± 0.1
1/2 Na mannitol	59	-14.1 ± 1.5	3	-19.6 ± 0.3
1/2 Na glucosamine	59	-21.4 ± 2.2	2	-19.1 ± 0.3
1/2 Na Mg	59	-24.5 ± 1.7	3	-15.8 ± 1.2
1/4 Na mannitol	30	-32.0 ± 3.1	3	-35.1 ± 0.8
1/4 Na Mg	30	-38.1 ± 2.9	2	-25.6 ± 3.0

Solution	$[K]_o$ (mM)	Experimental		GHK
		ε_o (mV)	n	ε_o (mV)
0.5 K	0.5	-5.4 ± 1.3	4	-2.7 ± 0.1
1.0 K	1.0	-3.6 ± 1.5	3	-2.6 ± 0.1
1.5 K	1.5	-3.1 ± 1.2	2	-2.5 ± 0.1
2.5 K(control)	2.5	-2.3 ± 0.4	23	-2.3
5 K	5.0	-0.9 ± 1.8	2	-1.8 ± 0.1
10 K	10.0	0.3 ± 2.1	4	-0.8 ± 0.3

was varied between 0.5 and 10 mM (see Fig. 5.1B). The experimental values and the GHK predictions for ε_o are given in Table 5.4. The observed K-dependence of ε_o appears to be well-described by the GHK equation, as has been previously reported (cf. Takeuchi & Takeuchi, 1960). Again, as noted for the Na-dependence of ε_o, the GHK predictions for ε_o with varying external K concentration are essentially unaffected by surface charge potential and the uncertainty in choosing the initial internal ion concentrations in control solution.

Miniature end-plate currents

End-plates were localized by recording m.e.p.c.s extracellularly or m.e.p.p.s with fast rise times ($\leq$ 1 ms) and amplitudes $\gtrsim$ 1 mV. Iontophoretic application of ACh to these regions produced large depolarizations with a rapid onset. The peak amplitude of m.e.p.c.s (I_p) was clearly dependent on the external Na concentration, as seen in Fig. 5.2. In 1/2 Na Mg solution, the average value of I_p at a holding potential of -50 mV was 1.2 ± 0.5 nA (n=4) while in 2 Na solution I_p was 4.3 ± 0.4 nA (n=4), which can be compared to the control (Na) value of 2.45 ± 0.2 nA (n=9). It was also apparent that Na concentration affected the time course of decay of m.e.p.c.s (Fig. 5.2). In solutions containing lowered Na concentrations, the time constant of decay (τ_D) of m.e.p.c.s was increased relative to the control value, while τ_D was decreased in high Na solutions. For example, τ_D was 5.0, 2.9 and 2.5 ms respectively, for averages of m.e.p.c.s obtained in 1/2 Na Mg, Na and 2 Na solutions, as illustrated in Fig. 5.2 (V_m = -50 mV, temperature, 15°C). Consistent with previous observations (e.g. Gage & McBurney, 1975), τ_D had an exponential dependence on membrane potential (Magleby & Stevens, 1972a,b). Average values of τ_D are shown plotted semilogarithmically against membrane potential in Fig. 5.2D for 1/2 Na Mg, Na and 2 Na solutions. The solid lines are least-squares regression fits to the equation (Magleby & Stevens,

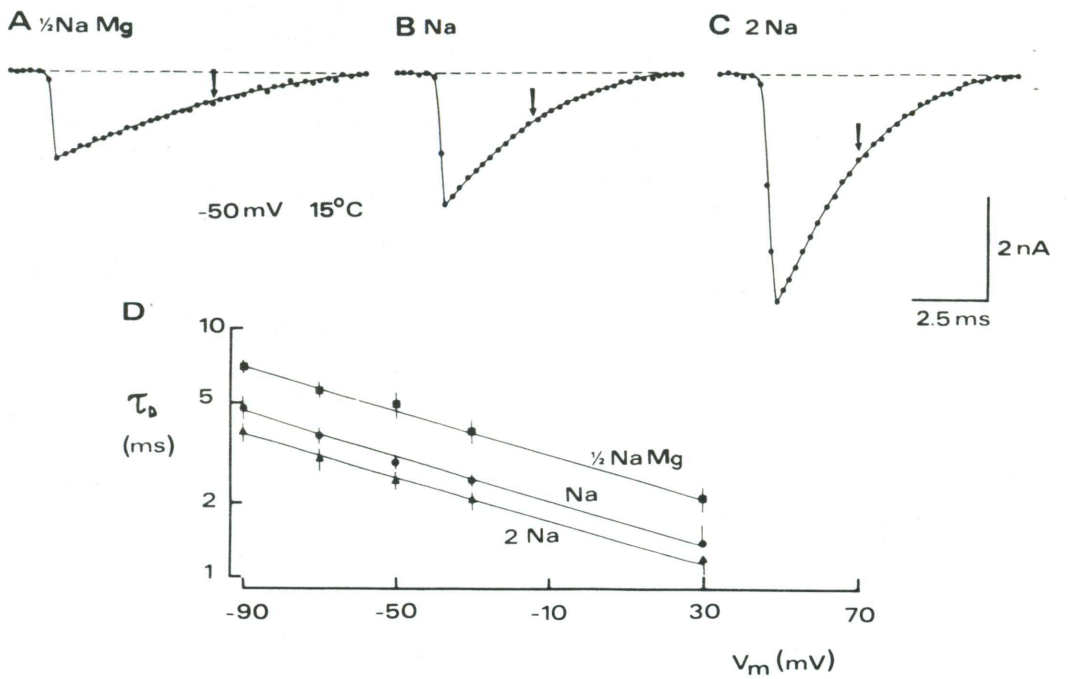

Figure 5.2. The effect of sodium concentration on m.e.p.c.s. Averaged m.e.p.c.s ($n \geq 15$) were obtained under voltage clamp (V_m = -50 mV) in: A, lowered Na solution (1/2 Na Mg). B, control solution (Na) and C, double Na solution (2 Na). M.e.p.c.s decayed exponentially and the time constant of decay (τ_D ; arrows) decreased with increasing [Na]: τ_D was 5.0, 2.9 and 2.5 ms, respectively in 1/2 Na Mg, Na and 2 Na solutions. The peak amplitude of m.e.p.c.s increased with increasing [Na].
D. Voltage dependence of τ_D. Average values of τ_D are shown at each potential. Regression lines were fitted to the data using: $\tau_D (V_m) = \tau_D(0)\exp(-V_m/H)$. Calculated H values were 98 mV (n=4), 100 mV (n=9) and 108 mV (n=4), respectively for 1/2 Na Mg, Na and 2 Na solutions.

1972a,b): $\tau_D(V_m) = \tau_D(0)\exp(-V_m/H)$, where H is the volt constant (or membrane potential required for an e-fold shift in τ_D) and $\tau_D(0)$ is the decay time constant at zero potential. It can be seen that τ_D (1/2 Na Mg) > τ_D (Na) > τ_D (2 Na) at all potentials and that the slopes of the lines (H values) were not significantly different from the control value of 100 mV. H values and $\tau_D(0)$ were also calculated for individual cells and are presented, averaged, in Table 5.5 for the different solutions.

Current-voltage curves for voltage-clamped m.e.p.c.s were obtained in solutions containing a variety of Na concentrations (Fig. 5.3A,B). It was clear that the peak m.e.p.c. amplitude (I_p) depended on Na concentration. Also, the I-V relationship was non-linear in all solutions: I_p at depolarized voltages was greater than I_p at (the same) hyperpolarized voltages, as has been previously reported (e.g. Kordaš, 1969; Magleby & Stevens, 1972a; Dionne & Stevens, 1975; Gage & Van Helden, 1979; Takeda et al., 1980, 1981). This non-linearity tended to be greater in high Na solutions (Fig. 5.3B).

The Na dependence of averaged time constants of decay of m.e.p.c.s (τ_D) is presented in Fig. 5.4A,B for a membrane potential of -90 mV. As the external Na concentration was raised, τ_D tended to decrease and appeared to 'saturate' at high Na concentrations. This apparent 'saturation' of τ_D with increasing Na concentration was suggestive of classical Michaelis-Menten enzyme kinetics (see Michaelis & Menten, 1913). The data shown in Fig. 5.4A were replotted in Fig. 5.4B as reciprocal rate constant (α^{-1}; ms) versus reciprocal external Na concentration ($[Na]_0^{-1}$; M^{-1}), following Lineweaver-Burk (1934). This transformation assumed that $\tau_D = 1/\alpha$ (i.e. that the opening rate constant $\beta \ll \alpha$;

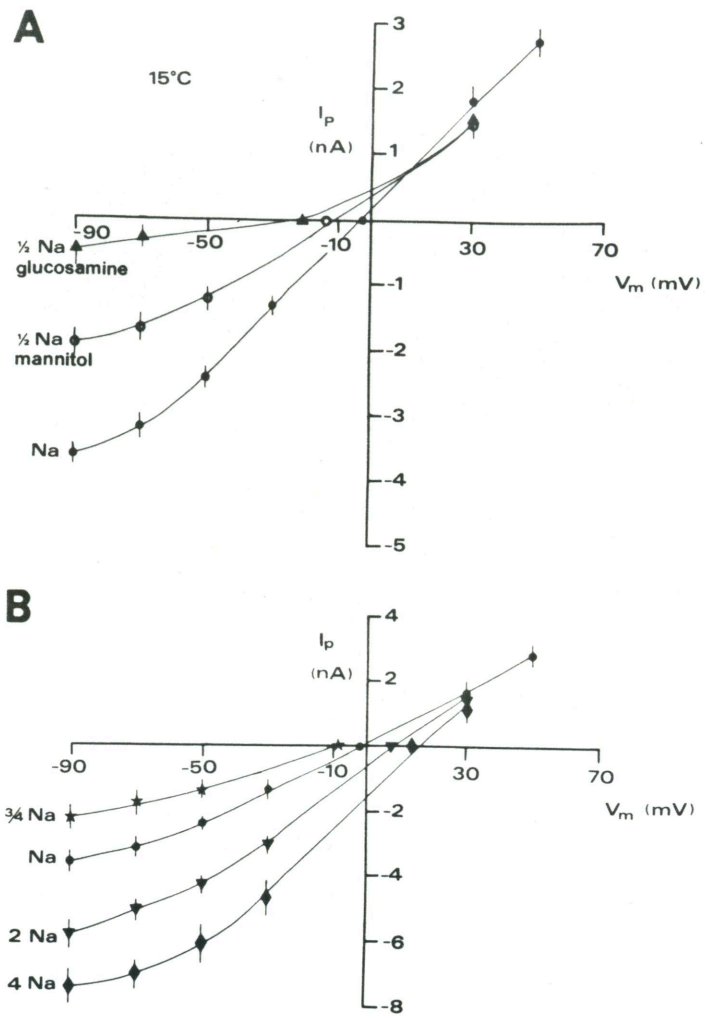

Figure 5.3. Effects of Na concentration on current-voltage relationships for voltage-clamped m.e.p.c.s. A. Peak m.e.p.c. amplitude (I_p) was reduced in decreased Na solutions, especially when glucosamine HCl (▲) was substituted for NaCl. No significant difference in I_p was apparent at positive membrane potentials. Data are averages from 3 cells (1/2 Na glucosamine), 4 cells (1/2 Na mannitol; o) and 8 cells (Na; ●), with the number of m.e.p.c.s at each potential ≥ 50. B. Increases in Na concentration result in larger values of I_p at negative, but not positive voltages. Averaged data from 3 cells (3/4 Na; ★), 4 cells (Na; ●), 3 cells (2 Na; ▼) and 4 cells (4 Na; ◆). Note the non-linearity of the I-V curves. Temperature, 15°C. The solid lines were drawn through the data points by eye.

Magleby & Stevens, 1972a,b; Anderson & Stevens, 1973; see Chapters One and Two) and that α would have a hyperbolic dependence on Na concentration (as is evident from the solid line shown in Fig. 5.4A). It was not a little surprising that the data fell on a fairly good straight line in the Lineweaver-Burk plot (Fig. 5.4B), especially if the 1/4 Na mannitol point is ignored - the correlation coefficient for the least squares regression line was 0.978. The inverse of the negative abscissal intercept (10.75 M^{-1}) is the Michaelis constant, K^m_{Na} (=93 mM). By analogy with enzyme kinetics, K^m_{Na} represents the apparent external Na concentration at which half-maximal velocity is reached (alternatively, the concentration at which one half of the 'sites' governing the channel closing mechanism are saturated). A note of caution should be sounded here, as no obvious reaction scheme in which the external Na concentration would affect the probability of channel closure (or protein conformational stability) is easily suggested (see Discussion). It should be noted that τ_D at low Na concentrations (e.g. 1/4 Na mannitol) or in the presence of glucosamine appears to deviate significantly from the regression line. However, m.e.p.c.s in these solutions have the smallest peak amplitudes and thus, the increase in τ_D is quite difficult to reliably measure because of the deteriorating signal-to-noise ratio.

As shown previously (Cohen & Van der Kloot, 1978; Ascher et al., 1978; Marchais & Marty, 1979; see Chapter 4), the presence of high Mg concentrations leads to an increased τ and a smaller I_p. However, the Na concentration here in 1/2 Na Mg solution is 58 mM, whereas it was 90 mM in 20 Mg solution (see Chapter 4). Adams et al. (1981) have also recently reported that τ was increased 2 to 3-fold in 1/2 Na glucosamine solution, while the single channel conductance was greatly decreased.

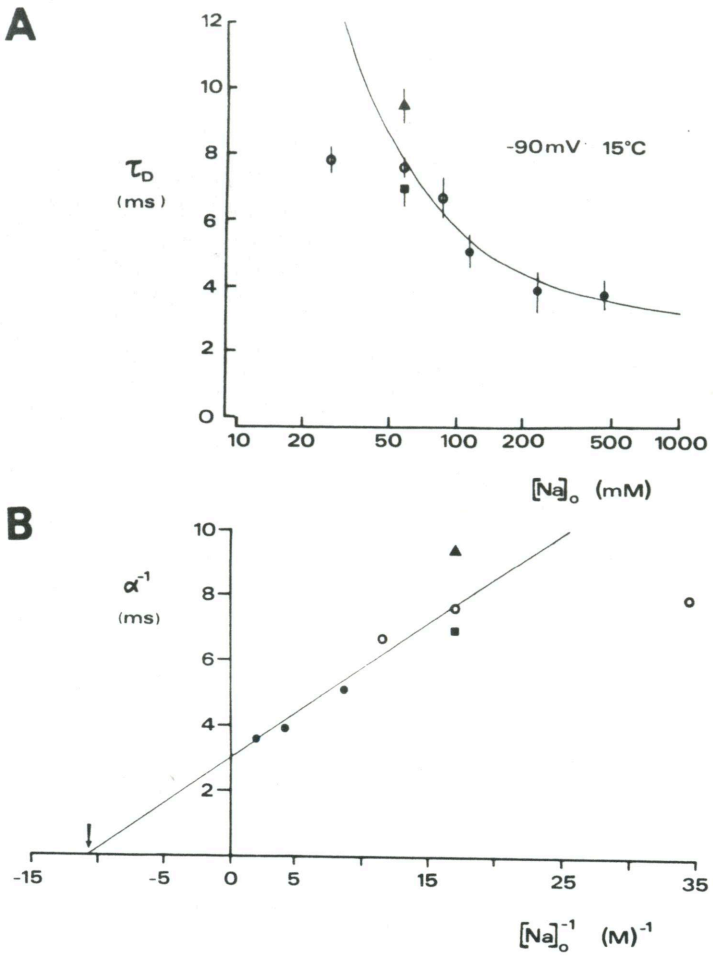

Figure 5.4. The time constant of decay (τ_D) of m.e.p.c.s depends on Na concentration. A. Average values of τ_D obtained under voltage clamp at -90 mV plotted as a function of Na concentration. NaCl was replaced with mannitol (o) or $MgCl_2$ (■) or glucosamine HCl (▲). The solid line is the predicted curve derived from the regression line shown in B. Note the logarithmic abscissa. B. Lineweaver-Burk plot of the reciprocal closing rate constant (α^{-1}) vs. reciprocal Na concentration. A least-squares regression line was fitted through the data, arbitrarily ignoring the points ■, ▲ and the 1/4 Na point (right most o). The correlation coefficient was 0.978. The negative abscissal intercept, 10.75 M^{-1}, yields the Michaelis constant (K^m_{Na}), which was 93 mM. Temperature, 15°C.

Glucosamine Containing Solutions

In addition to the increase in τ_D in 1/2 Na glucosamine solution, it was also observed that peak m.e.p.c. amplitude (I_p) was markedly decreased at hyperpolarized potentials when compared to I_p in 1/2 Na Mg or 1/2 Na mannitol solutions (see Fig. 5.3A), but not at depolarized potentials. Previous reports have suggested (Marchais & Marty, 1980; Adams et al., 1981) that glucosamine blocks open ACh-activated channels, and that this might partly account for its apparent low permeability (e.g. Lassignal & Martin, 1977; Dwyer, Adams & Hille, 1980; Adams et al., 1980; Marchais & Marty, 1980). Certainly, both m.e.p.c.s and ACh-induced current fluctuations were difficult to record at negative membrane potentials in solutions containing glucosamine at concentrations of 29, 58 and 87 mM. In order to increase the signal-to-noise ratio, nerve-evoked end-plate currents (e.p.c.s) were recorded under voltage-clamp in an effort to clarify the actions of glucosamine.

In $1/2\,\overset{Na}{\diagup}$ solutions with added glucosamine HCl, a decrease in pH occurred. Therefore, an increased amount of the HEPES buffer (6 mM; see Table 5.1) was used and the 1/2 Na glucosamine solution was titrated to pH 6.9-7.0 with NaOH. In control experiments, no obvious differences in either τ_D or I_p were evident when the HEPES concentration of normal toad Ringers was increased. Although decreases in pH have been reported to cause increases in τ_D in frogs (e.g. Scuka, 1975; Mallart & Molgó, 1978), in our hands, increased hydrogen ion concentrations have small effects ($\lesssim$10% change) on τ_D (see Chapter Three).

End-plate Currents

Glycerol-treatment of deeper muscle fibres was not always completely successful as some contraction occasionally occurred in response to nerve stimulation. As well, the distributed nature of the toad end-plate (up to 500 μm in length as judged from fibres stained for acetylcholinesterase) often resulted in a poor space clamp when using a two-microelectrode point voltage-clamp. This was seen as a 'kick' or deflection on the voltage trace (see Fig. 5.5A,C). To overcome these problems, 2 μM curare was included in the bathing solutions. The peak amplitude of e.p.c.s was reduced to 10-20 nA from a control level of 50-60 nA and the lack of a perfect space clamp was minimized. Data was rejected from cells having voltage deviations greater than 1 % of the total driving force.

In 1/2 Na solutions containing glucosamine, mannitol or Mg (Fig. 5.5A,B,C) the peak amplitude of e.p.c.s was reduced and the time course of decay was prolonged. E.p.c.s decayed exponentially as shown in the graphs of normalized amplitude vs. time after the peak (Fig. 5.5). Time constants of decay (τ_D) for e.p.c.s were similar to those obtained from m.e.p.c.s (see Table 5.5). For example, average values of τ_D obtained from e.p.c.s and m.e.p.c.s in 1/2 Na Mg solutions over a range of membrane potentials are plotted against each other in Fig. 5.5D. It is apparent that rather similar estimates of τ_D were derived from both e.p.c.s and m.e.p.c.s.

The effect of membrane potential on peak e.p.c. amplitude is illustrated in Fig. 5.6A. The I-V curves demonstrate the reduction in e.p.c. amplitude and the shift in the null potential in 1/2 Na solutions. Both these effects and the non-linear I-V relationship are qualitatively similar to the m.e.p.c. data (compare Fig. 5.3A). The voltage-sensitivity of τ_D measured from e.p.c.s in Na and 1/2 Na glucosamine solutions is shown in Fig. 5.6B. τ_D depended exponentially on membrane potential, as

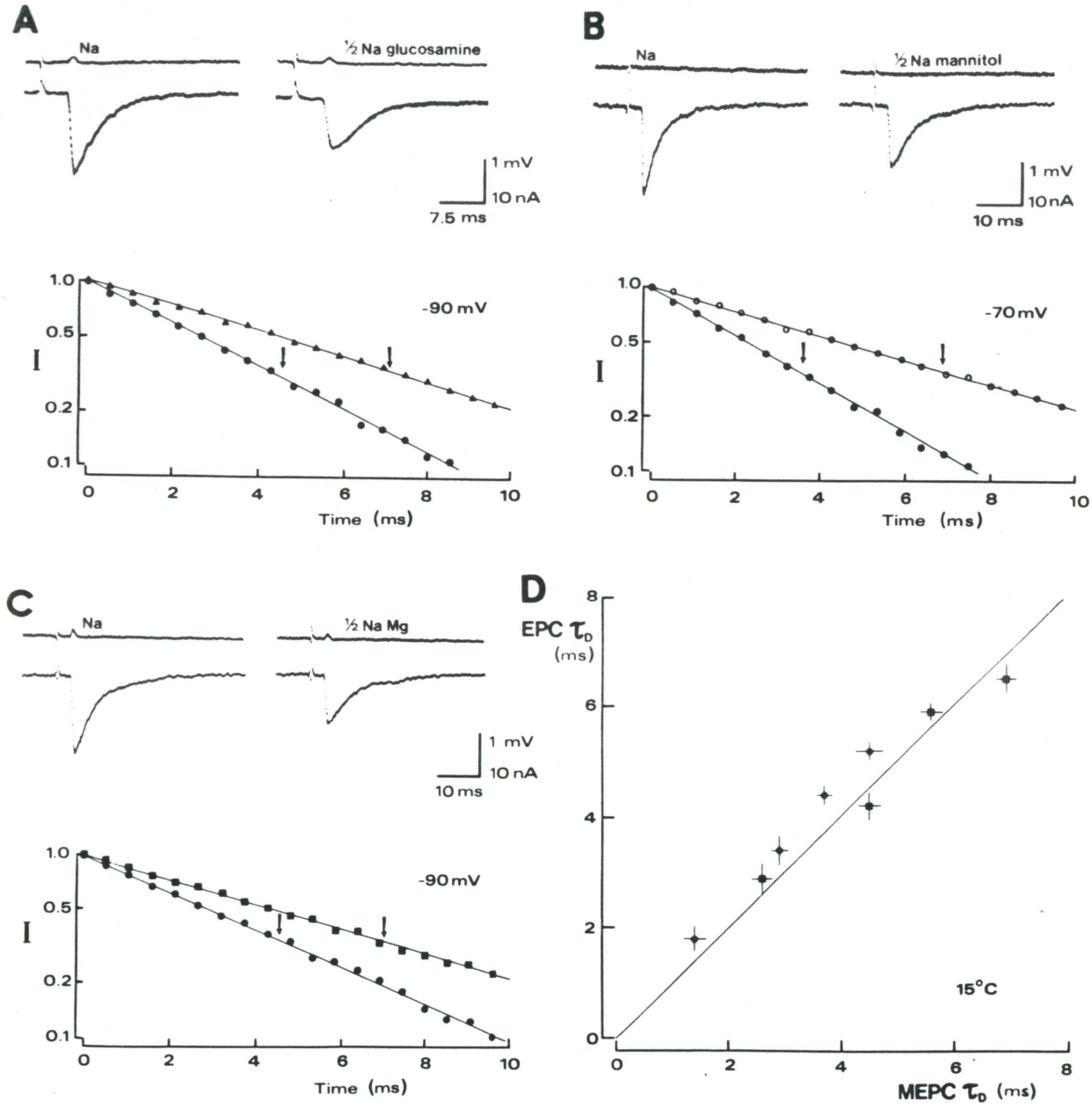

Figure 5.5. Nerve-evoked end-plate currents (e.p.c.s). A,B,C. Voltage-clamped e.p.c.s (upper traces) recorded in control (Na, ●) and 1/2 Na solutions (glucosamine, ▲ ; mannitol, o ; Mg, ■) for 3 different paired cells. Peak e.p.c. amplitude was decreased in all 1/2 Na solutions. Lower portion of each panel plots normalized e.p.c. amplitude vs. time. E.p.c.s decayed exponentially, with time constants of decay (ms; arrows) being (A): 4.5, 7.1; (B): 3.7, 6.8; (C): 4.7, 6.9, respectively, for control and test solutions. Holding potentials were -90 mV (A and C), -70 mV (B); temperature, 15°C. D. Both e.p.c.s and m.e.p.c.s gave similar estimates of τ_D. Data obtained from 3 cells in Na (●) and 4 cells in 1/2 Na Mg solution (■) over a range of membrane potentials. The line indicates equivalence.

Table 5.5. Voltage dependence of the time constant of decay (τ_D) for voltage-clamped m.e.p.c.s and nerve-evoked e.p.c.s. Values of $\tau_D(0)$ and H were calculated for individual cells from least-squares regression lines using the equation: $\tau_D(V_m) = \tau_D(0)\exp(-V_m/H)$. Results are shown as means ± 1 SEM. Temperature, 15°C; $\bar{r}$, correlation coefficient; n, number of fibres.

Solution	H (mV)	$\tau_D(0)$ (ms)	$\bar{r}$	n
m.e.p.c.s				
1/2 Na mannitol	101±4	2.74±0.46	.990	4
1/2 Na Mg	97±6	2.88±0.51	.998	4
3/4 Na	110±5	2.03±0.40	.983	3
Na (control)	95±4	1.83±0.09	.997	9
2 Na	109±8	1.57±0.25	.998	3
4 Na	115±7	1.41±0.33	.986	4
e.p.c.s				
1/2 Na mannitol	98±5	2.85±0.37	.987	3
1/2 Na Mg	101±5	2.81±0.42	.990	4
1/2 Na glucosamine	89±9	3.32±0.30	.941	3
Na (control)	93±6	2.31±0.24	.956	3

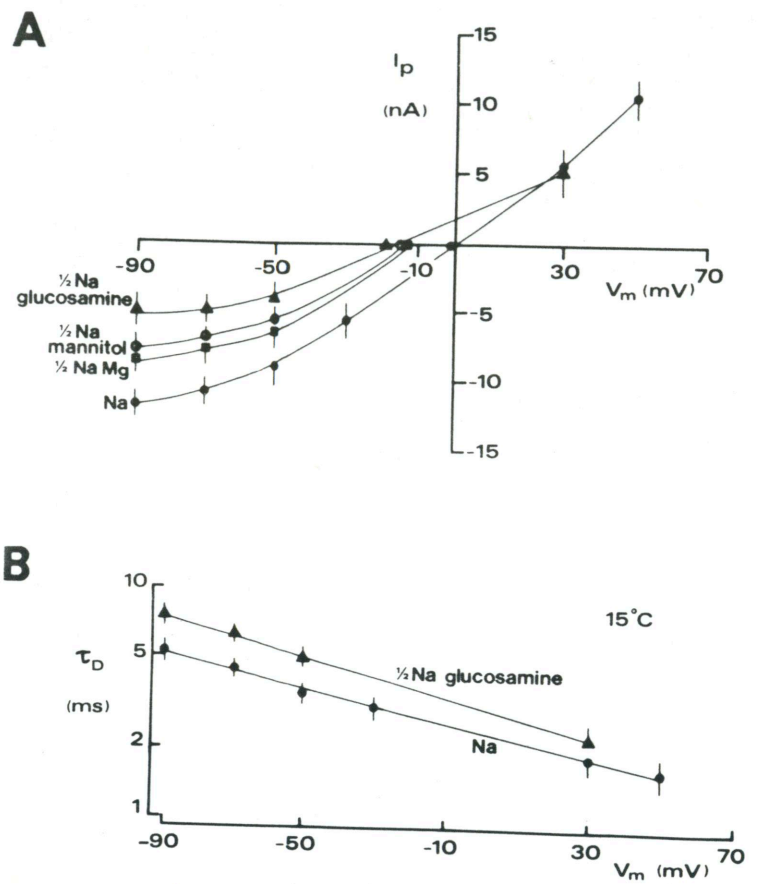

Figure 5.6. Voltage dependence of e.p.c. peak amplitude and time constant of decay. A. Current-voltage curves in control (Na, ● ; n=5) and 1/2 Na solutions (glucosamine, ▲ ; n=3; mannitol, O ; n=3; Mg, ■ ; n=4). E.p.c.s were recorded under voltage clamp. All solutions also contained 2 μM curare. Note the nonlinearity of the I-V curves. The lines were drawn through the data points by eye. Temperature, 15°C. B. Averaged values of τ_D at each potential plotted against holding potential. H values calculated from the regression lines were 87 mV (1/2 Na glucosamine, ▲) and 94 mV (Na, ●). $\tau_D(0)$ values were 2.4 and 3.1 ms, respectively for Na and 1/2 Na glucosamine solutions.

observed with m.e.p.c.s (see Fig. 5.2A). Average values of $\tau_D(0)$ and H are given in Table 5.5.

One interesting difference between the e.p.c. and m.e.p.c. data was noted. In 1/2 Na glucosamine solution, peak m.e.p.c. amplitude was reduced to a greater extent than was peak e.p.c. amplitude (compare Fig. 5.3A and Fig. 5.6A). A possible explanation is that glucosamine also exerts some presynaptic effect - the quantal size may be reduced while the quantal content was increased. No experiments were performed to pursue these possibilities.

Noise Analysis

ACh-induced end-plate current fluctuations were recorded in Na (control), 1/2 Na, 2 Na and 4 Na solutions. As in previous experiments, ACh was applied iontophoretically and spectra were computed after subtraction of base-line (in the absence of ACh) noise. Sample spectra in Na and 1/2 Na solutions are shown normalized in Fig. 5.7. Both these spectra, and those obtained in 2 Na and 4 Na solutions (not illustrated) were well-described by single Lorentzian curves. However, in 1/2 Na solutions, especially in the presence of glucosamine, deviations from Lorentzian behaviour were apparent at frequencies below ~15 Hz (Fig. 5.7). The average open channel lifetime (τ_N) was increased when the external Na concentration was halved as can be seen from the shifts in power density to lower frequencies. The half-power frequencies for the spectra illustrated in Fig. 5.7 were 32.5, 23.8, 21.5 and 17.9 Hz for Na, 1/2 Na Mg, 1/2 Na mannitol and 1/2 Na glucosamine solutions, respectively. The corresponding values of τ_N were 4.9, 6.7, 7.4 and 8.9 ms (membrane potential, -90 mV; temperature, 15°C). The increase in τ_N observed in 1/2 Na solutions was similar to the increase in τ_D obtained from m.e.p.c.s and m.e.p.c.s in the same solutions. When the external Na concentration was increased, τ_N became smaller. For example, in a paired cell, τ_N was 2.8 ms in Na solution and decreased to 2.4 ms

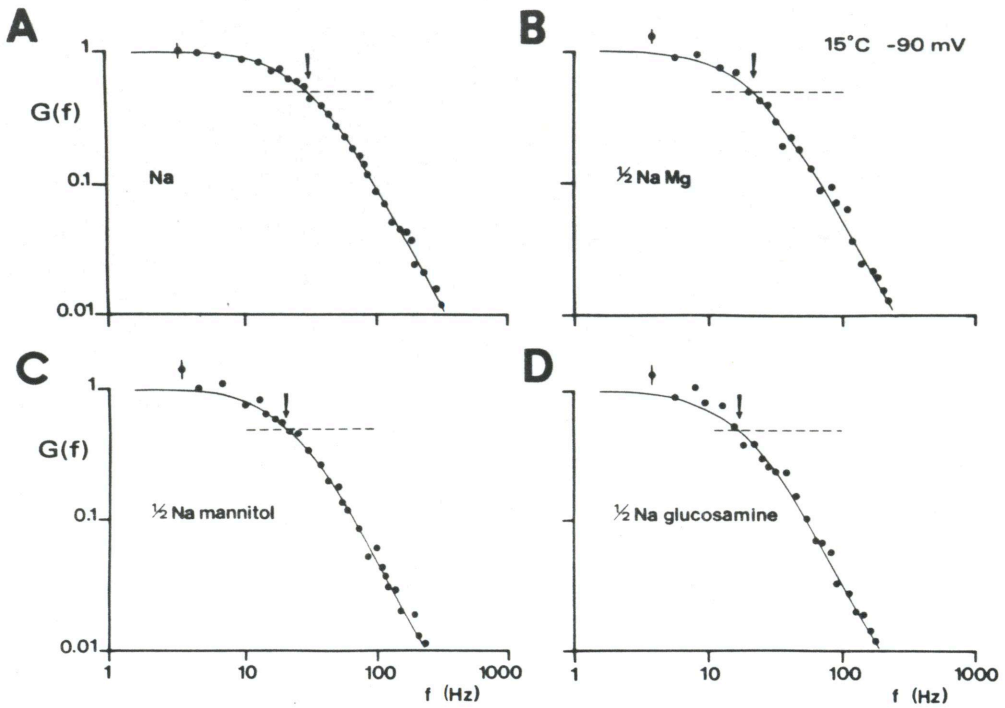

Figure 5.7. Noise spectra in control and 1/2 Na solutions. Spectra are shown normalized. The solid lines are least squares fits to single Lorentzian curves. The broken lines between 10 and 100 Hz indicate the half-power amplitude. Average open channel lifetime (τ_N) was estimated from the half-power frequencies (arrows). Similar estimates of single channel conductance (γ) were obtained from spectra and variance. Errors bars at 4 Hz indicate ±1 SEM. Holding potential, -90 mV; temperature, 15°C. Note the logarithmic axes. A. Control (Na) solution. τ_N = 4.9 ms. γ = 20.4 pS. Mean ACh-induced end-plate current, μ_i = 35nA. Zero-frequency asymptote, G(0) = 1.22×10^{-21} A^2s. B. 1/2 Na Mg solution. τ_N = 6.7 ms. γ = 16.1 pS. μ_i = 18 nA. G(0): 5.09×10^{-22} A^2s. C. 1/2 Na mannitol solution. τ_N = 7.4 ms. γ = 13.9 pS. μ_i = 15 nA. G(0) = 4.68×10^{-22} A^2s. D. 1/2 Na glucosamine solution. τ_N = 8.9 ms. γ = 6.9 pS. μ_i = 9 nA. G(0) = 1.52×10^{-22} A^2s.

in 2 Na solution (membrane potential, -50 mV; temperature, 15°C). In another paired cell, τ_N decreased from 3.0 ms in Na solution to 2.1 ms in 4 Na solution, under the same conditions. Average values of τ_N are presented in Table 5.6.

The single channel conductance (γ) depended on the external Na concentration. No differences in estimates of γ calculated from spectra ($\gamma_{p.s.d.}$) or variance ($\gamma_{var.}$; see Chapter Two) were evident. For 1/2 Na solutions, γ was 16.1 pS (Mg), 13.9 pS (mannitol) and 6.9 pS (glucosamine) for the cells shown in Fig. 5.7. Glucosamine clearly reduces γ to a greater extent than does halving the Na concentration. Values of $\gamma \lesssim 5$ pS approach the limit at which spectra could be reliably described by a single Lorentzian function, especially at low frequencies (e.g. see also spectra obtained in 80 Ca solution; Fig. 4.8). In 2 Na solution, γ was increased by 31% on average, while a 42% increase in γ in 4 Na solution was observed (membrane potential, -90 mV). Average values of γ from several cells are shown in Table 5.6.

It was of interest to examine the voltage dependence of γ in solutions containing differing external Na concentrations. Previous reports have indicated that γ is larger at positive potentials than at negative potentials in normal toad Ringers (e.g. Van Helden et al., 1979; Gage & Van Helden, 1979; Takeda et al., 1980, 1981). Figure 5.8 illustrates both the Na-dependence and the voltage-dependence of γ. At hyperpolarized potentials, γ increased with increasing Na concentration (Fig. 5.8A). In contrast, at positive membrane potentials, γ was much less dependent on the external Na concentration (Fig. 5.8B). Comparison of γ at -90 mV and 30 mV at similar external Na concentrations revealed that γ was greater at positive potentials in control and 1/2 Na solutions, but not in 2 Na or 4 Na solutions (see Table 5.6).

The Na dependence of the peak m.e.p.c. conductance (G_p) and the

Table 5.6. End-plate channel characteristics derived from noise analysis. Average open channel lifetime (τ_N) calculated from half-power frequencies of spectral density graphs. Single channel conductance (γ) was estimated both from spectra ($\gamma_{p.s.d.}$) and variance ($\gamma_{var.}$) and are presented pooled together, as no large differences in the calculated values were evident. Temperature, 15°C.

	τ_N (ms)			
solution	-90 mV	-50 mV	30 mV	n
Na (control)	4.7 ± 0.6	3.0 ± 0.3	1.9 ± 0.6	6
1/2 Na mannitol	7.0 ± 0.5	5.1 ± 0.3	2.3 ± 0.4	3
1/2 Na glucosamine	8.8 ± 0.9	6.5 ± 0.5	2.5 ± 0.5	2
1/2 Na Mg	6.4 ± 0.4	4.9 ± 0.6	2.2 ± 0.4	4
2 Na	4.1 ± 0.8	2.4 ± 0.7	1.9 ± 0.5	2
4 Na	3.9 ± 0.7	2.2 ± 0.4	1.6 ± 0.4	3

	γ (pS)			
	-90 mV	-50 mV	30 mV	n
Na (control)	20.4 ± 1.9	22.2 ± 2.1	27.8 ± 2.3	6
1/2 Na mannitol	13.7 ± 2.3	16.1 ± 1.9	24.6 ± 2.5	3
1/2 Na glucosamine	7.1 ± 3.7	7.9 ± 2.9	22.9 ± 3.9	2
1/2 Na Mg	15.2 ± 2.2	16.8 ± 2.3	23.8 ± 2.6	4
2 Na	29.5 ± 1.7	30.4 ± 1.8	29.1 ± 4.0	2
4 Na	35.1 ± 3.2	35.3 ± 3.4	30.1 ± 3.8	3

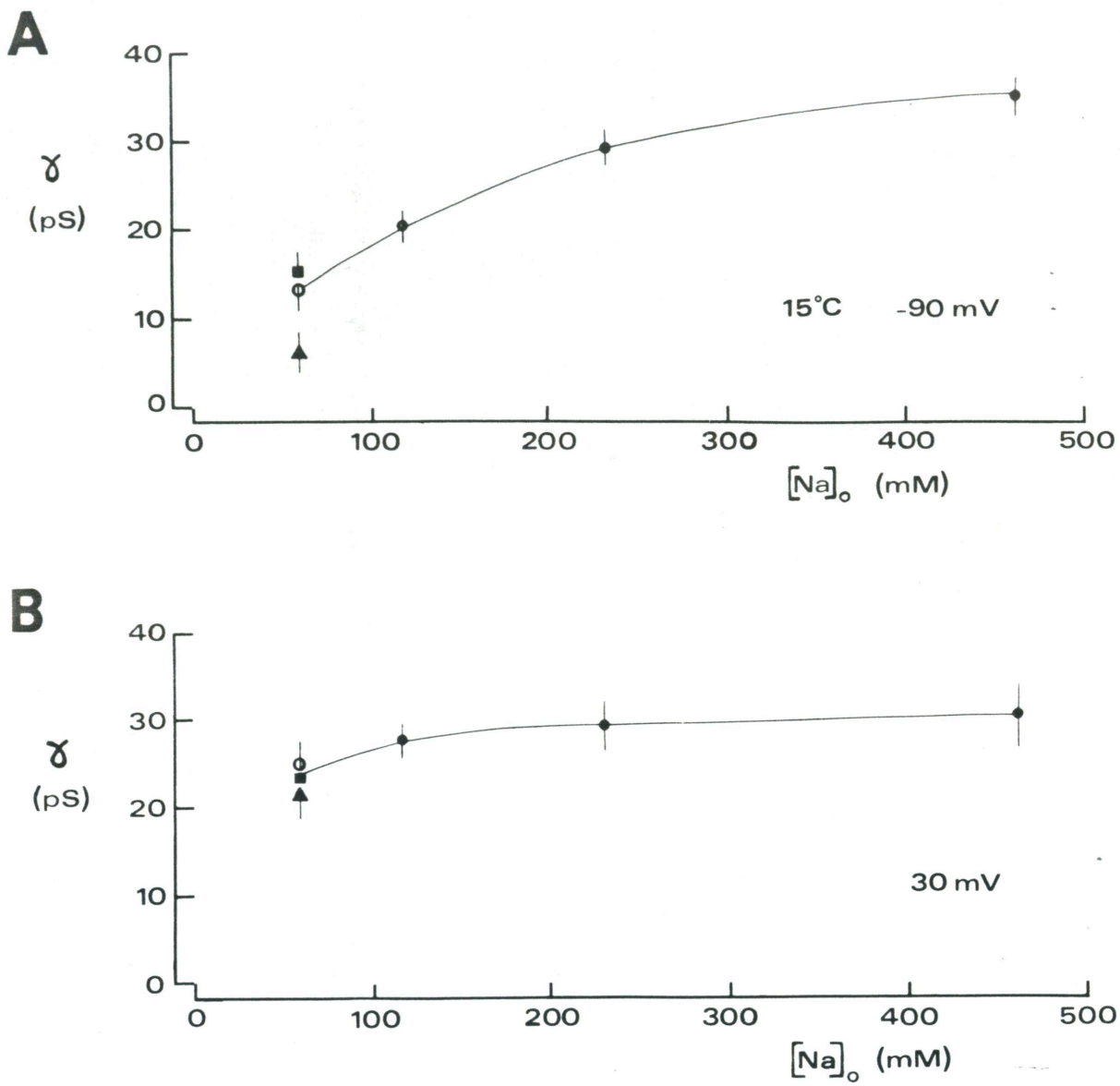

Figure 5.8. Single channel conductance (γ) is both Na and voltage-dependent. A. Average values of γ obtained at a holding potential of -90 mV vs. Na concentration. 1/2 Na solutions contained Mg (■), mannitol (o) or glucosamine (▲) as substitutes. Hypertonic solutions contained added Na glucuronate. B. The Na-dependence of γ is much less marked at a holding potential of 30 mV. Note that γ is larger in control and 1/2 Na solutions at positive potentials, but not in hypertonic solutions. The lines were drawn by eye through the data points. Temperature, 15°C.

single channel conductance (γ) appeared to 'saturate' at negative membrane potentials as the extracellular Na concentration was raised. This saturation was reminiscent of the effects of Na concentration on the time constant of decay of m.e.p.c.s (Fig. 5.4). Accordingly, the conductance data was replotted on Lineweaver-Burk plots (i.e. reciprocal conductance versus reciprocal Na concentration) in Fig. 5.9. The G_p data points in Fig. 5.9A were calculated from the I-V curves presented in Fig. 5.3 and the γ values used are given in Table 5.6. Good fits to straight lines were obtained (by least-squares regression) for both the G_p (correlation coefficient, $\bar{r} = 0.991$) and the γ data ($\bar{r} = 0.999$). The analysis ignored the conductance values obtained in 1/2 Na glucosamine solution, as these points deviated significantly from the apparent trend observed with the other solutions (see Fig. 5.9). Michaelis constants (K^m_{Na}) were calculated from the inverse of the negative abscissal intercept and for G_p, K^m_{Na} was 177 mM, while K^m_{Na} was 136 mM for the γ data. These estimates of K^m_{Na} are remarkably similar to the estimate of K^m_{Na} (=93 mM) derived from the Na-dependence of τ_D (see Fig. 5.4).

Charge Movement

The net ion movement during a m.e.p.c. (Q_m) or through a single channel (Q_c) tends to remain constant in the presence of different alkali monovalent cations (Van Helden et al., 1977; Gage & Van Helden, 1979) because of the opposite effects on I_p and τ_D. However, for some monovalent cations (e.g. ammonium, Takeda et al., 1980) and divalent cations (e.g. calcium and zinc, Takeda et al., 1981), charge transfer was not constant (see also Ascher et al., 1978; Marchais & Marty, 1979; Nonner et al., 1980; Adams et al., 1981). In 1/2 Na solutions, charge transfer was approximately the same as in Na solution, except at negative potentials in 1/2 Na glucosamine (Table 5.7) where it was less than in control. Charge movement in 2 Na and 4 Na solutions was clearly greater at negative potentials than in Na solution (Table 5.7).

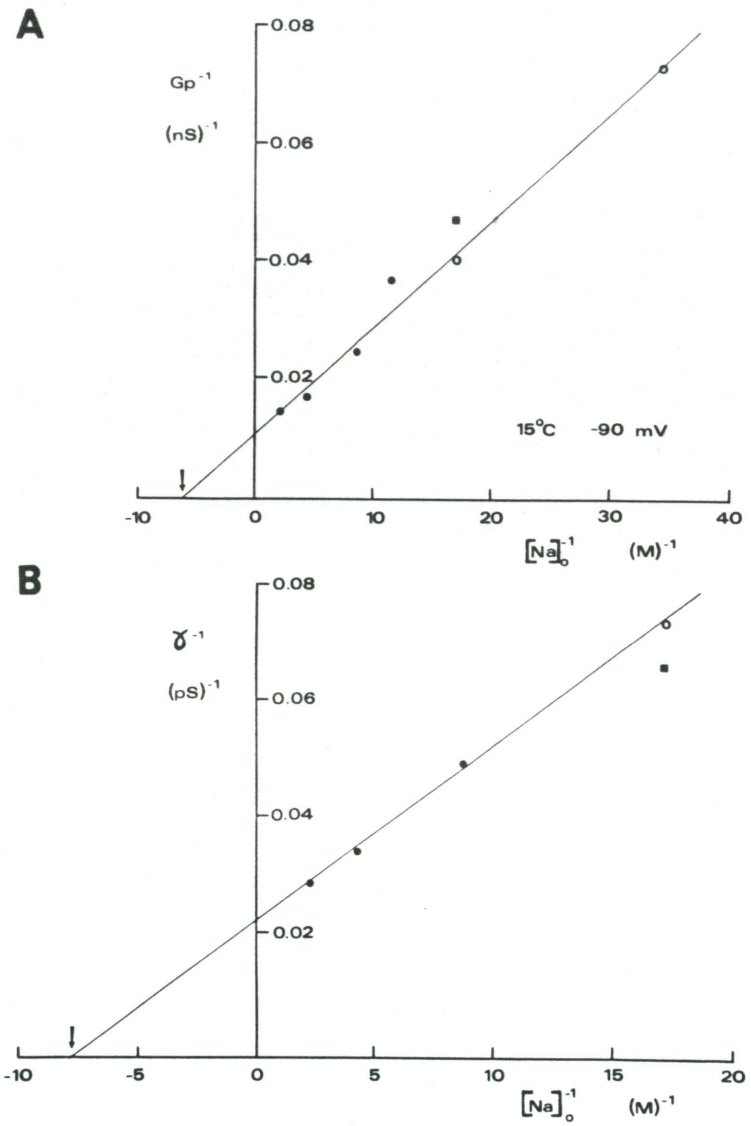

Figure 5.9. Lineweaver-Burk estimates of K_{Na}^m using peak m.e.p.c. conductance (G_p) and single channel conductance (γ). A. Reciprocal G_p vs. reciprocal Na concentration. G_p values were derived from the I-V plots shown in Fig. 5.3. Regression lines were fitted to the data, arbitrarily ignoring the 1/2 Na Mg (■) and 1/2 Na glucosamine (=0.137; not shown) values. Correlation coefficient = 0.991. The negative abscissal intercept was 5.65 M^{-1}, and K_{Na}^m was 177 mM. B. Reciprocal γ vs. reciprocal Na concentration. The regression line was fitted as described in A (1/2 Na glucosamine ordinate = 0.141; not shown). Correlation coefficient = 0.999. Note the change in abscissa scale. The negative abscissal intercept was 7.34 M^{-1}, and K_{Na}^m was 136 mM. Data obtained at a membrane potential of -90 mV, temperature 15°C.

Table 5.7. Voltage dependence of charge movement during a m.e.p.c. (Q_m) or through a single channel (Q_c). The amount of charge transferred during m.e.p.c. was calculated using $Q_m = I_p \cdot \tau_D$ and for single channels, the charge transferred was calculated using $Q_c = \gamma \cdot \tau_N \cdot (V_m - \varepsilon_o)$.

Temperature 15°C.

	Q_m (pC)			
Solution	-90 mV	-50 mV	30 mV	n
Na (control)	19.4 ± 1.6	7.1 ± 1.1	2.4 ± 0.9	9
1/2 Na mannitol	14.4 ± 1.8	6.8 ± 1.4	3.5 ± 1.1	4
1/2 Na Mg	12.4 ± 1.4	7.0 ± 1.5	3.2 ± 1.2	4
2 Na	23.0 ± 1.7	10.8 ± 1.2	2.2 ± 0.8	3
4 Na	27.7 ± 1.9	15.5 ± 1.6	1.9 ± 0.7	4

	Q_c (fC)			
	-90 mV	-50 mV	30 mV	n
Na (control)	8.3 ± 0.9	3.1 ± 0.8	1.7 ± 0.6	6
1/2 Na mannitol	7.3 ± 0.6	2.9 ± 0.6	2.3 ± 0.7	3
1/2 Na glucosamine	4.3 ± 0.9	2.2 ± 0.7	2.9 ± 0.8	2
1/2 Na Mg	6.4 ± 1.1	2.1 ± 0.8	2.7 ± 0.8	4
2 Na	11.8 ± 1.2	4.2 ± 1.0	1.2 ± 0.6	2
4 Na	14.0 ± 1.4	4.8 ± 0.9	0.9 ± 0.5	3

Discussion

The effects of varying the external Na and K concentrations on ε_o appear to be adequately described by the Goldman-Hodgkin-Katz equation, except in hypertonic Na solutions and when Mg was used as a Na substitute in low Na solutions having constant ionic strength. The results differ from the initial observations of Takeuchi & Takeuchi (1960) but agree with more recent studies (e.g. Adams et al., 1980; for review of earlier work, see Rang, 1975). The major reason for this discrepancy probably lies in the Takeuchis' determination of ε_o using linear extrapolation, whereas later investigators directly determined ε_o (see Chapter 1).

The deviation of the GHK predictions for ε_o from the experimental observations in hypertonic Na solutions is easily explained if the end-plate channel current 'saturates' with increasing permeant ion concentration, as the GHK equation has no allowance for saturation behaviour. This can be clearly seen as the GHK equation predicts a nearly linear increase in single channel conductance (γ) with increasing Na concentration (Table 5.8), while the results suggest that γ 'saturates' with increasing Na concentration (Fig. 5.8). There may be some uncertainty in the actual internal ion concentrations (Table 5.2) in high Na solutions, but the calculated estimates appear to be adequate inasmuch as good fits to the observed values of ε_o in the majority of the other solutions tested were obtained using the GHK equation. Moreover, the GHK predictions for ε_o were quite insensitive to variations in the assumed internal cation concentrations in control solution (see Methods; Table 5.4). Nevertheless, the adequacy of the calculated internal ion concentrations needs experimental support. One possibility would be to measure ε_o in solution made 4x hypertonic

Table 5.8. Na-dependence of single channel conductance (γ). Comparison between experimental and Goldman-Hodgkin-Katz (GHK) predictions. $P_{glucosamine}/P_K$ was assumed to be zero, and P_{Mg}/P_K was assumed to be 0.15. Calculated values of γ in pS are shown averaged for the 2 cases of initial internal ion concentrations in control solution (see Methods) and with no surface charge potential correction. Membrane potential, -50 mV; temperature, 15°C.

Solution	γ(experimental)	γ(GHK)
4 Na	35.3 ± 3.4	88.7
2 Na	30.4 ± 1.8	44.3
Na (control)	22.2 ± 2.1	22.2
3/4 Na	-	18.9
1/2 Na mannitol	16.1 ± 1.9	15.1
1/2 Na glucosamine	7.9 ± 2.9	14.9
1/2 Na Mg	16.8 ± 2.3	16.7

with mannitol (where presumably the internal concentrations would be greatly increased, although the Na/K pump may act to limit increases in internal Na; Table 5.2).

The effects of changing ionic strength are not clear. The differences between the observed and predicted values of ε_o in Mg-containing solutions may simply arise because the assumed P_{Mg}/P_K is too high. However, comparison of ε_o in 1/2 Na mannitol and 1/2 Na glucosamine solutions (Table 5.4) suggests that ionic strength does affect ion-selectivity. As Barry et al. (1979a) have proposed earlier, this may arise because decreases in ionic strength could cause less shielding of the polar intra-channel sites, thereby increasing their effective site strength. The net result would be an increased selectivity of Na compared to K. This hypothesis would account for the difference between the predicted and observed ε_o in 1/2 Na mannitol solution. An important point here is that corrections for surface charge potential result in very little change in the GHK predictions (at least for the surface charge densities assumed). A further alternative could be that Mg and glucosamine, which apparently have extremely low permeabilities (assumed to be zero) also act as channel blockers. Because of the asymmetry of the solutions, this may lead to an effective decrease in 'inward' Na permeability, while 'outward' K permeability would be unaffected. Although so far, channel blockers (e.g. local anaesthetics) have not been reported to change ε_o, relative ion permeabilities calculated from shifts in ε_o (e.g. Adams et al., 1980) should be treated cautiously in light of the differences when compared to measured conductances (e.g. Gage & Van Helden, 1979; Barry et al., 1979a; Takeda et al., 1980; Nonner et al., 1981; Adams et al., 1981). Channel block by permeant ions appears to be a definite

possibility (e.g. Adams, 1979; Gage & Hamill, 1981; Farley et al., 1981), but it remains to be resolved whether or not blocking ions and drugs act at the same 'blocking site' and whether or not the permeant ion, intrachannel binding site is the same as the 'blocking site'.

The effects of changes in external Na concentration on channel lifetime (τ) require some comment. In low Na solutions, τ is increased, whereas in high Na solutions, τ is decreased (Fig. 5.2). It is clear that changes in surface charge potential (e.g. Cohen & Van der Kloot, 1978) do not underly the observed effects, as decreases in ionic strength (in 1/2 Na mannitol) would tend to depolarize the actual transmembrane voltage and increases in ionic strength (in high Na solutions) would hyperpolarize the membrane voltage. These shifts in voltage (arising from screening of membrane surface charge) would lead to changes in τ opposite to those observed (remembering that the normal voltage dependence of τ results in an increase in τ with hyperpolarization). Further, τ in both 1/2 Na mannitol and 1/2 Na glucosamine solutions showed comparable increases (Table 5.5), even though the ionic strength in 1/2 Na mannitol solution was decreased. It may be that glucosamine exerts channel-blocking effects (Marchais & Marty, 1980; Adams et al., 1981), thereby increasing τ. To check this possibility, τ was measured in 1/2 Na Mg solution. Although τ was also increased by approximately the same amount (Table 5.5), it should be noted that 20 mM Mg causes comparable increases in τ in control solution (containing 90 mM Na; see Chapter 4; Cohen & Van der Kloot, 1978). Another possible explanation for the increase in τ seen in low Na solutions arises from Kordas' (1968) observation of a marked potentiation of acetylcholinesterase inhibitor action in low Na solutions. (i.e. acetylcholinesterase may be partially inhibited in low Na solutions). However, estimates of τ derived from noise analysis (Table 5.6) reveal similar increases in 1/2 Na solutions, when compared to τ measured from m.e.p.c.s.

Adams et al. (1981) have recently reported that τ is generally decreased in Na-free solutions. However, in their cut-fibre, vaseline gap preparation, CsF is the internal perfusate. Both Cs and F are known to alter τ: Van Helden et al. (1977) found that τ decreased by ~30% when CsCl was substituted for external NaCl while Kaibara et al. (1978) reported that the half-decay time of e.p.c.s was increased nearly 3-fold by 5 mM F. (The effects of F were also seen in the presence of an acetylcholinesterase inhibitor.) The results of Adams et al. (1981) show that τ in control solution increased from 1.71 to 2.54 ms when the internal CsF concentration was decreased from 120 mM to 12 mM (with 108 mM arginine aspartate). However, their value of τ in 1/2 Na mannitol solution increased from 1.23 to 1.76 ms with low internal CsF, which is still less than the control value. A 30% increase in τ was seen by Redmann (1980) when the control solution was made hypertonic with 460 mM sucrose, but when the Na concentration was raised to 345 mM (by adding Na glutamate), τ increased by about 60%. While the observations of Adams et al. (1981) on the Na-dependence of τ may not be incompatible with those reported here (in view of the uncertainties concerning the effects of internal CsF), no obvious reason for Redmann's (1980) opposite effect of high Na on τ is apparent.

The use of Lineweaver-Burk plots (Fig. 5.4) to describe the 'saturation' behaviour of the closing rate constant (α) may not be entirely appropriate. The calculated Michaelis constant suggests that Na concentration affects the normal closing rate. Kolb & Bamberg (1977) have previously proposed that increasing Na concentration 'stabilized' the 'conducting' (or open) Gramicidin A channel conformation, as the fraction of channels containing permeating cations increased with concentration. Similarly, Van Helden et al. (1977) and Gage & Van Helden (1979)

have suggested that permeant ions with high affinities for putative intrachannel binding sites resulted in longer channel open times. The observation here that τ decreases with increasing concentration seems to be at variance with the 'ion-binding stabilization' hypothesis (see also Marchais & Marty, 1979). However, the opposite effects of Na concentration on peak m.e.p.c. amplitude and on τ (Table 5.7) are reminiscent of the effects of the permeant, monovalent alkali cations (Van Helden et al., 1977; Gage & Van Helden, 1979). It is not at all obvious how permeant ions affect the gating structure of ionic channels. A recent report by Swenson & Armstrong (1981) showing that K channel lifetime in squid giant axons is influenced by some permeant cations lends support to the generality of ion effects on τ. It may be that the actual 'gate' corresponds to some channel protein (or at least, part of a protein) which physically moves (i.e. presumably, a conformational change) either in response to changes in the applied field (for excitable Na and K channels in nerve and muscle membranes) or upon agonist binding (for transmitter-activated, synaptic channels). Unfortunately, no clearer explanation of the molecular mechanisms underlying permeant ion effects on τ is presently available.

In Figure 5.10, the effect of changes in membrane voltage on the Na dependence of τ_D is illustrated. It is apparent that the slopes of the regression lines decrease with membrane depolarization, although the Michaelis constants (K^m_{Na}) are relatively unchanged. By analogy with enzyme kinetics, it can be imagined that α is 'inhibited', as the membrane is hyperpolarized. In fact, the data presented in Figure 5.10 resemble rather closely, classical noncompetitive inhibition of an enzyme catalyzed reation. Immediate problems present themselves, firstly in terms of the physical interpretation of K^m_{Na} and secondly, in identifying the 'inhibitor'. If our concept of the channel gate

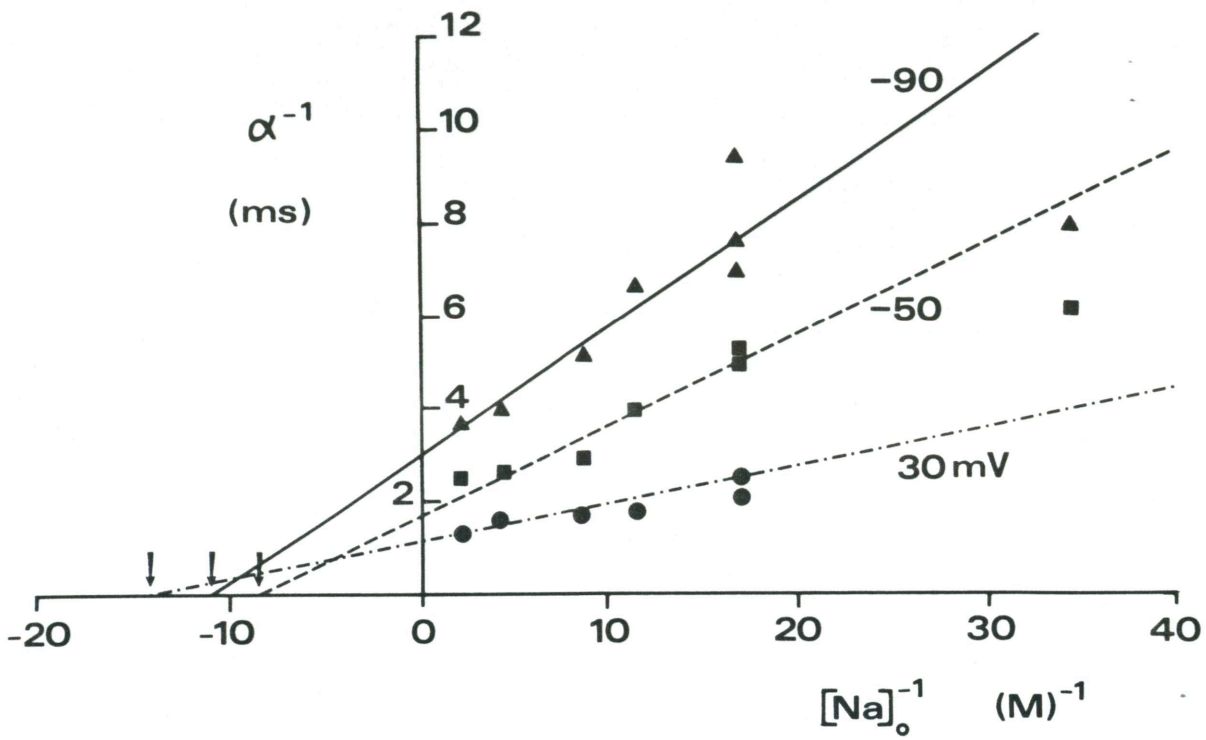

Figure 5.10. The effect of voltage on the Na dependence of τ_D. The average reciprocal closing rate constant for m.e.p.c.s, α^{-1}, is plotted against the reciprocal external sodium concentration, $[Na]_o^{-1}$, at three different membrane potentials. Regression lines were fitted by least-squares to the data ignoring the 1/4 Na data points (extreme right). The slopes of the lines decreased with increasing membrane depolarization. The Michaelis constant, K_{Na}^m was calculated from the negative abscissal intercept (arrows). For -90 mV (▲, ____), K_{Na}^m was 93 mM and the correlation coefficient ($\bar{r}$) was 0.978. For -50 mV (■, ----), K_{Na}^m = 116 mM and $\bar{r}$ = 0.974. For 30 mV (●, -·-·-·), K_{Na}^m = 71 mM and $\bar{r}$ = 0.955. Temperature, 15°C.

presented above is correct, then it may be that the critical 'movable' protein moiety possesses a regulatory site which binds permeant ions. The actual regulation process remains purely hypothetical, other than the obvious requirement of 'stabilizing' the channel in its open conformation. The identity of the 'inhibitor' species may be slightly more obvious, as there can be little argument that membrane depolarization increases the driving force on K ions. Hence, the intrachannel K concentration increases with depolarization, and decreases with hyperpolarization. (In the limit, at the K equilibrium potential, the intrachannel K concentration is finite, in spite of the zero net K flux). On Lineweaver-Burk plots, the slope of the inhibited reaction increases, so our hypothesis would be that the internal cation (K) would 'normally regulate' τ, and that Na is acting to 'inhibit' the normal rate of channel closure. Some support for this perhaps fanciful proposal can be raised from the changes in τ produced by differing internal concentrations of CsF (Adams et al., 1981). More recently, a Ca-activated K channel has been described (Pallotta, Magleby & Barrett, 1981) in patches of rat myotube membranes where channel lifetimes are affected by the internal free Ca concentration. Marty (1981) has also reported a similar Ca-activated K channel in cultured, bovine chromaffin cells, where the internal Ca concentration affects both channel lifetime and the probability of channel opening. The effects of the permeant, monovalent alkali cations on τ (Van Helden et al., 1977; Gage & Van Helden, 1979) can then be seen in terms of the extracellular cation 'competing' with K for the site 'regulating' τ. It is interesting to note that τ at 50 mV tends to the same (small) limiting value, essentially independent of the extracellular solution composition. This may arise because K ion-binding to the 'regulatory

site' normally determines the fastest rate of channel closure.

Previous reports have all indicated that the single channel conductance (γ) is reduced when the external Na concentration is decreased (Linder & Quastel, 1978; Lewis, 1979; Barry et al., 1979a; Adams et al., 1980; Horn & Patlak, 1980). When the Na concentration was greater than normal, both Horn & Patlak (1980) and Redmann (1980) found that γ increased, and in fact, tended to saturate at high Na concentrations. Quite similar saturation behaviour was seen here, especially at hyperpolarized membrane potentials (Fig. 5.8). Lineweaver-Burk plots were again used to describe the Na-dependence of γ (Fig. 5.9). The rationale for the use of such plots here appears to be somewhat sounder, in that some agreement exists for the concept of permeant ions binding to critical intrachannel site(s) as they traverse the channel (e.g. Stevens & Tsien, 1979). Such a reaction would seem to be more readily suited to analysis following classical enzyme kinetics compared to the hypothetical description given above for the Na-dependence of τ. The rate of ion translocation (hence, the conductance) through channels, if limited by the saturation of intrachannel binding sites, would tend towards a maximum value with increasing Na concentration (Fig. 5.8), in contrast to the Goldman-Hodgkin-Katz predictions (Table 5.8).

Lineweaver-Burk plots illustrating the Na-dependence of the peak m.e.p.c. conductance (G_p) at different membrane potentials are presented in Figure 5.11. Although the slopes of the lines in Figure 5.11 decreased with increasing membrane depolarization, this trend was much less clear-cut than observed with Na-dependence of τ (Fig. 5.10). The calculated Michaelis constant (K^m_{Na}) for the G_p data appeared to decrease with depolarization, but this was far from convincing. It was of interest to note that the values of K^m_{Na} found for the Na-dependence of τ were fairly similar to those for the Na-dependence of G_p (Figs. 5.10, 5.11). The effects of membrane voltage on the Na-dependence of γ are

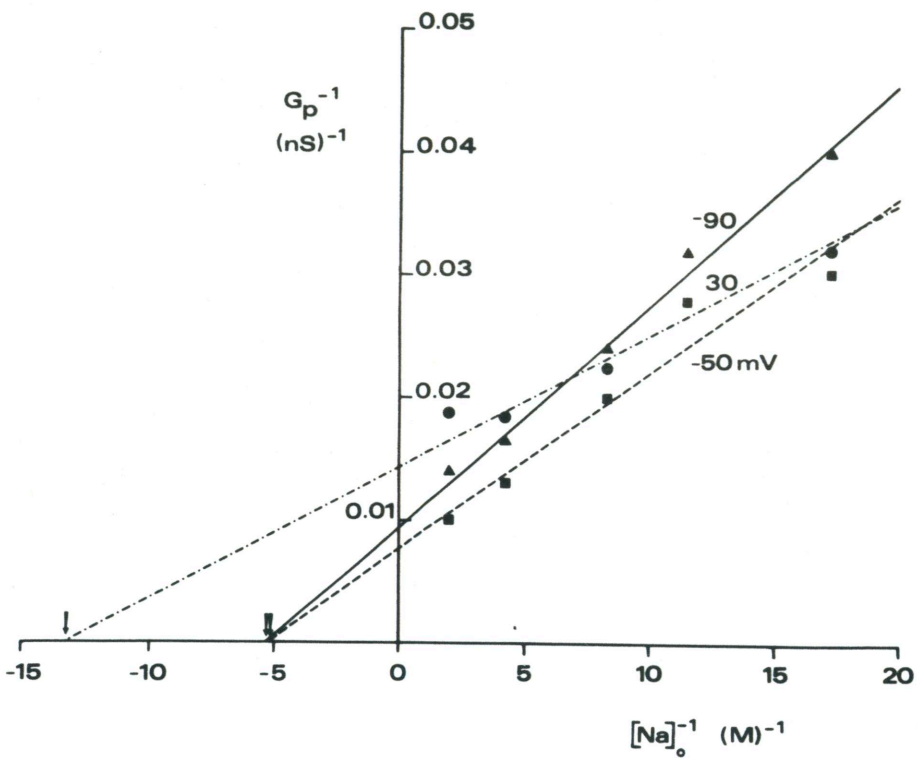

Figure 5.11. Voltage-dependence of Lineweaver-Burk plots of the average, reciprocal peak m.e.p.c. conductance (G_p^{-1}) versus reciprocal $[Na]_o$. Least squares regression lines were fit to the data. Note the decrease in slope with increasing depolarization. $K_{Na}^m = 190$ mM, $\bar{r} = 0.995$ (V_m = -90 mV; ▲ , ———). K_{Na}^m = 189 mM, $\bar{r}$ = 0.953 (V_m = -50 mV; ■ , -----). K_{Na}^m = 75 mM, $\bar{r}$ = 0.956 (V_m = 30 mV; ● , -·-·-·). Temperature, 15°C.

shown in Figure 5.12. The decrease in the slopes of the regression lines on the Lineweaver-Burk plots with depolarization is more obvious. Also, in this case, the values of K^{m}_{Na} decreased with membrane depolarization. The observed crossover, although not occurring at infinite Na concentration, suggests that classical competitive inhibition of an enzyme catalyzed reaction is occurring. A plausible explanation would be that Na ions compete with K ions for the critical ion-binding sites(s). As the slope of the inhibited reaction is steeper on Lineweaver-Burk plots, it could be imagined that K ions normally rate-limit ion translocation (or at least, ion occupancy of the binding site(s)) and that the higher channel Na concentrations at hyperpolarized voltages lead to competition for the binding site(s). Examination of the voltage dependence of γ at high Na concentrations (Fig. 5.12) reveals that it is opposite to that observed at lower Na concentrations. According to the explanation put forward by Barry et al. (1979a) for the voltage dependence of γ (in control solution), the relative partition coefficients (or equilibrium constant) and relative intra-channel mobilities differ for various permeant ions, and changes in membrane voltage act to alter the relative intrachannel ion concentration in asymmetric solutions (see Chapter 3). The reversed voltage dependence of γ in high Na solution may result from 'saturation' effects at the binding site(s) dominating the normally inferred equilibrium constants for Na and K. This implies that the normal relative partition coefficients for Na and K ($K_{Na}/K_{K} = 3\pm1$; Chapter 3) would be altered, effectively increasing the site affinity of K relative to Na.

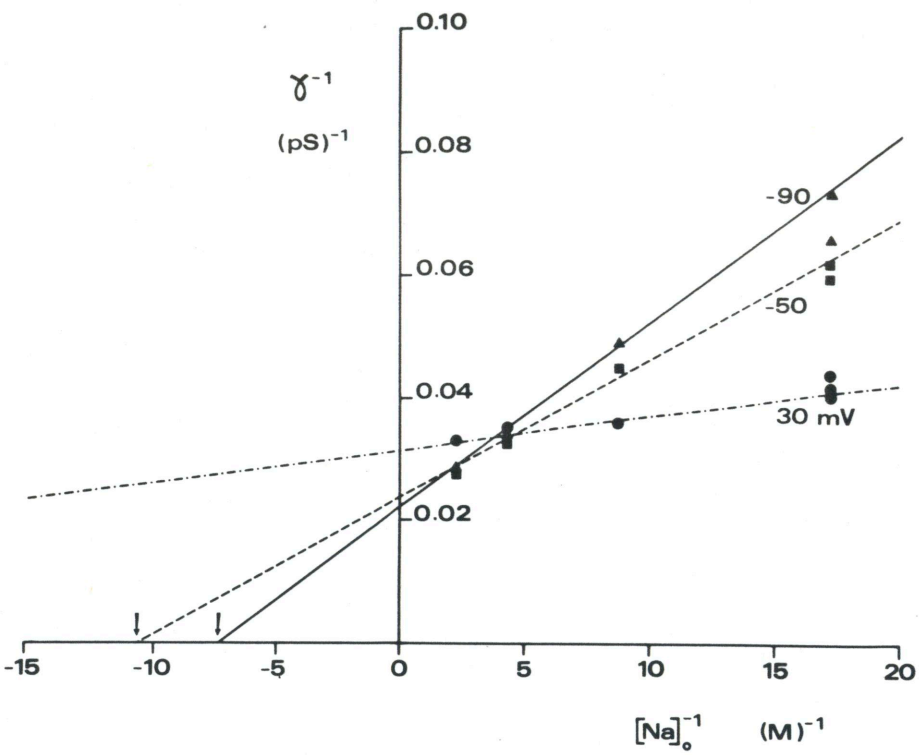

Figure 5.12. Voltage sensitivity of Lineweaver-Burk plots of average reciprocal single channel conductance (γ^{-1}) versus reciprocal $[Na]_o$. The slopes of the least-squares regression lines decreased with increasing depolarization. For V_m = -90 mV (▲, ———), K_{Na}^m = 136 mM, $\bar{r}$ = 0.999. For V_m = -50 mV (■, ----), K_{Na}^m = 97 mM, $\bar{r}$ = 0.997. For V_m = 30 mV (●, -·-·-·), K_{Na}^m = 17 mM, $\bar{r}$ = 0.998. Temperature, 15°C.

The apparent Michaelis constant (K^m_{Na}) calculated from the Na-dependence of γ (Fig. 5.8) was 136 mM. This can be compared to the values of about 140 mM and 400 mM found from the Na-dependence of outward single channel currents in rat myotubes (measured using a patch clamp technique) with the inside (myoplasmic side) Na concentration varying (Horn & Patlak, 1980) and from the Na-dependence of peak m.e.p.c. conductance in frog muscle (Redmann, 1980), respectively. (D.J.) Adams et al. (1981) hypothesized that the fraction of channels containing a 'bound ion' in control solution was 0.2, and assuming that channels contain a single ion only, calculated a value of K^m_{Na} (or ion dissociation constant) of 456 mM. It was implicit that the binding at equilibrium would follow the classical Langmuir curve (for review, see e.g. Colquhoun, 1973). Using a completely symmetrical barrier-well model for ion permeation, P.R. Adams (1979) derived a half-saturation concentration (i.e. K^m_{Na}) of >200 mM. This arises by analogy with the blocking kinetics of some local anaesthetics (e.g. Neher & Steinbach, 1978; Ogden et al., 1981). The 'dwell time' of a permeant ion in the channel can be estimated, knowing the single channel amplitude and the channel lifetime (e.g. If γ = 20 pS, V = 100 mV, and τ = 3 ms, then 3.75×10^4 ions cross a single open channel. One ion, on average, would spend 0.08 μs in crossing the channel (= the 'dwell time') assuming the channel contains a maximum of only one ion at any instant in time). The reciprocal of the dwell time gives an estimate of the outward jump rate (1.25×10^7 s^{-1}) and a K^m_{Na} of ~250 mM results if the inward rate is taken as ~5×10^7 M^{-1} s^{-1}. (The outward jump rate is the rate at which ions leave the binding site and cross towards the cell interior. The inverse inward jump rate is considered to be very small).

It may be possible to utilize these values of K^m_{Na} to calculate the average intrachannel Na concentration, and thus discriminate between a single ion versus a multi-ion pore. Another way of asking the same

question is to find the ion concentration which gives the apparent resistance of a single channel. If γ = 20 pS, and we represent the channel by a right cylinder of length 10 nm, and diameter 0.65 nm, then the equivalent conductivity is 6.03×10^{-3} $S.cm^{-1}$. This corresponds to a NaCl concentration of ~60 mM (at 20°C), if we assume that the ions move with their free solution mobilities (Robinson & Stokes, 1959). Since we know that P_{Cl} through end-plate channels is essentially zero, the intrachannel Na concentration is then ~120 mM. Using the channel dimensions given above, it follows that each channel contains on average 0.24 ions. However, intrachannel ion mobility is almost certainly less than in free solution, so that the ion concentration and, hence, the number of ions in the channel would have to be greater, in order to account for the same channel conductance. Obviously, the argument depends critically on choosing the appropriate channel volume.

An alternative calculation based on the linear velocity of ion movement (and independent of the actual channel cross-sectional area) is possible. Using the 'dwell time' of 0.08 μs derived earlier, and a channel length of 10 nm, then, on average, one ion would cross the channel with a velocity of 12.5 cm/s. The maximum possible velocity of a Na ion (moving with a free solution mobility (μ_e) of 4.43×10^{-8} $m^2.s.^{-1}V^{-1}$; calculated from the limiting equivalent conductivity at 18°C; Robinson & Stokes, 1959) in a field of 100 mV/10 nm is ~44 cm/s. The current per unit area, I (in A/m^2) is:

$$I = FJ \quad ,$$

where F is the Faraday and J is the ion flux (in $moles.m^{-2}.s^{-1}$). The flux, J, is given by:

$$J = C\mu_e.\frac{d\varepsilon}{dx} \quad ,$$

where C is the ion concentration (in $moles/m^3$), μ_e is the free solution mobility and $\frac{d\varepsilon}{dx}$ is the potential gradient (=100 mV/10 nm). The current, i (=2 pA), through one channel of area δa is:

$$i = FC\mu_e \cdot \frac{d\varepsilon}{dx} \cdot \delta a.$$

The concentration, C, can be replaced by:

$$C = \frac{N}{\delta a . \delta} \quad ,$$

where δa is the cross-sectional area, δ is the length of the channel (= 10 nm), and N is the number of moles of ions in the channel. Solving for N:

$$N = \frac{i.\delta}{F\mu_e . \frac{d\varepsilon}{dx}} = 4.68 \times 10^{-25} \text{ moles},$$

and, on average, the number of ions per channel is 4.68×10^{-25} x Avogadro's number = 0.28. This can be seen as internally consistent as the velocity of 1 ion moving at free solution mobility would be $12.5/0.28 \cong 44$ cm/s. If ions move with a mobility of 28% the free solution value, then on average channels would contain a single ion with velocity of 12.5 cm/s. Another possibility is that end-plate channels contain >1 ion at any time (each moving with <28% of their free solution mobility) and, although 1 ion is transferred in 0.08 μs (given that the entry of an ion into the channel causes the exit of an ion at the other end), the time for a single ion to traverse the channel would be >0.08 μs. For example, if permeant ions travel through the channel with a mobility of 10% of the free solution value, then there would be 2.8 ions per channel, on average, and each ion would have an average velocity of 4.4 cm/s.

What are the implications of these calculations? Firstly, Hille and co-workers (Dwyer et al., 1980; Adams et al., 1980, 1981) have proposed that ~20% of end-plate channels contain bound ions. If each channel has a single ion-binding site and the channel contains, at most one permeant ion, then the average number of ions per channel would be ~0.2. As shown above, this level of ion occupancy suggests that ions move through the channel with a mobility approaching their free solution value. Using the K^m_{Na} value found here (136 mM), classical binding theory predicts that ~ 43% of the channels would contain a bound ion (assuming

a maximum of one ion per channel). It is probable that permeant ions have intrachannel mobilities significantly smaller than in free solution, given the restricted nature of the channel lumen and the likelihood of the presence of one or more ion-binding sites. If true, then it may be that end-plate channels do contain several ions at any instant in time.

Secondly, the physical interpretation of the apparent K_{Na}^{m} becomes less clear, given the possibility of a multi-ion (and therefore, multi-site) channel. Levitt (1978a,b) has shown that the image force (which arises in moving charge between media of different dielectric constants) coupled with electrostatic forces between ions limit the number of monovalent cations contained in the Gramicidin A channel to a maximum of two (see also Parsegian, 1969, 1975; Jordan, 1981). If more ions are contained within the channel, then in order to overcome these energy considerations, one needs to postulate the presence of at least one low energy well (or binding site). Similarly, Adams (1979) shows that the very high image force barrier encountered by divalent cations (which are known to be permeant) can be lowered by the presence of a single negative charge within the channel. No unequivocal evidence exists which allows the determination of the number of ions contained within open end-plate channels at any given instant in time. Implicit in the neutral site model proposed by Barry et al. (1979a) is the assumption that end-plate channels contain several permeant cations (and their counterions) and sufficient ion-binding sites to warrant the use of a Nernst-Planck electrodiffusion approach in describing ion permeation. This style of analysis has also been successfully applied to ion permeation through the large aqueous channels found in gall-bladder epithelial membranes (see Barry & Diamond, 1971; Barry et al., 1971; Wright et al., 1971). On the other hand, ion permeation through a variety of pore-like channels in biological membranes and through (for e.g.) Gramicidin A channels in

artificial lipid bilayers appears to involve ions binding to a few, (usually < 3), discrete intrachannel sites (for review, see Stevens & Tsien, 1979). Little is known about the actual physical nature of these sites (c.f. Adams et al., 1981) or their numbers within end-plate channels. Both the partitioning of ions from the bulk solution into the channel lumen and the mobility of ions within the channel must be important parameters in determining not only the channel selectivity, but also the maximal channel conductance (e.g. Hille, 1975). Eyring rate theory has been favoured for the description of ion permeation where ions 'hop' over energy barriers or bind in a few critical energy wells (for review, see Glasstone, Laidler & Eyring, 1941; Hille, 1975; Stevens & Tsien, 1979). The question that needs answering relates to the meaning of the apparent Michaelis constant when there are many binding sites (with presumably no one rate-limiting step), as in the neutral-site model of Barry et al. (1979a).

Thirdly, both rate theory and electrodiffusion approaches become intractable when permeabilities appear to have concentration-dependence (see Fig. 5.1; Hille, 1975). The deviation between the observed and GHK predictions in hypertonic Na solutions needs confirmation. The explanation of this effect may critically alter our approach in modelling the other permeability data.

Lastly, specific experimental tests should be constructed that will clarify the different assumptions inherent in a thick, neutral-site pore model and one in which there are only a few significant energy barriers and wells (binding sites). P.R. Adams has suggested[1] that both the permeability and conductance of the neutral-site pore should change if the intrachannel anion concentration could be altered (e.g. by having an anion so large that it would be excluded from the channel lumen, thus

---

1 Personal communication.

affecting the macroscopic electroneutrality condition and the cation concentration). Another possibility is to examine how the discrepancy between permeability and conductance behaves in the limit of very low ion concentrations. The neutral-site model in its present form predicts that the discrepancy would remain unchanged (however, the model's assumptions of electroneutrality and the condition of continuity of the electro-diffusion equations obviously would have no validity in the limit of very low ion concentrations) whereas in a simple ion-binding - rate theory model, the conductances would become proportional to the permeabilities (i.e. at the end-plate, γ would tend to the (same) limiting value at very low monovalent, alkali cation concentrations, because the differences in permeability ratios calculated from ε_o's are small). This, of course, promises to be perhaps technically impossible with the present level of resolution available for the determination of γ.

In conclusion, several interesting points have arisen. The nature of permeant ions is known to influence both τ and γ, and now it appears that some of these effects are concentration dependent. Theoretical description of the observations will hopefully lead to a better understanding of the molecular mechanisms which normally control τ and γ.

CHAPTER SIX

GENERAL DISCUSSION

The major emphasis of this thesis has been towards a more complete characterization of ion permeation through ACh-activated ionic channels at the motor end-plate. Perhaps the most striking result that arises is the demonstration of the ion-dependence of end-plate channel lifetime and conductance, following on from the initial observations of Van Helden, Hamill & Gage (1977). In Chapter 3, the substitution of ammonium ions for external sodium ions resulted in an increase in both channel lifetime and conductance. The time constant of decay of m.e.p.c.s in the presence of low concentrations (20 mM) of calcium and magnesium ions was approximately 30% slower than normal. Higher concentrations of calcium (80 mM) resulted in a further increase in τ_D, and the single channel conductance was significantly reduced. Zinc or nickel ions, at concentrations of 0.1 to 5 mM were much more effective in prolonging τ_D, although they had essentially no effect on γ. Channel lifetime decreased with increasing external sodium concentration, while channel conductance increased with sodium concentration. As discussed in Chapter 5, the apparent 'saturation' of α (the closing rate constant) and γ suggests that, at the end-plate, ions binding to sites within the channel lumen may be the normal 'controlling' mechanisms.

The neutral-site pore model of Barry et al. (1979a) was successful in explaining both the ion and voltage-dependence of γ. Recently, Hamill et al. (1981) and Redmann, Clark & Adams[1] have found that single channel amplitudes measured with the patch clamp technique were increased in the presence of Cs, and decreased in the presence of Li, respectively. The key observation of the voltage dependence of γ (Van Helden et al., 1977, 1979) has received support from Adams et al. (1981) who showed γ was greater at positive voltages in asymmetric solutions (e.g. with Cs

---

[1] P.R. Adams, Personal communication.

inside, and Li outside), although the voltage dependence of γ in control solution is not universally seen by other investigators (see Discussions, Chapters 4 and 5). In crustacean muscles, Lingle & Auerbach (1980) have also reported that γ is voltage dependent at ACh-activated, excitatory synaptic channels found in the foregut muscles.

One of the most obvious differences between synaptic channels and voltage-activated Na and K channels in nerve membranes is the larger synaptic single channel conductance. At the end-plate, γ is typically about 25 pS, while estimates of γ for Na and K channels are in the 2 to 10 pS range (e.g. Fishman, 1975; Stevens, 1977). Taken together with the relatively weak selectivity of synaptic channels compared to Na and K channels, it thus seems likely that the molecular mechanisms of ion permeation will differ in detail, especially in terms of how selectivity and maximal conductances result (see Hille, 1975; Reuter & Stevens, 1980). Non-independent ion movement was first postulated by Hodgkin & Keynes (1955), who reported Ussing flux ratios with exponents $\neq 1$ in K channels of squid axons. The observed flux coupling resulted in the proposal of single-file ion movement in K channels, and the suggestion that the K channel was a 'long pore'.

Based on ion selectivity experiments, the minimal cross-sectional area of the end-plate channel appears to be about 0.65 nm x 0.65 nm (Maeno et al., 1977; Guy et al., 1977; Watanabe & Narahashi, 1979; Dwyer et al., 1980; Adams et al., 1980, 1981). For Na and K channels in nerve and muscle membranes, the narrowest part of the channel (or 'selectivity filter') is approximately 0.3 nm x 0.5 nm, and 0.3 nm x 0.3 nm, respectively (for review, see Hille, 1975; Armstrong, 1975). Hille has proposed that the selectivity filter in Na and K channels corresponds to a physical binding site, with permeant cations being stabilized (or bound) in a 'molecular fit' by oxygen ligands lining the

channel at its most constricted part. Anions would be excluded by these negatively charged oxygen groups. Following Hille (e.g., 1975), schematic representations of the selectivity filters in Na and K channels are given in Figure 6.1B and C. For comparison, a hypothetical end-plate 'selectivity filter' has been constructed (Fig. 6.1A) with the molecular dimensions of 0.65 nm x 0.65 nm. Putative oxygen ligands have been added, following Hille, and the channel, at its narrowest, can be seen to accommodate simultaneously, at least one Na and one K ion as well as two water molecules. No attempt was made to achieve the closest packing possible, nor were the oxygen groups arranged in any specific manner (e.g. to maximize H-bonding). The intent here is merely to demonstrate the relative sizes of these ion channels. Hille's (1971, 1972) selectivity filter for the Na channel is perhaps the most explicit proposal so far for an intra-channel ion binding site. In a side view (Fig. 6.1B), it is clear that the proposed binding site appears to occupy a molecular distance along the length of the channel. By contrast, a schematic representation of the end-plate channel (after Horn & Stevens, 1980) in side-view is illustrated in Fig. 6.1A. Although not constructed on the same scale compared to the Na and K channels in Fig. 6.1B and C, it is apparent that little structural evidence exists which would allow a detailed physical definition of the end-plate channel 'selectivity filter'. On the other hand, electrophysiological investigations have suggested that the lumen of end-plate channels contains at least one metal cation binding site (e.g. Van Helden et al., 1977; Gage & Van Helden, 1979; Barry et al., 1979a; Adams et al., 1981), a local anaesthetic or 'drug' binding site (e.g. Adams, 1976b; Neher & Steinbach, 1978; Redmann, 1980; Ogden et al., 1981), a site which binds decamethonium (a partial agonist) and perhaps, ACh (e.g. Sakmann et al., 1980; Adams & Sakmann,

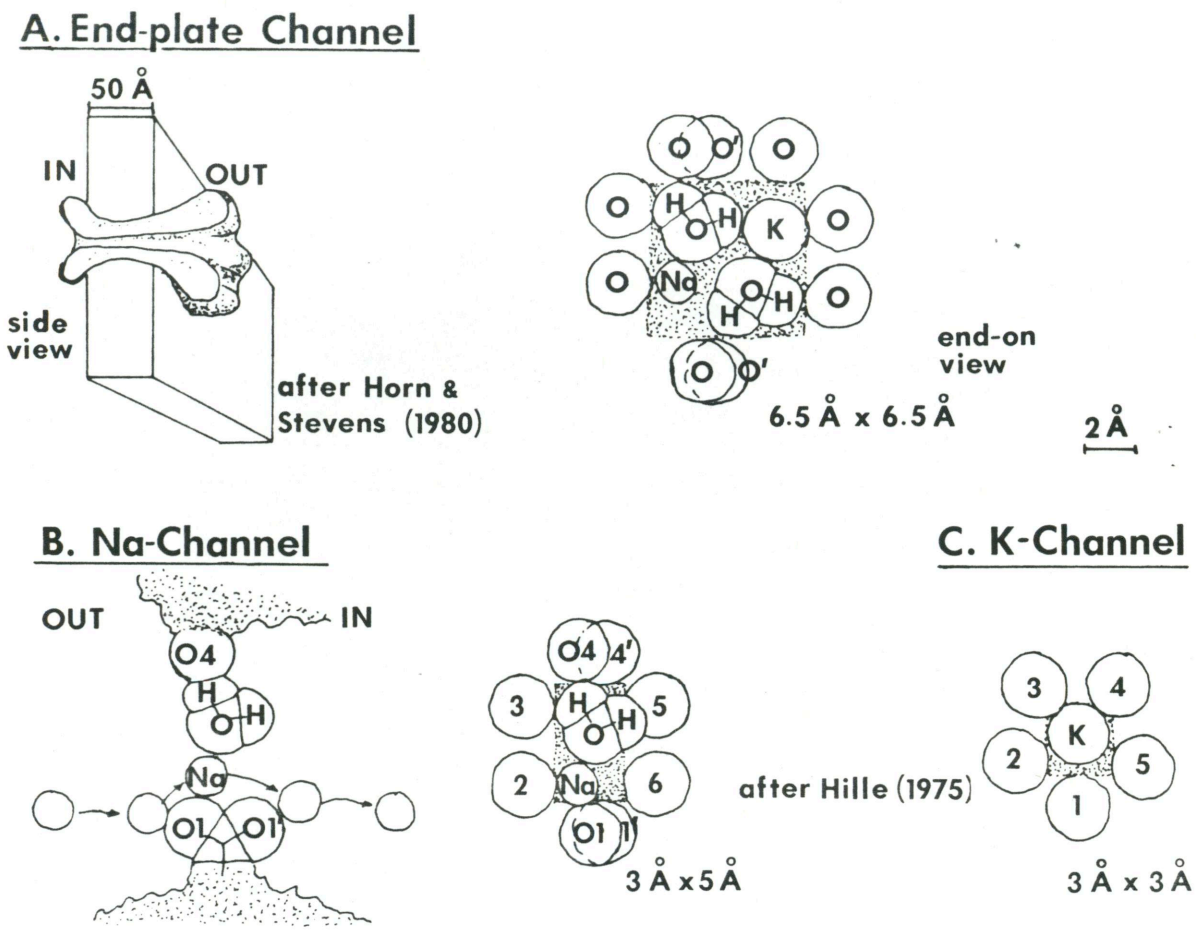

Figure 6.1. Schematic representations of ion channels and their 'selectivity filters'. Side views are shown on the left, and end-on views, on the right. The stippled areas in the end-on views represent the minimal cross-sectional channel lumen, as estimated from ion selectivity experiments. A. The ACh-receptor from Torpedo situated in the lipid bilayer is used to depict the end-plate channel (left). Structural information is derived from biochemical analysis, electron microscopy, x-ray diffraction and low-angle neutron scattering. Redrawn to scale, after Horn & Stevens (1980). The purely hypothetical end-on view (right) shows 2 water molecules, one Na, and one K ion in the 'selectivity filter', surrounded by potential H-bonding sites (oxygen, O; carboxyl oxygens, O-O'). The molecular dimensions are from Pauling (1960), and are drawn to scale, following Hille (1975). 'Selectivity filters' of the Na channel (B) and K channel (C) in the node of Ranvier, as proposed by Hille. H-bonding sites are provided by oxygen groups (numbered) and carboxyl oxygens. Redrawn to scale, after Hille (1975).

1978a,b), and finally, a hydrophobic site (Adams et al., 1981; Farley et al., 1981). In addition, permeant cations are known to alter channel lifetime (e.g. Van Helden et al., 1977; Ascher et al., 1978; Marchais & Marty, 1979; Takeda et al., 1980, 1981) and it may be that the mechanism of action results from permeant ions binding to another site which regulates channel lifetime (see Discussion, Chapter 5). No agreement appears to have been reached concerning just where in the channel these sites are located (but c.f. Neher & Steinbach, 1978; Lewis & Stevens, 1979; Horn & Brodwick, 1980; Farley et al., 1981; Adams et al., 1981), or whether or not a single site exists which exhibits all of the above characteristics. Finally, the known permeability of divalent cations and large organic cations (along with the weak selectivity between the alkali cations) in end-plate channels (see Chapters 3 and 4) indicates that the 'selectivity filter' must be quite different from that in Na and K channels, especially with respect to the molecular arrangement of the putative H-bonding ligands. It seems likely that there will be binding sites distributed along a sizeable length of the end-plate channel lumen, and that rate-theory models with a single, large, rate-limiting energy barrier may not be adequate for a description of ion permeation through end-plate channels (see Discussion, Chapter 5).

A further interesting point arises in comparing the known channel-blocking effects of tetrodotoxin (TTX) and tetraethylammonium ions (TEA) at Na and K channels, respectively (see e.g. Hille, 1970; Armstrong, 1975) with their effects at the end-plate. Low external concentration of TEA block open end-plate channels (e.g. Adler et al., 1979), whereas TEA has no effect on Na channels and blocks K channels only when present in the internal bathing solution (e.g. Armstrong, 1975). TTX has no effect on end-plate channels. The behaviour of these channel

blockers can be contrasted with effects of some drugs (e.g. barbiturates, some local anaesthetics, and octanol) which appear to exert similar qualitative effects (i.e. channel block) at both nerve (Blaustein, 1968; e.g. Hille, 1977; Swenson & Narahashi, 1980) and end-plate channels (e.g. Adams, 1976b; Neher & Steinbach, 1978; Gage et al., 1978; respectively for the drugs given above). A pertinent question would be when and how do permeant ions exert drug-like postsynaptic effects? Of course, the inverse should also be considered: i.e. when (and how) do drugs act like permeant ions? For some neutral drugs and aliphatic alcohols, it may be that the effects on channels are mediated via the hydrophobic membrane phase, (e.g. Gage et al., 1975; Hille, 1977), although direct channel blocking actions are certainly also possible (e.g. Adams, 1976b; Hille, 1977; Gage et al., 1978; Ogden et al., 1981). At the end-plate, quaternary ammonium derivatives like TEA, d-tubocurarine, gallamine (for review, see Katz & Miledi, 1980; see also, Adams et al., 1981) and the local anaesthetic QX-314 (a lidocaine derivative; Horn et al., 1980) are effective in reducing ACh-induced current only when applied extracellularly. In contrast, procaine, a tertiary amine blocks end-plate channels when present both externally (e.g. Adams, 1977b) and internally (Katz & Miledi, 1980; Hamill[1]), suggesting that its access to its site of action is via the lipid membrane phase. It will obviously prove fruitful to define the exact drug binding site and to investigate its relationship to the permeant cation binding site. For example, curare, in addition to its classical competitive antagonism of ACh binding, possesses channel blocking actions (e.g. Marty et al., 1976; Manalis, 1977; Katz & Miledi, 1978; Colquhoun et al., 1979). The ACh-receptor and ionophore functional groups appear to be separable

---

[1] O.P. Hamill, Personal communication.

by biochemical and pharmacological techniques (for review, see Heidmann & Changeux, 1978; Landau, 1978). However, should the curare channel blocking site be related to the agonist blocking site, it may be that the mechanics of ACh binding to its (classical) receptor is more intimately related to the ionophore process than is presently thought. In this vein, no strong explanation has been put forward to date for the apparent dependence of γ on agonist type (see e.g. Colquhoun et al., 1975; Colquhoun, 1979).

The non-independence of ion movement through Na and K channels in nerve and muscle membranes appears to be well-established (for reviews, see Hille, 1975; French & Adelman, 1976). Deviations from the independence principle are often observed experimentally in the form of flux coupling (e.g. Hodgkin & Keynes, 1955), anomalous mole fraction behaviour (e.g. Neher, 1975; Neher et al., 1978), saturation effects (Hille, 1975) or non-agreement of permeability ratios calculated from zero current potentials and measured conductances. Most of these discrepancies are explainable in terms of either ion-ion interactions, ion-channel interactions, ion-water interactions or strict 'knock-on', single-filing effects (for review, see French & Adelman, 1976; Hille & Schwarz, 1978). No suggestion of explicit single-filing in end-plate channels has appeared, and in view of the large channel diameter (Fig. 6.1A), it seems unlikely that ions would be so constrained in traversing the end-plate. Adams et al. (1980) have argued against flux interactions among Na, K and Tl ions, based on the good fit of a conventional electrodiffusion (i.e. GHK) description of null potentials in mixtures of these ions (see also Huang et al., 1978; Hille & Schwarz, 1978), although end-plate channels certainly do deviate from the classical assumption of independent ion movement. The evidence for non-independence falls into three areas. Firstly, the voltage

dependence of γ cannot be described theoretically by the GHK equation (Chapters 3 and 4). Secondly, permeability ratios calculated from null potential measurements are not in agreement with the measured conductance ratios (e.g. Van Helden et al., 1977; Gage & Van Helden, 1979; Barry et al., 1979a; Nonner et al., 1980; Takeda et al., 1980, 1981; Adams et al., 1981). Thirdly, γ does not increase linearly with increasing Na concentration, but rather displays apparent saturation behaviour (Chapter 5; Horn & Patlak, 1980; Redmann, 1980). Given that flux interaction and single-filing effects are not present in end-plate channels, it seems highly probable that the source of these deviations from independence will lie in ion-channel interactions. Comparatively little attention has been paid to the possibility of ion-water interaction in the form of electrokinetic or electroosmotic phenomena (e.g. Vargas, 1968) in end-plate channels (but c.f. Horn & Patlak, 1980). Although measurements of water fluxes across biological membranes (like the muscle end-plate preparation) promise to pose severe technical difficulties, they could provide critical data in evaluating the relative importance of 'frictional' hydrodynamic effects (see Adams et al., 1980) and ion-channel wall interactions. Of course, the number (and nature) of intrachannel ion-binding sites remains a crucial variable, which most certainly warrants further experimental definition.

No discussion of ion permeation through membrane channels would be complete without reference to the Gramicidin A channel (e.g. Hladky & Haydon, 1972; Myers & Haydon, 1972). An extensive literature exists which describes many of these special, channel forming proteins (for review, see Urry et al., 1975; Ehrenstein & Lecar, 1977; Urban et al., 1978).

A comprehensive survey of ion permeation through Gramicidin channels

would be outside the scope of the discussion here, but an attempt will be made to highlight those aspects which allow comment and comparison in relation to the properties of ionic channels in nerve membrane and at the end-plate described above. It is well established that the conducting form of the Gramicidin A channel is a dimer complex, having a length of 2.6 nm and a minimal inner diameter of about 0.38 nm (for recent reviews, see Andersen & Procopio, 1980; Finkelstein & Andersen, 1981). This lumen diameter is quite close to that inferred for Na and K channels in nerve (Fig. 6.1 B and C). By comparison with the end-plate (Fig. 6.1A), the Gramicidin A channel diameter is indeed significantly smaller. From X-ray crystallographic studies, it appears that the conducting complex contains two ion-binding sites (Koeppe et al., 1979). Ion selectivity studies suggest the presence of two or four (or possible more) ion-binding sites, and demonstrate clearly that ion movements in Gramicidin channels fail to obey the independence principle (e.g. Sandblom et al., 1977; Neher et al., 1978; Urban et al., 1980). For example, anomalous mole fraction behaviour, saturation and single-filing effects have all been observed. The narrow pore diameter imposes single-file transport on both permeant cations and on water molecules. In K channels of nerve membrane, it is not known whether ions and water molecules move in obligatory single file (Hodgkin & Keynes, 1955; Andersen & Procopio, 1980), although the small diameter (e.g. Hille, 1975) and the electroosmotic potentials measured by Vargas (1968) suggest that this is so. The number of water molecules that 'accompany' each permeant cation (in single file) in Gramicidin channels has been estimated to be 5 or 6 (Rosenberg & Finkelstein, 1978a,b) or 8 or 9 (Dani & Levitt, 1981a,b). One interesting aspect of this ion/water single-filing is the recent proposal (Finkelstein & Andersen, 1981) that the rate of ion translocation is limited, not

by any significant electrostatic barrier between the binding sites at either ends of the channel, but rather by the necessity of a permeant cation moving six water molecules (in single file) along with it (but c.f. Dani & Levitt, 1981a,b).

The Gramicidin single channel conductance and the average channel lifetime are ion-dependent and also concentration-dependent (e.g. Hladky & Haydon, 1972; Myers & Haydon, 1972; Kolb & Bamberg, 1977). As well, the composition and thickness of the lipid bilayer into which Gramicidin is inserted plays a critical role in determining lifetime, and perhaps conductance (e.g. Hladky & Haydon, 1972; Urry et al., 1975; Neher & Eibl, 1977; Rudnev et al., 1981). Structural modifications of single channel atoms can result in profound changes in channel characteristics. For example, substitution of a methyl group for the N-terminal hydrogen results in an approximately 100 fold decrease in τ and about a 50% decrease in γ (Szabo & Urry, 1979). With the reconstitution of isolated ACh receptors and their insertion into lipid bilayers as functional entities (recently, for e.g., Boheim et al., 1981; for review, see Heidmann & Changeux, 1978), it should prove possible to use similar experimental manipulations to gain further insight into end-plate channel permeation mechanisms.

One of the most puzzling features of ion channel behaviour relates to the normal channel closing mechanism. Channels open in response to applied voltage or upon agonist binding. For voltage-activated channels, some (e.g. Na and Ca channels) display inactivation (i.e. they shut, or move to a separate 'inactivated' state during prolonged depolarizing pulses), while K channels apparently do not. The inactivation of Na channels is poorly understood in terms of the molecular details describing the actual transition (for review, see Armstrong, 1975). Mullins (1959, 1960, 1968), who first emphasized the

importance of 'solvating' permeant ions as a prerequisite to their entry into the membrane hydrophobic phase, also constructed a specific excitation model which, perhaps accounted for inactivation (although ultimately, his model is probably inadequate in that it postulated only a single channel to carry both Na and K ions in the squid axon). The inactivation of Ca channels may not be directly voltage-dependent, but rather appears to depend on the entry of Ca itself (e.g. Tillotson, 1979; Standen, 1981). Inactivation of these ionic channels may be analagous to desensitization (Del Castillo & Katz, 1957; Katz & Thesleff, 1957) at ACh-activated end-plate channels. The normal voltage-dependence of τ observed in both excitable (see Hodgkin, 1964; Cole, 1972) and synaptic channels (e.g. Kordaš, 1969; Magleby & Stevens, 1972a,b) has been interpretated (especially for synaptic channels) as the effect of the applied field on a dipole present in the relaxing ionophore moiety (Magleby & Stevens, 1972a,b). Alternatively, Adams (1976a) has proposed that membrane potential affects τ because the ACh-binding step may be voltage-dependent. A recent report suggests that the durations of channel opening are directly related to ACh binding (Cohen, Van der Kloot & Attwell, 1981). If so, then the explanations for the voltage dependence of τ put forward by Magleby & Stevens (1972a,b) and Adams (1976a) would be inseparable, experimentally. The 'ion-binding stabilization' hypothesis (Van Helden et al., 1977; Ascher et al., 1978; Gage & Van Helden, 1979; Marchais & Marty, 1979) is a further alternative for the control of τ. As discussed in Chapter 5, there may be, in fact a separate intrachannel site which 'controls' τ, and which is affected by the presence of different permeant cations. Bearing in mind this seeming plethora of mechanisms regulating τ, it must be remembered that the effects of agonist species on τ (and γ; e.g. Katz & Miledi, 1973a; Colquhoun et al., 1975) remain largely

unexplained (see Colquhoun, 1979). One possibility that has received relatively little (biochemical) attention is the effect of the various (permeant) cations on agonist binding (but c.f. Neumann & Chang, 1976; Heidmann & Changeux, 1978). Obviously, these alternatives merit further study.

In summary, it would appear that our understanding of the molecular processes important in determining ion selectivity and γ has reached a fairly sophisticated level (although, less so, for τ). However, in spite of the intensive (and extensive) electrophysiological efforts in this direction, it may be that the satisfactory conclusion of this aspect of (classical) biophysics will rest in the hands of the biochemists and physical chemists, who have available more subtle techniques amenable to the problem. Nevertheless, the advent of the giga-ohm seal, patch clamp (e.g. Hamill et al., 1981) promises to provide an exceptionally potent method in the electrophysiolgists' armoury, ideally suited for investigating the distribution of lifetimes (and not subject to the vagaries of noise analysis). Finally, there can be no doubt that fresh challenges in ion channel research are forthcoming. For example, the recently described Ca-activated K channel, with its large γ (= 100 pS) and high selectivity (Pallotta et al., 1981; Marty, 1981), along with the large γ reported for glutamate-activated synaptic channels in locust muscle (e.g. Patlak et al., 1979; Gration et al., 1981) may pose problems for the theoreticians. Clearly these observations are music to the ears of the experimentalists.

ACKNOWLEDGEMENTS

It is a pleasure to acknowledge Professor W.E. Glover for facilitating my entry into the School as a graduate student, and for providing continued support throughout the duration of my stay here.

Professor Peter W. Gage and Dr. Peter H. Barry co-supervised my thesis. I thank them for stimulating discussion, constructive criticism, guidance and encouragement. The Biophysics group in Room 308 has provided a unique learning environment - I owe debts in particular to David Adams, Nick Datyner, Owen Hamill and Dirk Van Helden for their help in acquiring some of the more subtle research skills that I now possess. For their contribution to the milieu of Room 308 and for their friendship, I also thank my colleagues - Jude Allen, Sue Andrews, Ron Balnave, Angela Dulhunty, Chris French, Alan Harvey, Maureen Lonergan, John MacDonald, Sandy Murray, Nino Quartararo, Jamie Rist, Pankaj Sah, Hugh Spencer, Tom Torda, Peter Vaughan and Ruth Wachtel. Recent critical discussions of ion permeation concepts with Paul Adams are gratefully acknowledged.

The Electrical and Mechanical Workshops in the School were instrumental in the design, construction or maintenance of much of the equipment I used - thanks to Ted Crawford, Lumir Pek, Heinz Schneider and Colin Woods, and to Jack Aberhard and Bill Van Kalken. I am grateful to Wendy Cumines, Pegi Holtz, Barb Karet, Rodney Malbon and Mandy Winterbotham for their technical assistance over the years. Cynthia Prescott has been typist non pareil in the preparation of both this thesis, and the endless drafts of various papers. A special thanks to Dirk Van Helden for the use of his computer analysis programs and to Rodney Malbon for maintaining the computer facilities. The Medical Illustrations Unit at the Prince of Wales Hospital provided excellent photographic service in producing the final prints (and slides) of the figures.

I am thankful to the National Research Council of Canada for giving me financial sustenance in the form of a Postgraduate Scholarship.

Finally, Nancy, my wife, has been responsible for timely and professional comments on my progress, for maintaining my perception of the Alice-in-Wonderland nature of research and for much happiness.

REFERENCES

ADAMS, D.J. 1978. An analysis of ionic channels in Aplysia nerve cell-membrane. Ph.D. Thesis, University of New South Wales, Sydney, Australia.

ADAMS, D.J., DWYER, T.M. & HILLE, B. 1980. The permeability of end-plate channels to monovalent and divalent metal cations. J. Gen. Physiol. 75, 493-510.

ADAMS, D.J., NONNER, W., DWYER, T.M. & HILLE, B. 1981. Block of end-plate channels by permeant cations in frog skeletal muscles. J. Gen. Physiol. In press.

ADAMS, P.R. 1975. A study of desensitization using voltage clamp. Pflüg. Arch. 360, 135-144.

ADAMS, P.R. 1976a. Voltage dependence of agonist responses at voltage-clamped frog end-plates. Pflüg. Arch. 361, 145-151.

ADAMS, P.R. 1976b. Drug blockade of open end-plate channels. J. Physiol. 260, 531-552.

ADAMS, P.R. 1977a. Relaxation experiments using bath-applied suberyldicholine. J. Physiol. 268, 271-289.

ADAMS, P.R. 1977b. Voltage jump analysis of procaine action at frog end-plate. J. Physiol. 268, 291-318.

ADAMS, P.R. 1979. Ion movements in end-plate channels. Brain Res. Bull. 4, 147-148.

ADAMS, P.R. & FELTZ, A. 1980. Quinacrine (mepacrine) action at frog end-plate. J. Physiol. 306, 261-281.

ADAMS, P.R. & SAKMANN, B. 1978a. Decamethonium both opens and blocks end-plate channels. Proc. Natl. Acad. Sci. U.S.A. 75, 2994-2998.

ADAMS, P.R. & SAKMANN, B. 1978b. A comparison of current-voltage relations for full and partial agonists. J. Physiol. 283, 621-644.

ADLER, M., ALBUQUERQUE, E.X. & LEBEDA, F.J. 1978. Kinetic analysis of the action of end-plate currents altered by atropine and scopolamine. Molec. Pharmacol. 14, 514-529.

ADLER, M., OLIVEIRA, A.C., ALBUQUERQUE, E.X., MANSOUR, N.A. & ELDEFRAWI, A.T. 1979. Reaction of tetraethylammonium with the open and closed conformations of the acetylcholine receptor ionic channel complex. J. Gen. Physiol. 74, 129-152.

ADRIAN, E.D. 1914. The all-or-none principle in nerve. J. Physiol. 47, 460-474.

ALBUQUERQUE, E.X. & THESLEFF, S. 1967. Influence of phospholipase C on some electrical properties of the skeletal muscle membrane. J. Physiol. 190, 123-138.

ALEMÀ, S., CULL-CANDY, S.G., MILEDI, R. & TRAUTMANN, A. 1981. Properties of end-plate channels in rats immunized against acetylcholine receptors. J. Physiol. 311, 251-266.

ANDERSON, C.R. & STEVENS, C.F. 1973. Voltage clamp analysis of acetylcholine produced end-plate current fluctuations at frog neuromuscular junction. J. Physiol. 235, 655-691.

ANDERSEN, O.S. & PROCOPIO, J. 1980. Ion movement through gramicidin A channels. Acta Physiol. Scand. Suppl. 481, 27-35.

ARMSTRONG, C.M. 1975. Channels and voltage dependent gates in nerve. In: Membranes - A Series of Advances. Dynamic Properties of Lipid Bilayers and Biological Membranes. ed. Eisenman, G. vol. 3, Marcel Dekker, N.Y. Chap. 5. 325-358.

ARMSTRONG, C.M. & GILLY, W.F. 1979. Fast and slow steps in the activation of sodium channels. J. Gen. Physiol. 74, 691-711.

ASCHER, P., LARGE, W.A. & RANG, H.P. 1979. Studies on the mechanism of action of acetylcholine antagonists on rat parasympathetic ganglion cells. J. Physiol. 295, 139-170.

ASCHER, P., MARTY, A. & NEILD, T.O. 1978. Lifetime and elementary conductance of the channels mediating the excitatory effects of acetylcholine in Aplysia neurones. J. Physiol. 278, 177-206.

AXELSSON, J. & THESLEFF, S. 1959. A study of supersensitivity in denervated mammalian skeletal muscle. J. Physiol. 147, 178-193.

BAMBERG, E. & LÄUGER, P. 1977. Blocking of the Gramicidin channel by divalent cations. J. Membr. Biol. 35, 351-375.

BARRY, P.H. & DIAMOND, J.M. 1970. Junction potentials, electrode standard potentials, and other problems in interpreting electrical properties of membranes. J. Membr. Biol. 3, 93-122.

BARRY, P.H. & DIAMOND, J.M. 1971. A theory of ion permeation through membranes with fixed neutral sites. J. Membr. Biol. 4, 295-330.

BARRY, P.H., DIAMOND, J.M. & WRIGHT, E.M. 1971. The mechanism of cation permeation in rabbit gall bladder. Dilution potentials and biionic potentials. J. Membr. Biol. 4, 358-394.

BARRY, P.H., GAGE, P.W. & VAN HELDEN, D.F. 1979a. Cation permeation at the amphibian motor end-plate. J. Membr. Biol. 45, 245-276.

BARRY, P.H., GAGE, P.W. & VAN HELDEN, D.F. 1979b. End-plate channels behave as neutral site channels. Neurosci. Lett. 11, 233-237.

BARRY, P.H., GAGE, P.W. & VAN HELDEN, D.F. 1979c. Cation permeation through single end-plate channels. Excerpta Med. Int. Congr. Ser. 473, 174-184.

BEGENISICH, T. & LYNCH, C. 1974. Effects of internal divalent cations on voltage-clamped squid axons. J. Gen. Physiol. 63, 675-689.

BEN-HAIM, D., LANDAU, E.M. & SILMAN, I. 1973. The role of a reactive disulphide bond in the function of the acetylcholine receptor at the frog neuromuscular junction. J. Physiol. 234, 305-325.

BENNETT, M.V.L. 1966. Physiology of electrotonic junctions. Ann. N.Y. Acad. Sci. 137, 509-539.

BENNETT, M.V.L. 1974. Flexibility and rigidity in electrotonically coupled systems. In: Synaptic Transmission and Neuronal Interaction. ed. Bennett, M.V.L. Soc. Gen. Physiol. Series. Raven Press, N.Y. Vol. 28, 153-178.

BERNSTEIN, J. 1902. Untersuchungen zur Thermodynamik der bioelektrischen Ströme. I. (Erster Theil). Pflüg. Arch. 92, 521-562.

BLAUSTEIN, M.P. 1968. Barbiturates block sodium and potassium conductance increase in voltage-clamped lobster axon. J. Gen. Physiol. 51, 293-307.

BLAUSTEIN, M.P. & GOLDMAN, D.E. 1968. The action of certain polyvalent cations on the voltage-clamped lobster axon. J. Gen. Physiol. 51,279-291

BLINKS, L.R. 1930. The direct current resistance of Nitella. J. Gen. Physiol. 13, 495-508.

BOHEIM, G., HANKE, W., BARRANTES, F.J., EIBL, H., SAKMAN, B., FELS, G. & MAELICKE, A. 1981. Agonist-activated ionic channels in acetylcholine receptor reconstituted into planar lipid bilayers. Proc. Natl. Acad. Sci. USA, 78, 3586-3590.

BORON, W.F., & DE WEER, P. 1976. Intracellular pH transients in squid giant axons caused by CO_2, NH_3 and metabolic inhibitors. J. Gen. Physiol. 67, 91-112.

BOYLE, P.J. & CONWAY, E.J. 1941. Potassium accumulation in muscle and associated changes. J. Physiol. 100, 1-63.

BRAZIER, M.A.B. 1959. The historical development of neurophysiology. In: Handbook of Physiology. Section 1: Neurophysiology. eds. Field, J. & Magoun, H.W. Am. Physiol. Soc., Washington. Vol. 1, 1-59.

BREGESTOVSKI, P.D., CHAILACHJAN, L.M., DUNIN-BARKOVSKII, V.L., POTAPOVA, T.M. & VEPRINTSEV, B.N. 1972. Effect of temperature on the end-plate equilibrium potential. Nature 236, 453-454.

BREGESTOVSKI, P.D., MILEDI, R. & PARKER, I. 1979. Calcium conductance of acetylcholine induced end-plate channels. Nature 279, 638-639.

BREITSCHMID, P. & BRENNER, H.R. 1981. Channel gating at frog neuromuscular junctions formed by different cholinergic neurones. J. Physiol. 312, 237-252.

BRENNER, H.R. & SAKMANN, B. 1978. Gating properties of acetylcholine receptor in newly-formed neuromuscular synapses. Nature 271, 366-368.

COHEN, I. & VAN DER KLOOT, W.G. 1978. Effects of [Ca^{2+}] and [Mg^{2+}] on the decay of miniature end-plate currents. Nature 271, 77-79.

COHEN, I., VAN DER KLOOT, W.G. & ATTWELL, D. 1981. The timing of channel opening during miniature end-plate currents. Brain Res. 223, 185-191.

COLE, K.S. 1949. Dynamic electrical characteristics of the squid axon membrane. Arch. Sci. Physiol. 3, 253-258.

COLE, K.S. & MOORE, J.W. 1960. Liquid junction and membrane potentials of the squid giant axon. J. Gen. Physiol. 43, 971-980.

COLE, K.S. 1972. Membranes, Ions, and Impulses. A Chapter of Classical Biophysics. University of Calif. Press, Berkeley.

COLQUHOUN, D. 1973. The relation between classical and cooperative models for drug action. In: Drug Receptors. Ed. H.P. Rang. MacMillan, London. 149-182.

COLQUHOUN, D. 1979. The link between drug binding and response: theories and observations. In: The Receptors. A Comprehensive Treatise. Vol. 1. Ed. R.D. O'Brien. Plenum Press, N.Y. 93-142.

COLQUHOUN, D., DIONNE, V., STEINBACH, J.H. & STEVENS, C.F. 1975. Conductance of channels opened by acetylcholine-like drugs in the muscle end-plate. Nature 253, 204-206.

COLQUHOUN, D., DREYER, F. & SHERIDAN, R.E. 1979. The actions of tubocurarine at the frog neuromuscular junction. J. Physiol. 293, 247-284.

COLQUHOUN, D. & HAWKES, A.G. 1977. Relaxations and fluctuations of membrane currents that flow through drug-operated channels. Proc. R. Soc. Lond. B. 199, 231-262.

COLQUHOUN, D., LARGE, W.A., RANGE, H.P. 1977. An analysis of the action of a false transmitter at the neuromuscular junction. J. Physiol. 266, 361-395.

CONTI, F. & WANKE, E. 1975. Channel noise in nerve membranes and lipid bilayers. Quart. Rev. Biophys. 8, 451-506.

COUTEAUX, R. 1951. Remarques sur les méthodes actuelles de détection histochemique des activités cholinestérasiques. Arch. Int. Physiol. 59, 526-537.

CULL-CANDY, S.G., MILEDI, R. & TRAUTMANN, A. 1979. End-plate currents and acetylcholine noise at normal and myasthenic human end-plates. J. Physiol. 287, 247-265.

CURTIS, H.J. & COLE, K.S. 1942. Membrane resting and action potentials from the squid giant axon. J. Cell. Comp. Physiol. 19, 135-144.

DALE, H.H. 1914. The action of certain esters and ethers of choline, and their relation to muscarine. J. Pharmacol. Exp. Therap. 6, 147-190.

DALE, H.H., FELDBERG, W. & VOGT, M. 1936. Release of acetylcholine at voluntary motor nerve endings. J. Physiol. 86, 353-380.

DANI, J.A. & LEVITT, D.G. 1981a. Binding constants of Li^+, K^+ and Tl^+ in the gramicidin channel determined from water permeability measurements. Biophys. J. 35, 485-500.

DANI, J.A. & LEVITT, D.G. 1981b. Water transport and ion-water interaction in the gramicidin channel. Biophys. J. 35, 501-508.

DEGUCHI, T. & NARAHASHI, T. 1971. Effects of procaine on ionic conductances of end-plate membranes. J. Pharmacol. Exp. Therap. 176, 423-433.

DEL CASTILLO, J. & KATZ, B. 1954. The membrane change produced by the neuromuscular transmitter. J. Physiol. 125, 546-565.

DEL CASTILLO, J. & KATZ, B. 1955. Local activity at a depolarized nerve-muscle junction. J. Physiol. 128, 396-411.

DEL CASTILLO, J. & KATZ, B. 1957. Interaction at end-plate receptors between different choline derivatives. Proc. R. Soc. Lond. B. 146, 369-381.

DIONNE, V.E. & PARSONS, R.L. 1981. Characteristics of the acetylcholine-operated channel at twitch and slow fibre neuromuscular junctions of the garter snake. J. Physiol. 310, 145-158.

DIONNE, V.E. & RUFF, R.L. 1977. End-plate current fluctuations reveal only one channel type at frog neuromuscular junction. Nature 266, 263-265.

DIONNE, V.E. & STEVENS, C.F. 1975. Voltage dependence of agonist effectiveness at the frog neuromuscular junction. J. Physiol. 251, 245-270.

DULHUNTY, A.F. & GAGE, P.W. 1973. Electrical properties of toad sartorius muscle fibres in summer and winter. J. Physiol. 230, 619-641.

DUNIN-BARKOVSKII, V.L., KOVALEV, S.A., MAGAZANIK, L.G., POTAPOVA, T.V. & CHAYLAKHYAN, L.M. 1969. Equilibirum potentials of postsynaptic membrane activated with various cholinomimetics when the extracellular ionic medium is changed. Biofizika 14, 485-494.

DWYER, T.M., ADAMS, D.J. & HILLE, B. 1979. Ionic selectivity of end-plate channels. Biophys. J. 25, 67a.

DWYER, T.M., ADAMS, D.J. & HILLE, B. 1980. The permeability of end-plate channels to organic cations in frog muscle. J. Gen. Physiol. 75, 469-492.

ECCLES, J.C., KATZ, B. & KUFFLER, S.W. 1941. Nature of the 'end-plate potential' in curarized muscle. J. Neurophysiol. 4, 362-387.

EHRENSTEIN, G. & LECAR, H. 1977. Electrically gated ionic channels in lipid bilayers. Quart. Rev. Biophys. 10, 1-34.

EISENBERG, R.S., HOWELL, J.N. & VAUGHAN, P.C. 1971. The maintenance of resting potentials in glycerol-treated muscle fibres. J. Physiol. 215, 95-102.

EISENMAN, G. 1962. Cation selective glass electrodes and their mode of operation. Biophys. J. 2, 259-323.

EISENMAN, G. 1965. Some elementary factors involved in specific ion permeation. Proc. 23rd Int. Congr. Physiol. Sci. Tokyo. Reprinted from Exerpta Medica, International Congress Series, 87, 489-506.

EISENMAN, G. 1967. Particular properties of cation-selective glass electrodes containing Al_2O_3. In Glass Electrodes for Hydrogen And Other Cations. G. Eisenman, editor. Marcel Dekker, Inc., New York. Chap. 9.

ELLIOT, T.R. 1904. On the action of adrenalin. J. Physiol. 31, xx (Proc.)

FARLEY, J.M., YEH, J.Z., WATANABE, S. & NARAHASHI, T. 1981. End-plate channel block by guanidine derivatives. J. Gen. Physiol. 77, 273-293.

FATT, P. & KATZ, B. 1951. An analysis of the end-plate potential recorded with an intracellular electrode. J. Physiol. 115, 320-370.

FELTZ, A., LARGE, W.A. & TRAUTMANN, A. 1977. Analysis of atropine action at the frog neuromuscular junction. J. Physiol. 269, 109-130.

FELTZ, A. & MALLART, A. 1971a. An analysis of acetylcholine responses of junctional and extrajunctional receptors of frog muscle fibres. J. Physiol. 215, 85-100.

FELTZ, A. & MALLART, A. 1971b. Ionic permeability changes induced by some cholinergic agonists on normal and denervated frog muscle fibres. J. Physiol. 215, 101-116.

FIEKERS, J.F., SPANNBAUER, P.M., SCUBON-MULIERI, B. & PARSONS, R.L. 1980. Voltage dependence of desensitization. Influence of calcium and activation kinetics. J. Gen. Physiol. 75, 511-529.

FINKELSTEIN, A. & ANDERSEN, O.S. 1981. The gramicidin A channel: A review of its permeability characteristics with special reference to the single-file aspect of transport. J. Membr. Biol. 59, 155-171.

FINKELSTEIN, A. & MAURO, A. 1963. Equivalent circuits as related to ionic systems. Biophys. J. 3, 215-237.

FISCHBACH, G.D. & LASS, Y. 1978. Acetylcholine noise in cultured chick myoballs: A voltage clamp analysis. J. Physiol. 280, 515-526.

FISHMAN, H.M. 1975. Noise measurements in axon membranes. Fed. Proc. 34, 1330-1337.

FRENCH, R.J. & ADELMAN, W.J., Jr. 1976. Competition, saturation and inhibition - ionic interactions shown by membrane ionic currents in nerve, muscle and bilayer systems. In: Current Topics in Membranes and Transport. Academic Press, N.Y. Vol. 8, 161-207.

FRANKENHAEUSER, B. & HODGKIN, A.L. 1957. The action of calcium on the electrical properties of squid axons. J. Physiol. 137, 218-244.

FUJINO, M., YAMAGUCHI, T. & SUZUKI, K. 1961. 'Glycerol effect' and the mechanism linking excitation of the plasma membrane with contraction. Nature 192, 1159-1161.

FURSHPAN, E.J. & POTTER, D.D. 1959 . Transmission at the giant motor synapses of the crayfish. J. Physiol. 145, 289-325.

FURUKAWA, T., & FURUKAWA, A. 1959. Effects of methyl- and ethyl-derivatives of NH_4^+ on the neuromuscular junction. Japn. J. Physiol. 9, 130-142.

FURUKAWA, T., FURUKAWA, A. & TAKAGI, T. 1957. Fibrillation of muscle fibres produced by ammonium ions and its relation to the spontaneous activity at the neuromuscular junction. Japn. J. Physiol. 7, 252-266.

GAGE, P.W. 1976. Generation of end-plate potentials. Physiol. Rev. 56, 177-247.

GAGE, P.W. & ARMSTRONG, C.M. 1968. Miniature end-plate currents in voltage-clamped muscle fibres. Nature 218, 363-365.

GAGE, P.W. & EISENBERG, R.S. 1967. Action potentials without contraction in frog skeletal muscle fibres with disrupted transverse tubules. Science 158, 1702-1703.

GAGE, P.W. & HAMILL, O.P. 1980. Lifetime and conductance of acetylcholine-activated channels in normal and denervated toad sartorius muscle. J. Physiol. 298, 525-538.

GAGE, P.W. & HAMILL, O.P. 1981. Effects of anesthetics on ion channels in synapses. In: Int. Rev. Physiol., ed. R. Porter. Vol. 25, 1-45.

GAGE, P.W., HAMILL, O.P. & VAN HELDEN, D.F. 1979. Dual effects of ether on end-plate currents. J. Physiol. 287, 353-369.

GAGE, P.W. & McBURNEY, R.N. 1972. Miniature end-plate currents & potentials generated by quanta of acetylcholine in glycerol-treated fibres. J. Physiol. 226, 79-94.

GAGE, P.W. & McBURNEY, R.N. 1975. Effects of membrane potential, temperature and neostigmine on the conductance change caused by a quantum of acetylcholine at the toad neuromuscular junction. J. Physiol. 224, 385-407.

GAGE, P.W., McBURNEY, R.N. & SCHNEIDER, G.T. 1975. Effects of some aliphatic alcohols on the conductance change caused by a quantum of acetylcholine at the toad end-plate. J. Physiol. 244, 409-429.

GAGE, P.W., McBURNEY, R.N. & VAN HELDEN, D.F. 1974. End-plate currents are shortened by octanol: possible role of membrane lipid. Life Sci. 14, 2277-2283.

GAGE, P.W., McBURNEY, R.N. & VAN Helden, D.F. 1978. Octanol reduces end-plate channel lifetime. J. Physiol. 274, 279-298.

GAGE, P.W. & VAN HELDEN, D.F. 1979. Effects of permeant monovalent cations on end-plate channels. J. Physiol. 288, 509-528.

GINSBORG, B.L. 1967. Ion movements in junctional transmission. Pharmacol. Rev. 19, 289-315.

GINSBORG, B.L. 1973. Electrical changes in the membrane in junctional transmission. Biochim. Biophys. Acta 300, 289-317.

GLASSTONE, S., LAIDLER, K.J. & EYRING, H. 1941. The Theory of Rate Processes. 1-611. McGraw-Hill, N.Y.

GLAVINOVIC, M.I. 1979. Voltage clamping of unparalysed rat diaphragm for study of transmitter release. J. Physiol. 299, 467-488.

GOLDMAN, D. 1943. Potential, impedance and rectification in membranes. J. Gen. Phsyiol. 27, 37-60.

GRAHAME, D.C. 1947. The electrical double layer and the theory of electrocapillarity. Chem. Rev. 41, 441-501.

GRATION, K.A.F., LAMBERT, J.J., RAMSEY, R. & USHERWOOD, P.N.R. 1981. Non-random openings and concentration-dependent lifetimes of glutamate-gated channels in muscle membrane. Nature 291, 423-425.

GUY, H.R., DEKIN, M.S. & MORELLO, R. 1977. Effects of denervation on the permeability of acetylcholine-activated channels to organic cations. J. Neurobiol. 8, 491-506.

HAGINS, W.A. 1965. Electrical signs of information flow in photoreceptors. Cold Spring Harbor Symp. Quant. Biol. 30, 403-418.

HAMILL, O.P., MARTY, A., NEHER, E., SAKMANN, B. & SIGWORTH, F.J. 1981. Improved patch-clamp techniques for high-resolution current recording from cells and cell-free membrane patches. Pflüg. Arch. 391, 85-100.

HARVEY, A.L. & VAN HELDEN, D.F. 1981. Acetylcholine receptors in singly and multiply innervated skeletal muscle fibres of the chicken during development. J. Physiol. 317, 397-411.

HEIDMANN, T. & CHANGEUX, J.-P. 1978. Structural and functional properties of the acetylcholine receptor protein in its purified and membrane-bound states. Ann. Rev. Biochem. 47, 317-357.

HENDERSON, E.G. 1970. Potassium exchange and after potentials in frog sartorius muscles treated with glycerol. J. Gen. Physiol. 56, 692-715.

HLADKY, S.B. & HAYDON, D.A. 1972. Ion transfer across lipid membranes in the presence of Gramicidin A. I. Studies of the unit conductance channel. Biochim. Biophys. Acta 274, 294-314.

HILLE, B. 1970. Ionic channels in nerve membranes. Progr. Biophys. Mol. Biol. 21, 1-32.

HILLE, B. 1971. The permeability of the sodium channel to organic cations in myelinated nerve. J. Gen. Physiol. 58, 599-619.

HILLE, B. 1972. The permeability of the sodium channel to metal cations in myelinated nerve. J. Gen. Physiol. 59, 637-658.

HILLE, B. 1975. Ionic selectivity of Na and K channels of nerve membranes. In: Membranes - A Series of Advances, Vol. 3, Dynamic Properties of Lipid Bilayers and Biological Membranes. Ed. Eisenman, G. Marcel Dekker, N.Y. Chap. 4. 255-323.

HILLE, B. 1977. Local anesthetics: Hydrophilic and hydrophobic pathways for the drug-receptor reaction. J. Gen. Physiol. 69, 497-515.

HILLE, B. & SCHWARZ, W. 1978. Potassium channels as multi-ion single-file pores. J. Gen. Physiol. 72, 409-442.

HILLE, B., WOODHULL, A.M. & SHAPIRO, B.I. 1975. Negative surface charge near sodium channels of nerve: divalent ions, monovalent ions and pH. Philos. Trans. R. Soc. Lond. B. Biol. Sci. 270, 301-318.

HODGKIN, A.L. (1964). The Conduction of the Nervous Impulse. C.C. Thomas, Springfield.

HODGKIN, A.L. & HOROWICZ, P. 1959a. Movements of Na and K in single muscle fibres. J. Physiol. 145, 405-432.

HODGKIN, A.L. & HOROWICZ, P. 1959b. The influence of potassium and chloride ions on the membrane potential of single muscle fibres. J. Physiol. 148, 127-160.

HODGKIN, A.L. & HUXLEY, A.F. 1939. Action potentials recorded from inside a nerve fibre. Nature 144, 710.

HODGKIN, A.L. & KATZ, B. 1949. The effects of sodium ions on the electrical activity of the giant axon of the squid. J. Physiol. 108, 37-77.

HODGKIN, A.L. & KEYNES, R.D. 1955. The potassium permeability of a giant nerve fibre. J. Physiol. 128, 61-88.

HORN, R. & BRODWICK, M.S. 1980. Acetylcholine-induced current in perfused rat myoballs. J. Gen. Physiol. 75, 297-321.

HORN, R., BRODWICK, M.S. & DICKEY, W.D. 1980. Asymmetry of the acetylcholine channel revealed by quaternary anesthetics. Science 210, 205-207.

HORN, R. & PATLAK, J. 1980. Single channel currents from excised patches of muscle membrane. Proc. Natl. Acad. Sci. U.S.A. 77, 6930-6934.

HORN, R. & STEVENS, C.F. 1980. Relation between structure and function of ion channels. Comments Mol. & Cell. Biophys. 1, 57-68.

HOWELL, J.N., & JENDEN, D.J. 1967. T-tubules of skeletal muscle: morphological alterations which interrupt excitation-secretion coupling. Fed. Proc. 26, 553.

HUANG, L.M., CATTERALL, W.A. & EHRENSTEIN, G. 1978. Selectivity of cations and nonelectrolytes for acetylcholine-activated channels in cultured muscle cells. J. Gen. Physiol. 71, 397-410.

JAFFE, L.F. 1974. The interpretation of voltage-concentration relations. J. Theor. Biol. 48, 11-18.

JORDAN, P.C. 1981. Energy barriers for passage of ions through channels. Exact solution of two electrostatic problems. Biophys. Chem. 13, 203-212.

KAIBARA, K., KUBA, K., KOKETSU, K. & KARCZMAR, A.G. 1978. The mode of action of fluoride ions on neuromuscular transmission in frogs. Neuropharmacol. 17, 335-339.

KATZ, B. & MILEDI, R. 1969. Spontaneous and evoked activity of motor nerve endings in calcium Ringer. J. Physiol. 203, 689-706.

KATZ, B. & MILEDI, R. 1970. Membrane noise produced by acetylcholine. Nature, 226, 962-963.

KATZ, B. & MILEDI, R. 1971. Further observations on acetylcholine noise. Nature 232, 124-216.

KATZ, B. & MILEDI, R. 1972. The statistical nature of the acetylcholine potential and its molecular components. J. Physiol. 224, 665-699.

KATZ, B. & MILEDI, R. 1973a. The characteristics of "end-plate noise" produced by different depolarizing drugs. J. Physiol. 230, 707-712.

KATZ, B. & MILEDI, R. 1973b. The binding of acetylcholine to receptors and its removal from the synaptic cleft. J. Physiol. 231, 549-574.

KATZ, B. & MILEDI, R. 1975. The nature of the prolonged end-plate depolarization in anti-esterase treated muscle. Proc. R. Soc. B. 192, 27-38.

KATZ, B. & MILEDI, R. 1977. The reversal potential at the desensitized end-plate. Proc. R. Soc. Lond. B. 199, 329-334.

KATZ, B. & MILEDI, R. 1978. A re-examination of curare action at the motor end-plate. Proc. R. Soc. B. 203, 119-133.

KATZ, B. & MILEDI, R. 1980. Blockade of end-plate responses by intracellular application of procaine. In: Ontogenesis and Functional Mechanisms of Peripheral Synapses. INSERM Symposium No. 13, ed. J. Taxi. 171-178.

KATZ, B. & THESLEFF, S. 1957. A study of the "desensitization" produced by acetylcholine at the motor end-plate. J. Physiol. 138, 63-80.

KEHOE, J.S. 1972. Ionic mechanisms of a two-component cholinergic inhibition in aplysia neurones. J. Physiol. 225, 85-114.

KOELLE, G.B. 1950. The histochemical differentiation of types of cholinesterases and their localizations in tissues of the cat. J. Pharmacol. Exp. Therap. 100, 158-179.

KOEPPE, R.E., BERG, J.M., HODGSON, K.O. & STRYER, L. 1979. Gramicidin A crystals contain two cation binding sites per channel. Nature 279, 723-725.

KOKETSU, K. & NISHI, S. 1959. Restoration of neuromuscular transmission in sodium-free hydrazinium solution. J. Physiol. 147, 239-252.

KOLB, H.A. & BAMBERG, E. 1979. Influence of membrane thickness and ion concentration on the properties of the Gramicidin A channel. Autocorrelation, spectral power density, relaxation and single channel properties. Biochim. Biophys. Acta 464, 127-141.

KORDAŚ, M. 1968. A study of the end-plate potential in sodium deficient solution. J. Physiol. 198, 81-90.

KORDAŚ, M. 1969. The effect of membrane polarization on the time course of end-plate current in frog Sartorius muscle. J. Physiol. 204, 493-502.

KORDAŚ, M. 1972a. An attempt at an analysis of the factors determining the time course of the end-plate current. I. The effects of prostigmine and the ratio of Mg^{2+} to Ca^{2+}. J. Physiol. 224, 317-332.

KORDAŚ, M. 1972b. An attempt at an analysis of the factors determining the time course of the end-plate current. II. Temperature. J. Physiol. 224, 333-348.

KORDAŠ, M. 1977. On the role of junctional cholinesterase in determing the time course of the end-plate current. J. Physiol. 270, 133-150.

KROLENKO, S.A., ADAMJAN, S.J. SHVINKA, N.E. 1967. Vacuolization of skeletal muscle fibres. I. Vacuolization of fibres after discharging low-molecular non-electrolytes. Cytology (USSR), 9, 1346-1353.

KUBA, K., CHIKAZAWA, K. & KOKETSU, K. 1976. Novel action of a piperazine derivative on the end-plate of the frog. Japn. J. Physiol. 26, 159-175.

KUBA, K. & KOKETSU, K. 1976. Decrease of Na^+ conductance during desensitization of the frog end-plate. Nature 262, 504-505.

KUBA, K. & NISHI, J. 1979. Characteristics of fast excitatory post-synaptic current in bullfrog sympathetic ganglion cells. Effects of membrane potential, temperature and Ca ion. Pflüg. Arch. 378, 205-212.

KUFFLER, S.W. 1942. Electric potential changes at an isolated nerve-muscle junction. J. Neurophysiol. 5, 18-26.

KUFFLER, S.W. 1943. Specific excitability of the end-plate region in normal and denervated muscle. J. Neurophysiol. 6, 99-110.

KUFFLER, S.W. & YOSHIKAMI, D. 1975. The distribution of acetylcholine sensitivity at the postsynaptic membrane of vertebrate skeletal twitch muscles: iontophoretic mapping in the micron range. J. Physiol. 244, 703-730.

LAMBERT, D.H., SPANNBAUER, P.M. & PARSONS, R.L. 1977. Desensitisation does not selectively alter sodium channels. Nature 268, 553-555.

LAMBERT, J.J., VOLLE, R.L. & HENDERSON, E.G. 1980. An attempt to distinguish between the actions of neuromuscular blocking drugs on the acetylcholine receptor and its associated ionic channel. Proc. Natl. Acad. Sci. U.S.A. 77, 5003-5007.

LANDAU, E.M. 1978. The relation between function and structure of the ACh receptor at the muscle end-plate. Progr. Neurobiol. 10, 253-288.

LANDAU, E.M., GAVISH, B., NASCHEN, D.A. & LOTAN, I. 1981. pH dependence of the acetylcholine receptor channel. A species variation. J. Gen. Physiol. 77, 647-666.

LANGLEY, J.N. 1905. On the reaction of cells and of nerve-endings to certain poisons, chiefly as regards the reaction of striated muscle to nicotine and to curari. J. Physiol. 33, 374-413.

LASSIGNAL, N.L. & MARTIN, A.R. 1977. Effects of acetylcholine on postjunctional membrane permeability in eel electroplaque. J. Gen. Physiol. 70, 23-36.

LEVITT, D.G. 1978a. Electrostatic calculations for an ion channel. I. Energy and potential profiles between ions. Biophys. J. 22, 209-219.

LEVITT, D.G. 1978b. Electrostatic calculations for an ion channel. II. Kinetic behaviour of the Gramicidin A channel. Biophys. J. 22, 221-248.

LEWIS, C.A. 1979. Ion-concentration dependence of the reversal potential and the single channel conductance of ion channels at the frog neuromuscular junction. J. Physiol. 286, 417-445.

LEWIS, C.A. & STEVENS, C.F. 1979. Mechanisms of ion permeation through channels in a postsynaptic membrane. In: Membrane Transport Processes, Vol. 3. ed.: Stevens, C.F. & Tsien, R.W. Raven Press, N.Y. 133-151.

LINDEMANN, B. 1980. The beginning of fluctuation analysis of epithelial ion transport. J. Membr. Biol. 54, 1-11.

LINDER, T.M. & QUASTEL, D.M.J. 1978. A voltage-clamp study of the permeability change induced by quanta of transmitter at the mouse end-plate. J. Physiol. 281, 535-556.

LINEWEAVER, H. & BURK, D. 1934. The determination of enzyme dissociation constants. J. Amer. Chem. Soc. 56, 658-666.

LING, G. & GERARD, R.W. 1949. The normal membrane potential of frog sartorius fibers. J. Cell. Comp. Physiol. 34, 383-396.

LINGLE, C. & AUERBACH, A. 1980. Analysis of channels activated by acetylcholine and glutamate in crustacean muscles. Soc. Neurosci. Abstr. 6, 754.

LOEWI, O. 1921. Über humorale Übertragbarkeit der Herznervenwirkung. I. Mitteilung. Pflüg. Arch. 189, 239-242.

LUCAS, K. 1908-1909. The "all-or-none" contraction of amphibian skeletal muscle fibre. J. Physiol. 38, 113-133.

MACDERMOTT, A.B., CONNOR, E.A., DIONNE, V.E. & PARSONS, R.L. 1980. Voltage clamp study of fast excitatory synaptic currents in bull-frog sympathetic ganglion cells. J. Gen. Physiol. 75, 39-60.

MAENO, T. 1966. Analysis of sodium and potassium conductances in the procaine end-plate potential. J. Physiol. 183, 592-606.

MAENO, T., EDWARDS, C. & ANRAKU, M. 1977. Permeability of end-plate membrane activated by acetylcholine to some organic cations. J. Neurobiol. 8, 173-184.

MAENO, T., EDWARDS, C. & HASHIMURA, S. 1971. Differences in effects on endplate potentials between procaine and lidocaine as revealed by voltage clamp experiments. J. Neurophysiol. 34, 32-46.

MAGAZANIK, L.G. & POTOPOVA, V.T. 1969. Equilibrium potentials of the extrasynaptic membrane of denervated muscle with change in the extracellular ionic medium. Biofizika, 14, 658-661.

MAGAZANIK, L.G. & VYSKOCIL, F. 1973. Desensitization at the motor end-plate. In: Drug Receptors. Ed. H.P. Rang. MacMillan, N.Y. 105-119.

MAGLEBY, K.L. & STEVENS, C.F. 1972a. The effect of voltage on the time course of end-plate currents. J. Physiol. 223, 151-171.

MAGLEBY, K.L. & STEVENS, C.F. 1972b. A quantitative description of end-plate currents. J. Physiol. 223, 173-197.

MAGLEBY, K.L. & WEINSTOCK, M.M. 1980. Nickel and calcium ions modify the characteristics of the acetylcholine receptor-channel complex at the frog neuromuscular junction. J. Physiol. 299, 203-218.

MALLART, A., DREYER, F. & PEPER, K. 1976. Current-voltage relation and reversal potential at junctional and extrajunctional ACh-receptors of the frog neuromuscular junction. Pflüg. Arch. 362, 43-47.

MALLART, A. & TRAUTMANN, A. 1973. Ionic properties of the neuromuscular junction of the frog: effects of denervation and pH. J. Physiol. 234, 553-567.

MALLART, A. & MOLGŐ, J. 1978. The effects of pH and curare on the time course of end-plate currents at the neuromuscular junction of the frog. J. Physiol. 276, 343-352.

MANALIS, R.S. 1977. Voltage-dependent effect of curare at the frog neuromuscular junction. Nature 267, 366-367.

MARCHAIS, D. & MARTY, A. 1979. Interaction of permeant ions with channels activated by acetylcholine in Aplysia neurones. J. Physiol. 297, 9-45.

MARCHAIS, D. & MARTY, A. 1980. Action of glucosamine on acetylcholine-sensitive channels. J. Membr. Biol. 56, 43-48.

MARMONT, G. 1949. Studies on the axon membrane; I. A new method. J. Cell. Comp. Physiol. 34, 351-382.

MARTY, A. 1980. Action of calcium ions on acetylcholine-sensitive channels in aplysia neurones. J. Physiol., Paris 76, 523-527.

MARTY, A. 1981. Ca-dependent K channels with large unitary conductance in chromaffin cell membranes. Nature 291, 497-500.

MARTY, A., NEILD, T.O. & ASCHER, P. 1976. Voltage sensitivity of acetylcholine currents in Aplysia neurones in the presence of curare. Nature 261, 501-503.

McLACHLAN, E.M. & MARTIN, A.R. 1981. Non-linear summation of end-plate potentials in the frog and mouse. J. Physiol. 311, 307-324.

McLAUGHLIN, S.G.A., SZABO, G. & Eisenman, G. 1971. Divalent ions and the surface potential of charged phospholipid membranes. J. Gen. Physiol. 58, 667-687.

MICHAELIS, L. & MENTEN, M.L. 1913. Der kinetik der invertwirkung. Biochem. Zeitschr. 49, 333-369.

MILEDI, R. & PARKER, I. 1980. Effects of strontium ions on end-plate channel properties. J. Physiol. 306, 567-577.

MILEDI, R. & UCHITEL, O.D. 1981. Properties of postsynaptic channels induced by acetylcholine in different frog muscle fibres. Nature 291, 162-165.

MOORE, W.J. 1972. In: Physical Chemistry. 5th Ed. Prentice-Hall, Inc., New Jersey, p.435.

MORENO, J.H. & DIAMOND, J.M. 1975. Cation permeation mechanisms and cation selectivity in 'tight junctions' of gall bladder epithelium. In: Membranes - A Series of Advances, Vol. 3, Dynamic Properties of Lipid Bilayers and Biological Membranes, ed. Eisenman, G. Marcel Dekker, N.Y. Chap. 7. 383-497.

MULLINS, L.J. 1959. An analysis of conductance changes in squid axon. J. Gen. Physiol. 42, 1013-1025.

MULLINS, L.J. 1960. An analysis of pore size in excitable membranes. J. Gen. Physiol. 43, Suppl. 1, 105-117.

MULLINS, L.J. 1968. A single channel or a dual channel mechanism for nerve excitation. J. Gen. Physiol. 52, 550-556.

MYERS, V.B. & HAYDON, D.A. 1972. Ion transfer across lipid membranes in the presence of Gramicidin A. II. The ion selectivity. Biophys. Biochim. Acta 274, 313-322.

NASTUK, W.L. 1953. The electrical activity of the muscle cell membrane at the neuromuscular junction. J. Cell. Comp. Physiol. 42, 249-272.

NASTUK, W.L. 1959. Some ionic factors that influence the action of acetylcholine at the muscle end-plate membrane. Ann. N.Y. Acad. Sci. 81, 317-327.

NASTUK, W.L. & HODGKIN, A.L. 1950. The electrical activity of single fibres. J. Cell. Comp. Physiol. 35, 39-73.

NASTUK, W.L. & PARSONS, R.L. 1970. Factors in the inactivation of postjunctional membrane receptors of frog skeletal muscle. J. Gen. Physiol. 56, 218-249.

NEHER, E. 1975. Ionic specificity of the Gramicidin channel and the thallous ion. Biochim. Biophys. Acta 401, 540-544.

NEHER, E. & EIBL, H. 1977. The influence of phospholipid polar groups on Gramicidin channels. Biochim. Biophys. Acta 464, 37-44.

NEHER, E. & SAKMANN, B. 1975. Voltage-dependence of drug-induced conductance in frog neuromuscular junction. Proc. Natl. Acad. Sci. U.S.A. 72, 2140-2144.

NEHER, E. & SAKMANN, B. 1976a. Single-channel currents recorded from membrane of denervated frog muscle fibres. Nature 260, 799-802.

NEHER, E. & SAKMANN, B. 1976b. Noise analysis of drug induced voltage clamp currents in denervated frog muscle fibres. J. Physiol. 258, 705-729.

NEHER, E., SANDBLOM, J. & EISENMAN, J. 1978. Ionic selectivity, saturation, and block in Gramicidin A channels. II. Saturation behaviour of single channel conductances and evidence for the existence of multiple binding sites in the channel. J. Membr. Biol. 40, 97-116.

NEHER, E. & STEINBACH, J.H. 1978. Local anaesthetics transiently block currents through single acetylcholine channels. J. Physiol. 277, 153-176.

NEHER, E. & STEVENS, C.F. 1977. Conductance fluctuations and ionic pores in membranes. Ann. Rev. Biophys. Bioeng. 6, 345-381.

NEUMANN, E. & CHANG, H.W. 1976. Dynamic properties of isolated acetylcholine receptor protein: Kinetics of the binding of acetylcholine and Ca ions. Proc. Natl. Acad. Sci. U.S.A. 73, 3994-3998.

NONNER, W., ADAMS, D.J., DWYER, T.M. & HILLE, B. 1980. Conductance fluctuation measurements with organic cations at the end-plate channel. Fed. Proc. 39, 2064.

OGDEN, D.C., SIEGELBAUM, S.A. & COLQUHOUN, D. 1981. Block of acetylcholine-activated ion channels by an uncharged local anaesthetic. Nature 289, 596-598.

OOMURA, Y. & TOMITA, T. 1960. Study on properties of a neuromuscular junction. In: Electrical Activity of Single Cells. Ed.: Y. KATSUKI, Igaka Shoin, Ltd., Tokyo. 181-205.

OSTERHOUT, W.J.V. 1931. Physiological studies of large plant cells. Biol. Rev. 6, 369-411.

OVERTON, E. 1902. Beiträge zur allgermeinen Muskel-und Nervenphysiologie. Pflüg. Arch. 92, 346-386.

PALLOTTA, B.S., MAGLEBY, K.L. & BARRETT, J.N. 1981. Single channel recordings of Ca^{2+}-activated K^{+} currents in rat muscle cell culture. Nature 293, 471-474.

PARSEGIAN, V.A. 1969. Energy of an ion crossing a low dielectric membrane: Solutions to four relevant electrostatic problems. Nature 221, 844-846.

PARSEGIAN, V.A. 1975. Ion-membrane interactions as structural forces. Ann. N.Y. Acad. Sci. 264, 161-174.

PATLAK, J.B., GRATION, K.A.F. & USHERWOOD, P.N.R. 1979. Single glutamate-activated channels in locust muscle. Nature 278, 643-645.

PAULING, L. 1960. Nature of the Chemical Bond. Cornell Univ. Press, N.Y. 3rd Ed. 260, 514.

RANG, H.P. 1975. Acetylcholine receptors. Quart. Rev. Biophys. 7, 283-399.

RANG, H.P. 1981. The characteristics of synaptic currents and responses to acetylcholine of rat submandibular ganglion cells. J. Physiol. 311, 23-55.

RANG, H.P. & RITTER, J.M. 1970. On the mechanism of desensitization at cholinergic receptors. Molec. Pharmacol. 6, 357-382.

REDMANN, G.A. 1980. Local anaesthetic block of the endplate channel in high external sodium. Soc. Neurosci. Abstr. 6, 693.

REUTER, H. & STEVENS, C.F. 1980. Ion conductance and ion selectivity of potassium channels in snail neurones. J. Membr. Biol. 57, 103-118.

RITCHIE, A.K. & FAMBROUGH, D.M. 1975. Ionic properties of the acetylcholine receptor in cultured rat myotubes. J. Gen. Physiol. 65, 751-767.

ROBINSON, R.A., STOKES, R.H. 1959. In: Electrolyte Solutions. 2nd Ed. Butterworths, London. pp 461, 463.

ROSENBERG, P.A. & FINKELSTEIN, A. 1978a. Interaction of ions and water in Gramicidin A channels. Streaming potentials across lipid bilayer membranes. J. Gen. Physiol. 72, 327-340.

RUDNEV, V.S., ERMISHKIN, L.N., FONINA, L.A. & ROVIN, Y.G. 1981. The dependence of the conductance and lifetime of Gramicidin channels on the thickness and tension of lipid bilayers. Biochim. Biophys. Acta 642, 196-202.

ROSENBERG, P.A. & FINKELSTEIN, A. 1978b. Water permeability of Gramicidin A treated lipid bilayer membranes. J. Gen. Physiol. 72, 341-350.

RUFF, R.L. 1977. A quantitative analysis of local anaesthetic alteration of miniature end-plate currents and end-plate current fluctuations. J. Physiol. 264, 89-124.

SACHS, F. & LECAR, H. 1977. Acetylcholine-induced current fluctuations in tissue-cultured muscle cells under voltage clamp. Biophys. J. 17, 129-143.

SAKMANN, B. & ADAMS, P.R. 1979. Biophysical aspects of agonist action at frog endplate. In: Advances in Pharmacology & Therapeutics, Vol. 1, ed. Jacob, J. Pergamon Press, Oxford. 81-90.

SAKMANN, B., PATLAK, J. & NEHER, E. 1980. Single acetylcholine-activated channels show burst kinetics in presence of desensitizing concentrations of agonist. Nature 286, 71-73.

SANDBLOM, J., EISENMAN, G. & NEHER, E. 1977. Ionic selectivity, saturation and block in Gramicidin A Channels. I. Theory for the electrical properties of ion selective channels having two pairs of binding sites and multiple conductance states. J. Membr. Biol. 31, 383-417.

SCUKA, M. 1975. The amplitude and the time course of the end-plate current at various pH levels in the frog sartorius muscle. J. Physiol. 249, o83-195.

SPIVAK, C.E., WITKOP, B. & ALBUQUERQUE, E.X. 1980. Anatoxin-a: A novel, potent agonist at the nicotinic receptor. Mol. Pharmacol. 18, 384-394.

STANDEN, N.B. 1981. Ca channel inactivation by intracellular Ca injection into Helix neurones. Nature 293, 158-159.

STEINBACH, A.B. 1968. Alteration by xylocaine (Lidocaine) and its derivatives on the time course of endplate potential. J. Gen. Physiol. 52, 162-180.

STEINBACH, J.H. 1975. Acetylcholine responses on clonal myogenic cells in vitro. J. Physiol. 247, 393-405.

STEINBACH, J.H. 1980. Activation of nicotinic acetylcholine receptors. In: The Cell Surface and Neuronal Function, eds. Cotman, C.W., Post, G.&Nicholson, G.L. Elsevier, Amsterdam. 119-156.

STEINBACH, J.H. & STEVENS, C.F. 1976. Neuromuscular transmission. In: Frog Neurobiology. Ed.: Llinás, R. & Precht, W. Springer Verlag, Berlin. 33-92.

STEVENS, C.F. 1972. Inferences about membrane properties from electrical noise measurements. Biophys. J. 12, 1028-1047.

STEVENS, C.F. 1977. Study of membrane permeability changes by fluctuation analysis. Nature 270, 391-396.

STEVENS, C.F. & TSIEN, R.W. (eds). 1979. Ion Permeation Through Membrane Channels. Membrane Transport Processes. Vol. 3, 1-168. Raven Press, N.Y.

SWENSON, Jr., R.P. & ARMSTRONG, C.M. 1981. K^+ channels close more slowly in the presence of external K^+ and Rb^+. Nature 29, 427-429.

SWENSON, R.P. & NARAHASHI, T. 1980. Block of sodium conductance by n-octanol in crayfish giant axons. Biochim. Biophys. Acta 603, 228-236.

SZABO, G., EISENMAN, G., LAPRADE, R., CIANI, S.M., & KRASNE, S. 1973. Experimentally observed effects of carriers on the electrical properties of bilayer membranes-equilibrium domain. In Membranes - A Series of Advances, Vol. 2, Lipid Bilayers and Antibiotics. G. Eisenman, editor. Marcel Dekker, Inc., New York. Chap. 3.

SZABO, G. & URRY, D.W. 1979. N-acetyl Gramicidin: Single-Channel properties and implications for channel structure. Science 203, 55-57.

TAKEDA, K., BARRY, P.H. & GAGE, P.W. 1980. Effects of ammonium ions on end-plate channels. J. Gen. Physiol. 75, 589-613.

TAKEDA, K., DATYNER, N.B., BARRY, P.H. & GAGE, P.W. 1978. Postsynaptic effects of Zn^{2+} at the motor end-plate. Proc. Aust. Physiol. Pharmacol. Soc. 9, 126p.

TAKEDA, K., GAGE, P.W. & BARRY, P.H. 1981. Effects of divalent cations on toad end-plate channels. J. Membr. Biol. in the press.

TAKEUCHI, A. & TAKEUCHI, N. 1959. Active phase of frog's endplate potential. J. Neurophysiol. 22, 395-411.

TAKEUCHI,. A. & TAKEUCHI, N. 1960. On the permeability of end-plate membrane during the action of transmitter. J. Physiol. 154, 52-67.

TAKEUCHI, N. 1963a. Some properties of conductance changes at the end-plate membrane during the action of transmitter. J. Physiol. 167, 128-140.

TAKEUCHI, N. 1963b. Effects of calcium on the conductance change of end-plate membrane during the action of transmitter. J. Physiol. 167, 141-155.

TERRAR, D.A. 1978. Effects of dithiothreitol on end-plate currents. J. Physiol. 276, 403-417.

THOMAS, R.C. 1976. The effect of carbon dioxide on the intracellular pH and buffering power of snail neurones. J. Physiol. 255, 715-735.

TILLOTSON, D. 1979. Inactivation of Ca conductance dependent on entry of Ca ions in molluscan neurons. Proc. Natl. Acad. Sci. U.S.A. 76, 1497-1500.

TRAUTMANN, A. & ZILBER-GACHELIN, N.F. 1975. Further investigations on the effect of denervation and pH on the conductance change at the neuromuscular junction of the frog. Pflüg. Arch. 364, 53-58.

TSAI, M.C., OLIVEIRA, A.C., ALBUQUERQUE, E.X., ELDEFRAWI, M.E. & ELDEFRAWI, A.T. 1979. Mode of action of quinacrine on the acetylcholine receptor ionic channel complex. Mol. Pharmacol. 16, 382-392.

URBAN, B.W., HLADKY, S.B. & HAYDON, D.A. 1978. The kinetics of ion movements in the Gramicidin channel. Fed. Proc. 37, 2628-2632.

URBAN, B.W., HLADKY, S.B., & HAYDON, D.A. 1980. Ion movements in Gramicidin pores. An example of single file transport. Biochim. Biophys. Acta 602, 331-354.

URRY, D.W., LONG, M.M., JACOBS, M. & HARRIS, R.D. 1975. Conformation and molecular mechanisms of carriers and channels. Ann. N.Y. Acad. Sci. 264, 203-220.

VAN DER KLOOT, W.G. & COHEN, I. 1979. Membrane surface potential changes may alter drug interactions: an example, acetylcholine and curare. Science 203, 1351-1353.

VAN HELDEN, D.F., GAGE, P.W. & HAMILL, O.P. 1979. Conductance of end-plate channels is voltage dependent. Neurosci. Lett. 11, 227-232.

VAN HELDEN, D.F., HAMILL, O.P. & GAGE, P.W. 1977. Permeant cations alter end-plate channel characteristics. Nature 269, 711-713.

VARGAS, F.F. 1968. Water flux and electrokinetic phenomena in the squid axon. J. Gen. Physiol. 51, 1225-1305.

VENOSA, R.A. & HOROWICZ, P. 1973. Effects on sodium efflux of treating frog sartorius muscles with hypertonic glycerol solutions. J. Membr. Biol. 14, 33-56.

VERVEEN, A.A. & DE FELICE, L.J. 1974. Membrane noise. Progr. Biophys. Mol. Biol. 28, 189-265.

VERVEEN, A.A. & DERKSEN, H.E. 1965. Fluctuations in membrane potential of axons and the problem of Coding. Kybernetik, 2, 152-160.

WATANABE, S. & NARAHASHI, T. 1979. Cation selectivity of acetylcholine-activated ionic channels of frog endplate. J. Gen. Physiol. 74, 615-628.

WONG, F. 1978. Nature of light-induced conductance changes in ventral photoreceptors of Limulus. Nature 276, 76-79.

WOODHULL, A.M. 1973. Ionic blockage of sodium channels in nerve. J. Gen. Physiol. 61, 687-708.

WRAY, D. 1980. Noise analysis and channels at the postsynaptic membrane of skeletal muscle. Progr. Drug Res. 24, 9-56.

WRIGHT, E.M., BARRY, P.H. & DIAMOND, J.M. 1971. The mechanism of cation permeation in rabbit gallbladder. Conductances, the current-voltage relation, the concentration dependence of anion-cation discrimination, and the calcium competition effect. J. Membr. Biol. 4, 331-357.